

Solvent Freeze Out (SFO) Technology for Protein Crystallization  
-Optimization and Applicability-

Dissertation

Zur Erlangung des  
Doktorgrades der Ingenieurwissenschaften (Dr. -Ing.)

des

Zentrums für Ingenieurwissenschaften

der Martin-Luther-Universität

Halle-Wittenberg,

vorgelegt

von Frau M.Sc. Viviana Patricia Díaz Borbón

geb. am 05.10.1981 in Bogotá, Kolumbien

Gutachter: 1. Prof. Dr. –Ing. Dr. hc. Joachim Ulrich  
2. apl. Prof. Dr. rer. nat. habil. Heike Lorenz

Datum der Verteidigung: 28.03.2013

Düsseldorf, den 19.06.2013

## Acknowledgments

---

During the Christmas party of the year 2009, Professor Joachim Ulrich announced to me that I have been accepted as one of his PhD students. Since that day until today, when I am writing these sentences, I have been deeply grateful for this opportunity.

I very much appreciated the support of Prof. Ulrich during the time I was his student. In our meetings and discussions, he always showed me the right way to the fulfillment of my tasks and aims.

All the experiences gained through several congresses, seminars and exchange journeys are also of high value to me and I am very grateful for them.

Special acknowledgments are directed to Prof. Dr. M. Pietzsch and Dr. Hertel, members of the Downstream Processing group which belongs to the Institute of Pharmacy of the MLU Halle-Wittenberg, for sharing their laboratories and valuable proteins with us.

I would like to thank Dr. Spohn from Fraunhofer Institute for Mechanics of Materials IWM, for the supply of the silk proteins.

Thanks to Ms. Andrea Alles, account manager of European STEM, for providing us with the STEAM Integrity 10 system used in a crucial part of my experiments.

A special thank you goes to the students which were under my supervision: Steven, Annika, Steffi, Maria and Boat. We built this work together!

I want to thank Tao, with whom I had some common aims and worked together in order to reach them. We had therefore, several fruitful discussions and learned a lot from each other.

I would like to thank all my TVT colleagues and team members, for their support, help and especially for the moments we spent together. I wish all of them the best in their careers and personal life, for now and for the future.

I thank my husband for his support, patience and love and his family, which has been my family here in my second home: Germany.

The love to my parents and grandparents has been the motor of my life and their love to me has been the element which permits my life to be so precious. Thank God for letting us be.

Oh! And thanks to my cat –Tiga. Because of him, I was awake and “fit” early in the morning to start a new working day.

## Table of Contents

---

1.	Introduction.....	5
2.	Theoretical Background .....	7
2.1	Basics of Crystallization .....	7
2.1.1	Phase Diagrams .....	8
2.1.2	Industrial Crystallization.....	10
2.2	Melt Crystallization.....	11
2.3	Solvent Freeze Out Crystallization (SFO) Technology .....	13
2.4	Protein Crystallization .....	15
2.4.1	Industrial Application of Protein Crystallization .....	18
2.5	Process Optimization.....	19
3.	Aim of the Work .....	22
4.	Materials and Methods.....	23
4.1	Chemicals.....	23
4.2	Identification of Regions for Crystallization .....	25
4.2.1	Evaluation of Solubility Curve for Lysozyme by van't Hoff Equation.....	25
4.2.2	Screening Tests for Protein Crystallization .....	26
4.2.3	Turbidity Measurements for Determination of Nucleation and Solubility Curves..	29
4.3	Solvent Freeze Out Process .....	30
4.3.1	Protein Crystallization from Pure Solutions .....	31
4.3.2	Protein Crystallization from Mixture.....	31
4.4	Evaluation and Characterization of the Crystals .....	32
4.5	Optimization Strategy.....	32
4.5.1	Fractional Factorial Design .....	34
4.5.2	Central Composite Design.....	35
5.	Results .....	37
5.1	Determination of Solubility Curves of Lysozyme.....	37
5.2	Screening Test for Lysozyme Crystallization .....	39
5.2.1	Pure Lysozyme Solutions.....	39
5.2.2	Lysozyme Ovalbumin Mixtures .....	47
5.3	Pseudo-phase Diagrams: Solubility and Nucleation.....	48
5.3.1	Lysozyme in Pure Solutions.....	49
5.3.2	Lysozyme-Ovalbumin Mixture .....	53
5.4	Crystallization of Lysozyme by Solvent Freeze Out .....	55
5.4.1	Crystallization of Lysozyme from Pure Solutions .....	56

5.4.2	Crystallization of Lysozyme from Lysozyme-Ovalbumin Mixtures .....	61
5.4.2.1	Preliminary Crystallization of Lysozyme by SFO .....	61
5.4.2.2	Advanced Crystallization of Lysozyme by SFO .....	64
5.5	Process Optimization .....	69
5.5.1	Fractional Factorial Designs .....	70
5.5.2	Significant Effects .....	77
5.5.3	Central Composite.....	78
5.5.3.1	Surface Response .....	82
5.5.3.2	Desirability Profile.....	83
6.	Discussion.....	85
6.1	Determination of Pseudo-Phase Diagrams for Lysozyme .....	85
6.2	Crystallization of Lysozyme from Pure Solutions and Mixtures .....	88
6.2.1	Screening Tests.....	88
6.2.2	Solvent Freeze Out -SFO.....	89
6.3	Effects of Parameters and Interactions on Process Responses .....	91
6.4	Optimization of the Process Parameters in the SFO Crystallization of Lysozyme .....	94
6.5	Considerations on the Design of Solvent Freeze Out Process .....	95
7.	Conclusions.....	101
8.	Summary .....	102
9.	Appendix.....	114

## 1. Introduction

One of the greatest challenges with respect to protection and preservation of the environment is the replacement of many synthetic materials with biodegradable and environmentally friendly materials [Fro10]. Nowadays proteins, such as biopolymers, play an important role as an alternative to synthetic polymers in products, such as packing films [Mec06, Fro10]. Proteins are likewise present within and all around human and animal beings, in the cells, in food [Mot98, Pro88, Yok04], in cosmetic products [Ant06, Chv85], in medicaments, and in an almost endless list.

Industry needs to uphold the production of proteins to satisfy the increasing demand for proteins. Therefore, efficient methods for protein extraction and purification from their original source are necessary on an industrial scale [Cha86, Tam11]. One of the most common methods for protein purification is ion exchange chromatography [Cha86, Por92]. This method involves high investment and operating costs and furthermore, additional steps are often required until a protein with high purity and stability [Chi90] is obtained.

Another popular method for protein purification is the use of salts for precipitation of the proteins (salting-out) or their drowning-out with polymers or additives [Wie99]. These methods have become more and more undesirable on an industrial scale, specifically the salting-out, because it requires high amounts of salts and often long operation times [Ald46]. Besides the requirement for reasonable operating times, low investment and operating costs, industrial processes should be above all ecologically sustainable. Therefore, efforts are continuously carried out to find alternative methods for protein purification [Hek07, Lig04] which fulfill industrial requirements.

Crystallization processes for industrial applications in protein purification appear to be attractive at first because they are relatively economical processes. Moreover, proteins possess more stability in their crystalline state than in solution [Dre92] and besides that; the purity of a protein is a requirement for its folding into an organized structure like a crystal [Jud98].

Ryu et al. [Ryu10a] introduced a novel method for protein crystallization named solvent freeze out (SFO) with the crystallization of hen egg white lysozyme as the first achievement in this area. This technology employs the fusion of a solid layer melt crystallization and solution crystallization in one single process. By means of the solid layer melt crystallization, the water of a protein solution is removed by freezing the solvent on a cooled surface [Ulr03]. The solution is therefore concentrated and eventually supersaturated in protein, which promotes the

formation and growth of protein crystals within the solution –classical solution crystallization-. This technology is equipped in such a way that the command of the parameters, such as temperature profiles, allows the control of the nucleation and the growth of the two kinds of crystals formed: the water ice and the protein crystals.

Among the benefits of this technology are its reasonable operating time, its affordability, its low impact against the environment (low salt requirement), and above all it preserves the quality of the proteins.

As any novel technology in its early stage of development, it presents some disadvantages and problems. For instance, there are difficulties common to the two processes involved in it. In order to solve this group of problems, an optimization is necessary. To accomplish this, the new technology has to be analyzed in order to allow a process control and produce an optimal product.

A further objective was to extend the applicability of the method as a proven technology for the purification of proteins out of a protein mixture, since the application of the solvent freeze out technology to protein crystallization had up until now been only reported for lysozyme in pure solutions [Ryu10a, Ryu10b]. The achievement of these goals was the main objective that prompted the realization of this work.

This work combines interdisciplinary tasks consisting of three interconnected, but not identical phases: finding crystallization conditions of the protein in different systems, evaluation of the reproducibility of the process and optimization of the process.

The first chapter gives a brief insight into the basics of protein and the industrial crystallization processes. The state of the art is presented as an important key for the comprehension of the achieved efforts, opening the path to new approaches which became the aim of the actual research. This aim is described shortly in the third chapter.

The fourth chapter offers a detailed description of the materials and methods applied in this investigation. As mentioned before the investigation consisted of three interconnected phases or focuses, therefore it is not prudent to present the results of each isolated from the others. Nevertheless, it is possible to approximate that the results of the first phase, the finding of crystallization conditions can be found in the chapters 5.1 and 5.2 . The results of the second phase, the reproducibility of the processes, are mainly treated in chapters 5.3 and 5.4. And the results of the optimization of the process, which used information from the two previous phases, can be found in chapter 5.5.

## 2. Theoretical Background

### 2.1 Basics of Crystallization

A crystallization process is part of the nature, taking place in several natural phenomena, for instance in the formation of snow flakes, sugar and salts, icicles, among others. Crystals such as calcium carbonate and calcium phosphates are present in the shells of eggs and mollusks or in bones and teeth [Dav00].

Crystallization can also be defined in different contexts as a purification technique, a separation process, a branch of particle technology, within others. But deepening in its physical meaning, it is a supramolecular phenomenon by which an ensemble of randomly organized molecules, ions or atoms come together to form an ordered three-dimensional ions or molecular array called crystal [Dav00]. This phenomenon can occur within a fluid and as a consequence a phase change takes place in a solution and a solid crystalline material is obtained.

In this context two definitions are relevant, which cause some polemical discussions regarding their similarities and differences: solution and melt. A solution is a mixture of two or more species that form a homogeneous single phase. It consists of a liquid solvent and a solute at determined conditions. Melts may be pure materials or mixture of materials, therefore, a homogeneous melt with more than one component at determined conditions is a solution as well [Scw02]. So, the crystallization can take place in the solution or in the melt just under determined conditions which are governed in principle by the thermodynamics of the system. Nevertheless, the kinetics of the process is relevant as well and concerns the formation of the new crystals and of their growth.

The growth of the crystals starts with a single molecule/ion or with a group of molecules/ions which are arranged in a symmetrical array. The ordered packed molecules in the crystal lead to solids with regular shapes and specific symmetries, which together characterize the morphology of the crystal [Dav00].

The morphology in crystals enables the identification of the nature of crystalline materials which can be done by the use of different techniques. For instance, by optical microscopy, crossed polars or by measuring melting points which give an indication of crystallinity, crystalline solids demonstrate a further property which is the diffraction of X-rays and electrons [Dav00].

### 2.1.1 Phase Diagrams

When crystallization do take place in a system, it is important to know. It is useful to use a map in which thermodynamic conditions are located and related to the presence of one or more phases. This map is known as phase diagram and it should provide information on equilibrium data -in a heterogeneous system, the equilibrium exists if the internal energy  $U$  is minimal-. With regard to crystallization, the knowledge of the liquid-solid equilibrium data is most important [Kön03].

The physical nature of a system can be expressed in terms of number of phases, which can change by altering one or more of these variables: temperature, pressure or concentration. In most crystallization processes, as mentioned above the main interest lies in the liquid and solid phases of the system. Since the pressure has a little effect on the equilibrium liquid-solid, this data can be accurately represented as a line in a temperature- concentration diagram [Kön03].

In a phase diagram the composition is plotted on the abscissa and the temperature on the ordinate. Sometimes, only part of the phase diagram is represented, then the independent variable, temperature, is plotted on the abscissa and the dependent variable, concentration on the ordinate, called solubility diagram [Kön03].

Phase diagrams have an important meaning for crystallization process design, since crystallization is achieved just when the concentration of the main component is greater than the equilibrium value. In this case the solution or melt is supersaturated and the degree of supersaturation is the driving force of crystallization processes [Dav00]. The nucleation or formation of a new crystal or cluster, takes place at high supersaturation values. The region of conditions in which nucleation occurs is known to be the limiting of the labile zone and the line is commonly known as the nucleation curve. The region limited between the solubility curve and the boundary of the labile zone (nucleation curve) corresponds to the metastable zone. The width of the metastable zone is the maximum supersaturation achievable before nucleation takes place and the growth of the crystals is only possible in this region. A solution which has conditions above the solubility curve is termed supersaturated and which conditions lay below the solubility curve is undersaturated. Existing crystals dissolve if they fall within this region. This description is represented in the hypothetical solubility diagram in Figure 2-1.



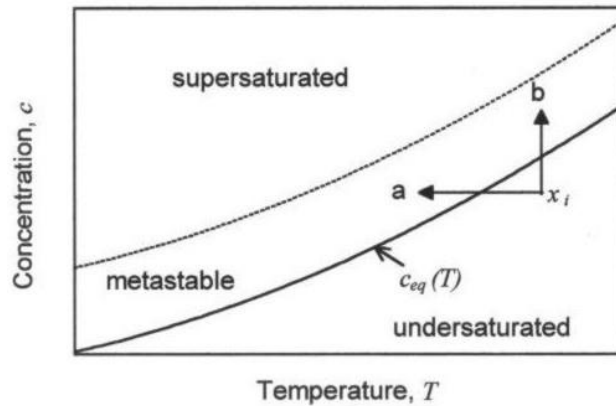


**Figure 2-1:** Hypothetical solubility diagram. A solution with starting conditions  $x_i$  is undersaturated. If the solution is supersaturated above the equilibrium curve  $c_{eq}(T)$  by increasing  $C$  (b path) or decreasing  $T$  (a path), crystals can be formed [Dav00].

In order to design a crystallization process, it is of great importance to have the knowledge of the phase diagram of the system or the metastable zone width. There are different techniques for measuring the nucleation curve which are based on the detection of changes of a physical property of the system. The most common properties considered in this respect are the light and sound transmission. Moreover, since the change of phase from the liquid to the solid state is accompanied by a heat release, the detection of a sudden temperature change may be also used to determine the nucleation point. The nucleation curve and therefore the metastable zone width, depends on the melt composition, the presence of crystals or other particles, the fluid dynamic in the vessel and on the cooling rate. Therefore, the nucleation is a kinetic property of the system unlike the solubility [Chi03].

In order to initiate a crystallization process the difference in chemical potential between the crystallizing substance in the crystal and in the melt must be negative. In other words a determined value of supersaturation should be reached. This value is located above the upper limit of the metastable zone, so crossing the nucleation curve. The concentration of the solution is therefore dropped by the formation of the new crystal and the system finds place within the metastable zone, in which the supersaturation values are adequate for the growth of the crystal. The conditions should stay within this region and a drop below the equilibrium curve should be avoided since the dilution of the new crystals is undesired. In a similar way the conditions should not reenter the labile zone because that would initiate formation of new nuclei.

### 2.1.2 Industrial Crystallization

The bulk production of crystalline materials is also known as mass crystallization. This crystallization is usually carried out in industry for the production of intermediary or end products. In an industrial process, crystallization is preferred in order to attain better quality and physical properties of the final product [Hof95, Nyv78].

Crystalline products have usually very high purity after being separated from an impure solution with a very low energy input. Moreover, crystalline products present good appearance and good handling characteristics, which avoids undesirable properties such as caking tendency, hygroscopicity and handling losses, within others [Ben02, Nyv78].

In order to design an industrial crystallization process, the required final characteristics of the product must be taken into account. For instance, the product has to meet a required purity, crystal size, crystal size distribution (CSD), determined storage characteristics and/or some properties in regard to its further processing [Nyv78, Roy04, Sch04]. Furthermore, some chemical products can be present as different polymorphs, solvates (hydrates) compounds or they might present chirality. If the desired product must fulfill one specific morphology, the selectivity becomes a further constrain to be controlled. In consequence, the selection of the proper process, equipment and operational regime has to be done based on these specifications. Besides the individual characteristics of the material processed, the economic and environmental aspects should be also considered for maximum benefits.

The complexity of a mass crystallization process consists of the presences of a liquid and solid phase in contact, mostly in a non equilibrium state [Nyv78]. Moreover, the nucleation and crystal growth are influenced by a great number of factors. There is a key variable in any crystallization process: the supersaturation [Gar95]. It determines the nucleation and growth kinetics in the process in a wide range and once it is possible to be controlled, the process itself can be controlled as well. The supersaturation may change during the course of a crystallization process, influencing the performance of the crystallization process and consequently the crystal product. For instance it influences the crystal growth which has an influence in the purity of the crystals, their size and size distribution [Gar95]. A scheme showing the influencing parameters in an industrial crystallizer is presented as follows in Figure 2-2 .

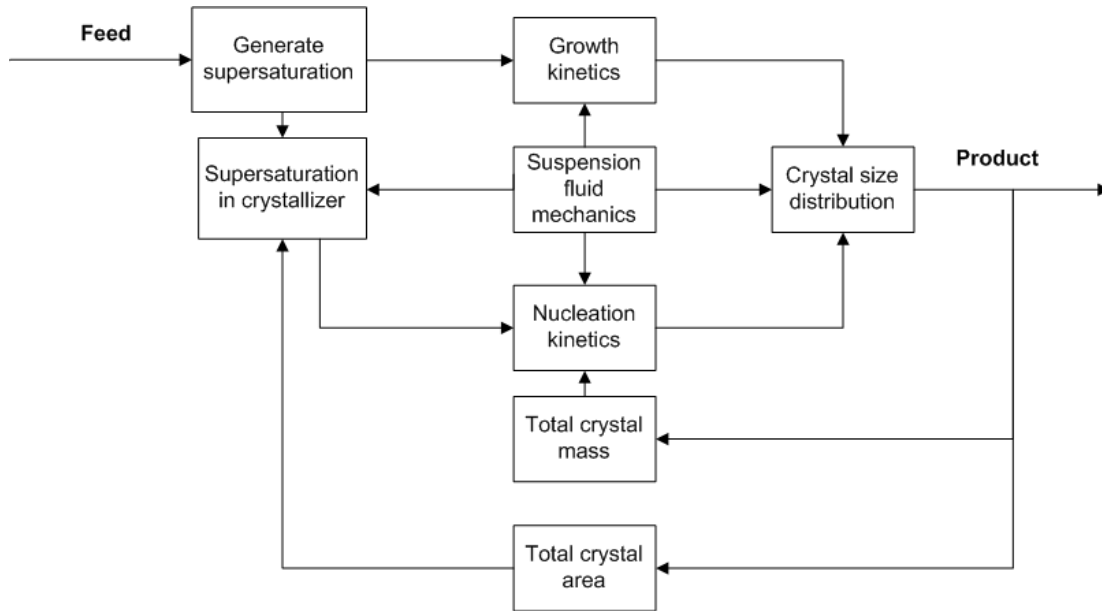


**Figure 2-2:** Interactions affecting crystallizer behavior [Gar95]

## 2.2 Melt Crystallization

Melt crystallization is an important separation, purification and concentration technique used in the chemical, pharmaceutical and food industry. It is a unit operation in chemical engineering and it is based on differences of the equilibrium composition of a substance in its solid or liquid states within a mixture.

This is called melt crystallization and not solution crystallization because, the desired product is considered to be a fraction of a mixture in which the other component (s) is the impurity (rest). This is the reason why the composition of the melt is usually presented in binary phase diagram for a complete range of concentrations or in a solubility diagrams for a limited section of concentrations [Ulr02].

In comparison to distillation as separation process, melt crystallization requires lower energy as the main advantage. The transition of solid-liquid involves lower temperatures and smaller difference in latent heats than the liquid-vapor transition [Ulr03]. Furthermore, this method is of great advantage for separation of organic compounds and heat sensible substances.

Suspension and solid layer melt crystallization are the kind of methods based on this technique and they are described in the following paragraphs.

The solid layer crystallization technique has been used since the last decades to recover a product out of mixtures by crystallization of the desired compound on a cooled surface [Ulr03]. It is based on the separation of a component of a melt due to its phase change and consequent

formation of a crystal layer on a cooled surface of a heat exchanger. The crystal layer grows perpendicular to the cooled surface and in direction to the bulk of the melt (mother liquor). The driving force for crystal growth is the temperature gradient between the equilibrium temperature in the front of the growing layer and the bulk temperature of the feed melt. It is described in other words, as the difference of the equilibrium conditions of solid and liquid phase in a mixture [Ulr03].

Since it is possible to control the temperature of the cooled surface and consequently the temperature difference in the interface, the crystal growth rate (layer growth rate) can be controlled. At the end of a crystallization process, the solid layer is re-molten and the product recovered. This method does not present problems with regard to solid-liquid separation, since the liquid residue is drained by gravity and separately discharged.

Due to the available surface area for crystallization which is in the order of  $100 \text{ m}^2/\text{m}^3$  high the growth rates in solid layer crystallization are in the order of  $10^{-5} - 10^{-7} \text{ m/s}$ . The growth rates can be as high as the purity of the crystal layer allows it, since too high growth rates enhance the kinetic incorporation of impurities and reduce the separation efficiency [Ulr03, Ulr02].

Solid layer crystallization is a proven technology for various industrial applications (e.g. [Ulr02, Sch93]). A quite simple but efficient technique to find out whether crystallization from the melt on a cooled surface can be used for separation is the so-called cooled surface experiments [Özo92, Sch93, Wan94, Neu95, Bie98]. The cooled surface apparatus which allows a static process mode is shown in Figure 2-3.

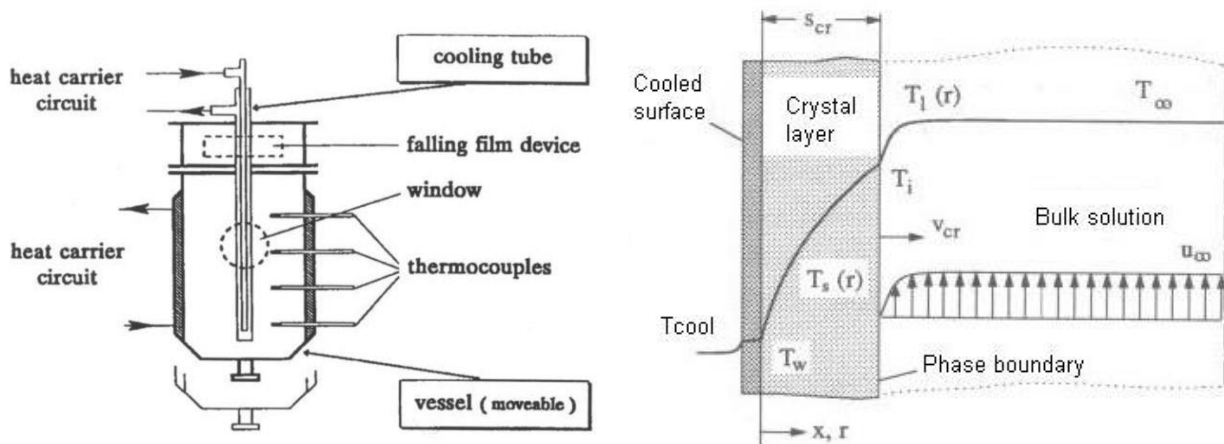


**Figure 2-3:** Left: Solid layer melt crystallization laboratory equipment (falling film) [Neu95]. Right: Scheme of the boundary layer, in accordance with [Sch93].

A tube internally cooled by a circulating coolant is placed in a temperature-controlled vessel containing the feed melt. By means of a thermostat the temperature of the cooled surface is controlled. Since the temperature difference is the driving force and it determines the growth rate and the purity of the layer, optimal temperature programs should be applied. Since the crystal layer thermally insulates the cooled surface, the cooling needs to be increased to compensate this and maintain a constant driving force for a constant optimal growth rate. Otherwise the crystallization process slows itself down and then stops itself when equilibrium of the temperature is reached. The growing crystal layer is exposed to a thermal gradient due to the flow of the heat of crystallization through the crystal layer and the wall of the crystallizer (see right of Figure 2-3).

With regard to suspension crystallization, the crystals made in the crystallizer are usually very pure but a small portion of the mother liquor can deteriorate the product purity dramatically. As the crystal product is obtained suspended in the mother liquor, the separation solid liquid is necessary and it should be done in an optimal way [Ulr03].

Moreover, the control of temperature and supersaturation are important points of attention because the strong temperature dependence of the supersaturation on the temperature for high concentration feeds. The method and controllability of the cooling are very important for the design and operation in suspension crystallization processes. A suspension with a distribution of several small particles would feature a high interface area which favors separation processes [Ulr02]. The surface area on which the crystallization occurs in suspension based processes is relatively large (in the order of  $10^4 \text{ m}^2/\text{m}^3$ ). This implies that relatively low growth rates (in order of  $10^{-7}$ - $10^{-9}$  m/s) are already enough to attain an acceptable production capacity. Low growth rates offer the advantage that the incorporation of impurities is significantly reduced, which in turn leads to very high separation efficiency in one process step [Ulr03]. Furthermore, suspension crystallization methods offers high crystal production rate per volume unit of equipment.

### 2.3 Solvent Freeze Out Crystallization (SFO) Technology

In a SFO process, the two melt crystallization processes take place simultaneously: The crystallization of the solvent (water) which occurs on the surface of the cooled surface (in principle solid layer melt crystallization) and the crystallization of the proteins which takes place within the solution/suspension crystallization). This description is depicted Figure 2-4.

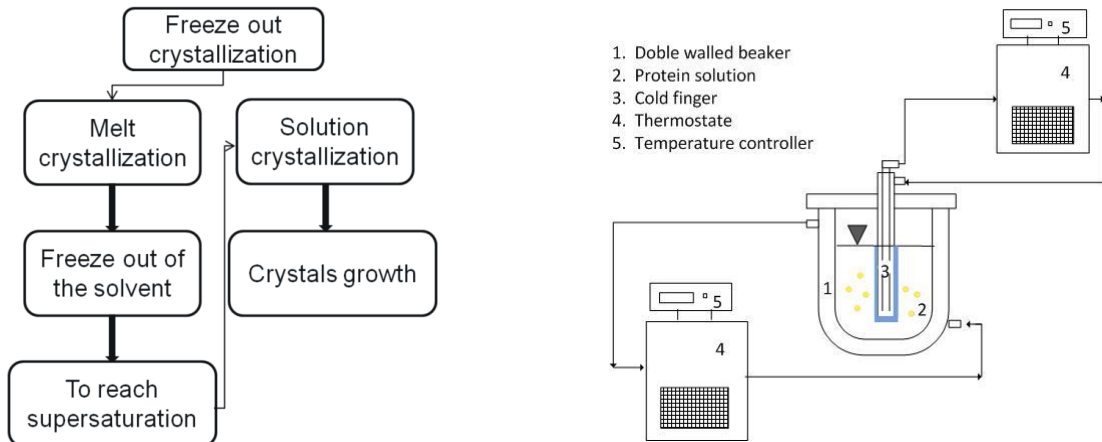


**Figure 2-4:** Left: Conceptual diagram of the solvent freeze out process. Right: Set up of a simple equipment for solvent freeze out crystallization of proteins [Dia10a].

The formation of ice is governed by the phase separation of the ice and all in water dissolved substances. The formation of protein crystals is governed by the phase behavior of aqueous protein solutions (here lysozyme). Only when the conditions of the system are set at determined values, either the water or protein separation by crystallization will take place. In other words, the driving force for nucleation and crystal growth will be supplied just when the system is located within the crystallization region.

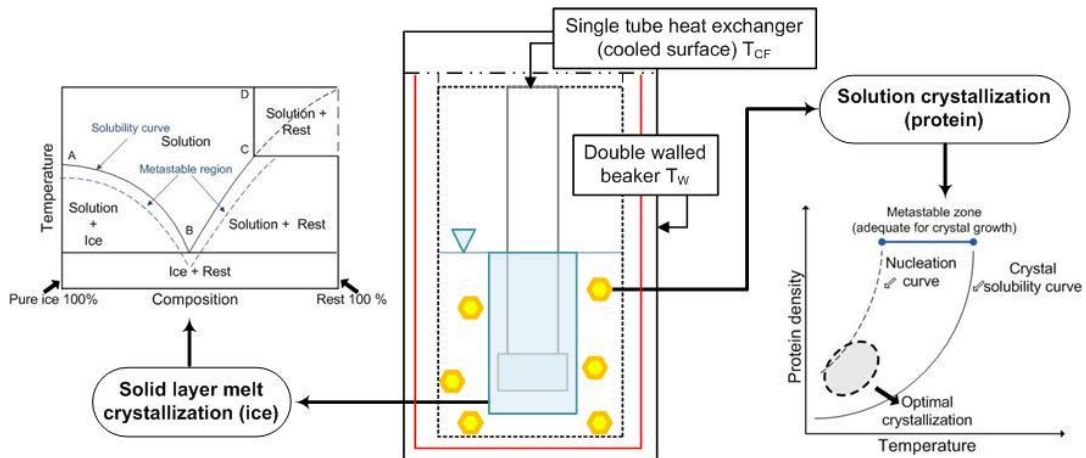


**Figure 2-5:** Representation of the solvent freeze out (SFO) crystallization process. Two crystallization processes take place. One is the crystallization of melt (water) on a cooled surface. The other is the crystallization of the protein within the solution [Dia10d].

For the solid layer melt crystallization the conditions of the solution in front of the cooled surface should be located below the A-B line of the simplified two compounds phase diagram water-“rest” (Figure 2-5, left). For the solution crystallization of the proteins, the conditions of the solution within the confines of the container should fall in between the solubility curve and

the limit of the metastable liquid-liquid region in the generic phase diagram of proteins (Figure 2-5, right).

In the case of the protein crystallization the solid layer is the solvent and the undesired impurities are drops of protein solution. This last phenomenon becomes one of the problems to be solved in this optimization. Ryu et al. [Ryu10a] described this behavior in dependence on the cooling rate and protein concentration in solution. Nevertheless, it was not taken into account the influence of the salt concentration, possible influence of agitation, cooling surface area or dynamic temperature profiles. Here are the motivations to investigate more these influences on the process in order to minimize impurities in the frozen solvent layer.

## 2.4 Protein Crystallization

Proteins are macromolecules which in turn consist of several molecules with determined structure named amino acids. An amino acid molecule has within its structure an  $\alpha$ -amino, an  $\alpha$ -carboxyl group, a hydrogen and a compound R linked to a carbon atom ( $\alpha$ -carbon). The compound R can be a hydrogen atom or any of the 19 hydrocarbon groups that in totally form the 20 kind of amino acids [Ber07].

The amino acids are linked each other by the formation of a peptide bond between the  $\alpha$ -amino group of one amino acid with the  $\alpha$ -carboxyl group of its neighbor. Several amino acids can be joined in a linear sequence, and form a polypeptide chain which determines the primary structure of a protein. A polypeptide chain can be formed from 100 up to 27000 amino acids with an average molecular weight between 5500 and 220000 g/mol<sup>-1</sup>. The side chains of the amino acids can rotate about the peptide bonds and induce different conformations of the polypeptide chain. These different conformations can be  $\alpha$ -helix or  $\beta$ -sheet and determine the secondary structure of the proteins. In a polypeptide chain, the electrochemical structure of the side chains can be different each other creating forces in between them. The interaction forces between functional groups cause the folding of the polypeptide chain into a three-dimensional structure called tertiary structure. Some proteins are complexes formed by the arrangement of different polypeptide chains with their own specific tertiary structure called subunits. These arrangements leaded by covalent or non-covalent forces determine the quaternary structure of the proteins [Ber07].

Proteins present a net charge on their surface, which is a result of the contributions of the side chain groups of the amino acids and the pH of the solution. Polar and non-polar, hydrophilic and hydrophobic interactions, negative and positive charges, all of them influence on the actual net

charge of the protein surface [Dur96, Wie99]. At the iso-electric point  $-pI$ , the net charge on the protein surface is screened by positive and negative charges, therefore it is neutralized. Proteins reach a minimum solubility at proton concentration corresponding to their iso-electric point (e.g. [Ber07, Phe90]).

Moreover, hydration of proteins is necessary for their solubility in water. If the hydration of a protein in solution is reduced, it will tend to fulfill its charges and replace the hydration forces within its structure itself. The water of hydration in a protein solution can be reduced by addition of a competitor compound which uptakes the water molecules such as a polymer or a salt. This effect is named “salting-out” and if the amount of removed active water is high enough the protein would precipitate. The solubility of some proteins can be increased by the addition of salts in an effect called “salting in” [Phe90, Phe09].

The crystallization of a protein occurs when it is arranged in a three dimensional organized structure, composed of a number of regular packed units [Cac91]. The free energy of the protein is minimized when the protein is crystallized, in a similar way as it was minimized when it is at a totally solvated state. These two states have in common that the charges and forces satisfied by the hydration bonds are then satisfied by forces within the protein molecule.

A protein that is in solution would stay in this stage up to certain concentration. If this concentration is exceeded the solution will no stay homogeneous and a new state or phase will appear. Therefore, modifications in the solubility of the protein are the key for the successful crystallization of the protein. The solubility of the protein is a function of the thermodynamic properties of the system. This means that in order to carry out a crystallization process, changes in the composition or the temperature (supersaturation) should be applied (see e.g. [Web97]).

A change in the composition means a change in the concentration of the protein, the pH of the system and/or the addition of an additive. If the pH of the protein in solution corresponds to the  $pI$ , the attraction forces of the protein are very strong and it will precipitate. In order to crystallize the protein, the pH must be set at a different value than its  $pI$ , in which there is a fine tuning between the intermolecular attractive and repulsive forces [Ros96].

In this way, the conditions of the system in a set determine the state of the protein, whether it is in solution, in crystalline or in precipitate state. In a phase diagram, the conditions and the state of the different compounds in the system are represented.

There is a generic phase diagram proposed for proteins and reported by several authors, e.g. [Haa98, Mus97, Ash04]. This phase diagram has been obtained by experimentation with



different proteins such as lysozyme and  $\gamma$ -crystalline. The experimental data are displayed in agreement with the model for hard spheres [Mus97]. At molecular level the salt-protein and protein-protein interactions determine the crystallization behavior [Tre08, Cur06]. This determines the osmotic second virial coefficient of the proteins and it has a determined value at which the protein would crystallize [Dur96, Ros96a].

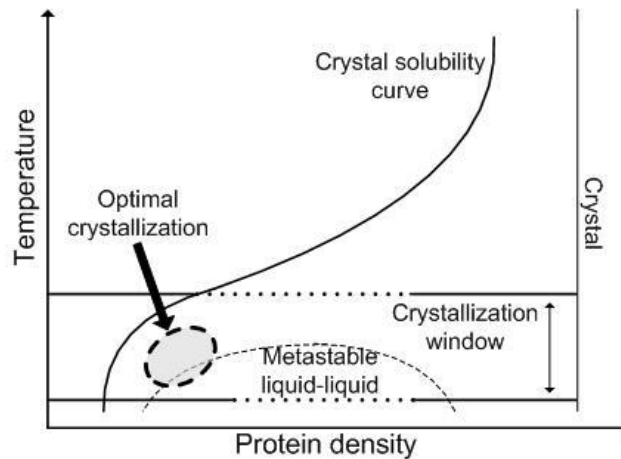


**Figure 2-6:** Generic Phase diagram with crystallization window [Cur06].

Moreover, one of the most important findings in protein crystallization has been the identification of a crystallization window within wide conditions of protein solutions [Cur06]. This crystallization window appears in between the solubility line and the liquid-liquid curve in the phase diagram.

This indicates that if the conditions at equilibrium (solubility) of the system are known it is possible to estimate the crystallization region and even with higher precision if the boundaries of the liquid-liquid region are known. It seems that the nucleation or formation of the protein crystals take place within drops with high concentrations of proteins present in the liquid-liquid metastable region. To subject the protein solution under these conditions for a while permits the formation of the protein nuclei. These protein nuclei would grow further in the region below the liquid – liquid boundary but far enough from the solubility curve to avoid crystals dissolution. This describes then the metastable a similarity to the classical diagram of nucleation in the supersaturated region, then crystal growth in the metastable region. In this region the driving for crystal growth is the concentration and temperature gradient from the equilibrium.

The conditions of a protein system can be described by the supersaturation value which is the actual concentration by the equilibrium concentration at actual temperature [DeM92].

It appears to be straight forward, well either the solubility curve is known or the conditions of the system lead to a second virial coefficient value adequate for crystallization. But, if none of this information is available? This is the difficult issue in protein crystallization. There are just few proteins that have been deeply investigated and from which the thermodynamic conditions are known, Lysozyme from Hen Egg White -HEW is one of those.

As protein crystallization is strongly influenced by many environmental influences such as temperature, pH, ionic strength, solvent composition, concentration of an auxiliary ion, within others. Finding crystallization conditions consist of a systematic search of a set of parameters that would impact upon formation of an appropriated crystal. It is therefore necessary to conduct a high number of crystallization experiments in certain ranges of the influencing parameters, evaluating the results and using the information obtained to improve and find the optimal set of conditions [Phe09].

Screening experiments are the most popular strategy to find the crystallization conditions of determined protein [Phe09, Wie99]. In this kind of experiments the conditions of the protein systems are varied in a wide range and the results are observed and analyzed. Furthermore, it is possible to represent then the results within pseudo-phase diagrams. The conditions under determined phase was observed is located on them and then a broader knowledge of the phase behavior is available.

#### **2.4.1 Industrial Application of Protein Crystallization**

Protein crystals are not only important for the crystallographer, but they have more applications. As it mentioned above, protein molecules in the crystalline state are more stable than in solution and therefore denature less easily [Dre92].

The industrial demand of proteins is growing in pharmaceutical, cosmetic and food markets. Biopharmaceuticals constituted approximately 10 % of the global prescription drug market in 2007. After separation and purification, proteins including pharmaceutical and industrial enzymes are high-value-added products [Tam11].

For example lysozyme, the protein present in the egg white, is widely used for food preservation, as well as in pharmaceutical industry due to its antibacterial activity. The addition of proteins to cosmetics seems to be effective in attaining cosmetic goals such as protection of the structure and function of skin and hair. Therefore, proteins are now a standard raw material in the cosmetic industry offering new possibilities in skin- and hair-care cosmetics [Chv85]. In food industry several application of proteins play an important role, for instance, the

modification of food proteins by the protein transglutaminase leads to textured products, improved elasticity and water-holding capacity, modified solubility and functional properties. In addition it produces food proteins of higher nutritive value through cross-linking of different proteins [Zhu95].

A variety of techniques is used to produce protein crystals (good reviews can be found e.g. in [Web97, Wie99 and Dur96]). Techniques differ in the parameters manipulated to bring about supersaturation and the degree of control over the process. Most techniques are based on evaporation, cooling or salting out to achieve supersaturation. So far, protein crystallization currently employs salting-out or drowning-out techniques, in order to achieve the necessary supersaturation for nucleation and crystal growth.

## 2.5 Process Optimization

Optimizing a process means finding a vector of processes variables  $\vec{x}$  which lead to the desired process responses  $\vec{y}$ . Therefore a process is considered as a black box with a number of input variables and a number of output variables [Loh04]. In order to optimize a process, it is first necessary to investigate experimentally it by carrying out a number of experiments with different processor vectors and recording the process responses [Loh04].

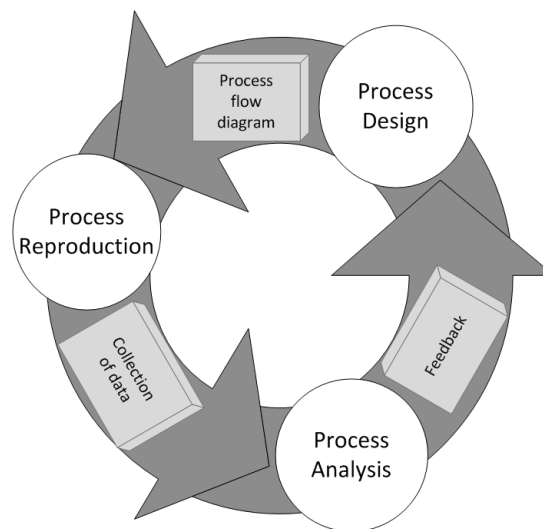


**Figure 2-7:** Procedure in cycling flow required for the optimization of a process [Dia10a].

When an optimization procedure should be taken in consideration, it is necessary to find the way to distribute the process vectors in order to gain as much information on the process with as a limited number of experiments as possible [Hun67]. Moreover, it is necessary to identify which process vector leads to the target response.

The steps of experimentations are described as:

- recognition and statement of the problem
- choice of the factors and levels
- selection of the response variables
- choice of the experimental design
- conduction of the experiments and data analysis.

The relevant background consists on information from previous experiments, routinely collected data, physical laws and expert opinion, are the fundamental part when the optimization is started. Above all it is fundamental to understand clearly what new knowledge can be gained besides the relevant available knowledge.

The experiment is therefore a test in which purposeful changes to the process vectors are made so that resulting changes in the response can be observed.

The components of the process vector are called factors.  $K$ , the number of factors is usually kept below 15. The basic experiments are used for the calculation of all the main effects in full or fractional factorial designs.

Full factorial designs are given if there are  $r$  levels for each of the  $k$  factors and if the experiments are replicated  $n$  times the number of experiments to carry out is [Loh04]:

$$\text{Number of experiments} = n \times r^k \quad \text{Eq. 2.1}$$

Even for small values of  $n$ ,  $r$  and  $k$  the number of experiments can be significantly large. Such full factor designs are popular only for very limited problems. It is particularly popular for 2-level designs. The effect of one or more parameters is calculated by averaging the differences of the other parameters. The reduction in experimental effort can be very notable for large number of factors.

### Fractional factorial designs

With the aim of keeping experimental efforts reasonably low and still to obtain the relevant information the fractional factorial design has been proposed [Mon97]:

$$\text{Number of experiments} = r^{(k-p)} \quad \text{Eq. 2.2}$$

$K$ =number of factors,  $p$ = number of factors generated from the interactions of a full factorial design [Box78, Mon97, Hun67].

### Central composite experiments

In order to assess the independent contributions of two factors, the factor levels must be set to that the columns in the design are independent of each other. The columns in the design matrix should be orthogonal. In this way the main effect and interactions estimates of interest are independent to each other. This is named orthogonality, the more orthogonal the columns are, the better the design because the more the independent information extracted from the design. The designs must be also rotatable, in order to extract the maximum amount of information as well. In order to estimate the second order, quadratic or non-linear component of the relationship between a factor and the dependent variable, one needs at least 3 levels for the respective values. By adding in star points to a simple square or cube 2 level factorial design points, one can achieve rotatable and often orthogonal designs [Sta02].

### Response surface and Response optimization

The shape of fitted overall responses can be summarized in graphs known as contour plots and response surface plots for the fitted model.

The procedures used in product development generally involve two steps. The first step consists of predicting responses on the dependent variables  $y$ , by fitting the observed characteristics of the product using a regression equation or  $x$  variables. The second step consists of finding the levels of the  $x$  variables which simultaneously produce the most desirable predicted responses on the  $y$  variables [Sta02].

### Profiling predicted responses and response desirability

A prediction profile for a dependent variable consists of a series of graphs, holding the levels of the others independent variables constant at specified values, called current values. If appropriated current values for the independent variables are selected, the inspection of the prediction profile can show which levels of the predictor variables produce the most desirable predicted response on the dependent variable. To profile the predicted responses on the dependent variables as well as the overall response desirability, the first step is to specify the desirability function of each dependent variable. The relationship between predicted responses on a dependent variable and the desirability of responses is called the desirability function [Sta02].

### 3. Aim of the Work

The industrial demand for proteins is growing year by year. In order to satisfy this increasing demand, methods on industrial scale are necessary for protein extraction and purification.

Since proteins are having a complex structure and are sensitive to environmental conditions, it is desirable to have them at their maximum stability. This would allow a better handling and improve storage conditions and their usage would be on top by keeping their properties unchanged, like activity in the case of enzymes.

Current techniques used to purify and crystallize proteins are chromatography, cooling or salting out crystallization techniques. They present significant disadvantages such as the requirement of high quantities of salt, energy and long crystallization times. Moreover, if the crystallization step would make other extraction and purification steps unnecessary, it would be of great advantage and benefit with regard to investment and profit.

Protein crystallization for industrial applications demands efficient processes that can be carried out within hours that are reproducible and environmental friendly. The solvent freeze out SFO was presented as an innovative technology that promises to overcome current obstacles in the industrial crystallization of proteins [Ryu10a]. Nevertheless,

- this process presents problems common to melt and suspension crystallization
- as a novel technique it must be optimized, and
- its development and optimization in terms of yield, crystal quality, environmental impact and energy is required.

The achievement of these three points became the aim of this work and its accomplishment is described throughout the following pages.

## 4. Materials and Methods

The methods and the respective materials involved in this study can be classified into three main groups consisting of:

- Production of the crystals in either screening tests or by the solvent freeze out method.
- Characterization of the crystals, which has been done through activity tests, SDS-PAGE analysis, gravimetric methods and light microscopy.
- Collection of data and statistical evaluation of the results obtained out of the crystallization processes and the consequent analytical methods.

### 4.1 Chemicals

Hen egg white lysozyme is the main protein used in this work. This protein has been purchased from Fluka and applied without any further purification. Sodium chloride (NaCl) ( $\geq 95\%$ ) purchased from Carl Roth was used as crystallizing agent. The egg protein albumin purchased from Fluka as well, has been applied as foreign protein in the crystallization tests of the lysozyme. Protein and salt (NaCl) solutions were treated in 0.1 M sodium acetate buffer with pH values of 4.4 and 5.0. Different concentrations of protein (lysozyme, ovalbumin) and crystallizing agent (NaCl) were applied as a function of the experimental aim. The sodium acetate buffers were prepared by titration of a sodium acetate solution with an acetic acid solution until the desired pH value was reached.

The microorganism *micrococcus lysodeikticus (micrococcus luteus)* (ATCC No. 4698) was utilized in the enzymatic activity tests of the commercial lysozyme and the produced lysozyme crystals. The activity tests were carried out in a phosphate buffer media with pH 7, which is prepared by the adequate combination of disodium-phosphate, monopotassium und dipotassium phosphates.

Different buffers were required in the implementation of the SDS-PAGE analysis, such as the buffers for the gel preparation, for the dissolution of the samples and for the electrophoresis running. For instance, the accumulative gel consisted of a 0.5 M Tris buffer with a pH value adjusted to 6.8. The separation gel buffer contained 1.5 M Tris buffer with a pH value of 8.8. The running buffer consisted on Tris, Glycin and Sodiumdodecylsulphate (SDS). The sample buffer has been obtained by mixing Tris, Sodiumdodecylsulphate (SDS), bromophenol blue, glycerol and Urea in adequate proportions at a pH value of 8.0.

In addition to the buffer solutions for the implementation of the SDS-PAGE other solutions are necessary, on one side, the solutions for the preparation of the gel, and on the other side the solutions for the treatment of the gel after electrophoresis.

The overview list of the chemicals used in the process, analysis and characterization of the crystals is shown in Table 4-1.

**Table 4-1:** Overview of the used chemical substances: proteins, microorganisms and chemicals.

Substance			Supplier
<b><i>Proteins</i></b>			
	Molecular weight [kDa]	Cas No.	
Hen egg white lysozyme (HEWL)	14.3	12650-88-3	Fluka Analytika
Albumin from egg	44.5	9006-59-1	Fluka Analytika
<b><i>Microorganism</i></b>			
Micrococcus lysodeikticus	Lyophilized cells	ATCC No. 4698	Sigma Aldrich
<b><i>Chemicals</i></b>			
	Molar mass [g/mol]	Lot. No.	
Acetic acid (C <sub>2</sub> H <sub>4</sub> O <sub>2</sub> )	60.05	10784671	Carl Roth GmbH & CoKG
Ammonium persulfate (APS)(NH <sub>4</sub> ) <sub>2</sub> S <sub>2</sub> O <sub>8</sub>	228.18	-	
Bromophenol blue (C <sub>19</sub> H <sub>10</sub> Br <sub>4</sub> O <sub>5</sub> S)	669.96	8D006192	Applichem
Dipotassium phosphate (K <sub>2</sub> HPO <sub>4</sub> )	174.2	24897389	Carl Roth GmbH & CoKG
Disodium phosphate (Na <sub>2</sub> HPO <sub>4</sub> )	141.96	40467540	Carl Roth GmbH & CoKG
Formaldehyd (CH <sub>2</sub> O)	30.03	416SM	Riedel-de Haën
Hydrochloric acid (HCl)	36.46	-	Bernd Kraft GmbH
Isopropanol (C <sub>3</sub> H <sub>8</sub> O)	60.1	607461	Carl Roth GmbH & CoKG
Mercaptoethanol (C <sub>2</sub> H <sub>6</sub> OS)	78.13	-	
Monopotassium phosphate (KH <sub>2</sub> PO <sub>4</sub> )	136.086	24897389	Carl Roth GmbH & CoKG
N-(4-hydroxyphenyl)glycine (C <sub>8</sub> H <sub>9</sub> NO <sub>3</sub> )	167.16	81HO4651	Sigma Aldrich
Tetramethylethylenediamine (C <sub>6</sub> H <sub>16</sub> N <sub>2</sub> )	116.2	48792069	Carl Roth GmbH & CoKG
Silver nitrate (AgNO <sub>3</sub> )	169.87	-	Merck
Sodium carbonate (Na <sub>2</sub> CO <sub>3</sub> )	105.98	929A427192	Merck
Sodium chloride (NaCl)	58.44	170154798	Carl Roth GmbH & CoKG
Sodium dodecyl sulphate (C <sub>12</sub> H <sub>25</sub> Na S O <sub>4</sub> )	288.37	49467326	Carl Roth GmbH & CoKG
Sodium hydroxide (NaOH)	39.99	71692	Fluka Chemika
Sodium sulphate (Na <sub>2</sub> SO <sub>4</sub> )	142.04	37466168	Carl Roth GmbH & CoKG
Sodium thiosulfate (Na <sub>2</sub> S <sub>2</sub> O <sub>3</sub> )	158.11	37466168	Carl Roth GmbH & CoKG
Tris(hydroxymethyl)-aminomethane (C <sub>4</sub> H <sub>11</sub> NO <sub>3</sub> )	121.14	49574655	Sigma Aldrich
Urea (CH <sub>4</sub> N <sub>2</sub> O)	60.06	7163	Grüssing GmbH



## 4.2 Identification of Regions for Crystallization

As it has been mentioned at the beginning of this chapter, the first section of this investigation consisted on the production of the lysozyme crystals. In order to achieve the crystallization of lysozyme, it was necessary to find the region of conditions which lead to the formation of a desired crystal. Since crystals form in supersaturated solutions, the knowledge of the solubility curve is the first approach to get information on the possible conditions for crystal formation and growth, e.g. [Ash04, Sch04]. Being the HEWL a well-studied protein, information on its solubility at a wide range of conditions can be obtained from literature, e.g. [Cac91, For99]. Nevertheless, the provided solubility data covers only temperatures between 2 and 25 °C, leaving the solubility data for lower and higher temperatures as unknown. In order to solve this problem, a method described in the following chapter has been applied to calculate the missing solubility data by extrapolation of already available data [For99].

### 4.2.1 Evaluation of Solubility Curve for Lysozyme by van't Hoff Equation

The van't Hoff equation which is shown in Eq. 4.1, deals with the relationship between the temperature and the equilibrium constants of a system. It can be arranged in order to obtain information on the solubility of the lysozyme at a determined temperature.

$$\ln\left(\frac{k_{T_2}}{k_{T_1}}\right) = \frac{\Delta H^\circ}{R} \left(\frac{1}{T_1} - \frac{1}{T_2}\right) \quad \text{Eq. 4.1}$$

For the reactions which take place in solution, the concentrations of insoluble or temporary existing solid substances correspond to 1 [Wie99]. Therefore the equilibrium constant can be expressed as follows in Eq. 4.2:

$$k_{T_1} = \frac{1}{c_1} ; k_{T_2} = \frac{1}{c_2} \quad \text{Eq. 4.2}$$

The two equilibrium constants are taken back and replaced into the original van't Hoff equation (Eq. 4.1) to get a new equation concerning to the temperature and concentration of the protein (Eq. 4.3).

$$\ln\left(\frac{C_1}{C_2}\right) = \frac{\Delta H^\circ}{R} \left(\frac{1}{T_1} - \frac{1}{T_2}\right) \quad \text{Eq. 4.3}$$

$C_1$  is the solubility of the protein at a temperature  $T_1$  and  $C_2$  denotes the solubility of the protein at a temperature  $T_2$ .

Once the solubility of the protein at a determined temperature is known, it is possible to calculate the supersaturation of the system which is as shown expressed in Eq. 4.4.

$$s = \frac{C}{C_{eq}} \quad \text{Eq. 4.4}$$

#### 4.2.2 Screening Tests for Protein Crystallization

With the knowledge of the solubility data of the protein in a determined system, it is possible to get an idea about the possible conditions for protein crystallization. Nonetheless, it is necessary to locate the regions in which the formation and the growth of the crystals take place and even more, if it possible, the limits between them.

Therefore, it was useful to carry out a number of crystallization trials in which the most important factors which influence crystallization such as the temperature and the concentrations of protein(s) and salt were changed.

The screening tests have been carried out in 96-well plates with a volume of 150  $\mu\text{L}$  per well. Protein and salt solutions were prepared separately in 2 or 10 mL sample tubes and then mixed in a determined proportion to reach a desired final composition of the solution. Furthermore, 100  $\mu\text{L}$  of the supersaturated solutions were sampled and added into the wells. Subsequently, the micro-titer plates were sealed and vacuum packed in plastic bags to be then immersed in a water bath for 5 or 24 hours. The fundamental sketch of the screening tests is represented in Figure 4-1.

In Figure 4-1, it is possible to observe an example of the arrangement of the wells in a micro-titer plate, in which each or some of the wells would contain protein solutions with initial conditions (A). After the 5 or 24 hours of the experiment and therefore the immersion in a water-ethylenglycol bath, the solutions have final conditions (B). Moreover, it can be counted which solution is with or without the presence of solid particles, which would be crystals if the crystallization has succeeded, or espherulites, or solids with irregular shapes. Therefore, once the screening tests were carried out, the protein solutions were investigated by means of a light microscope (Keyence VHX-500F).

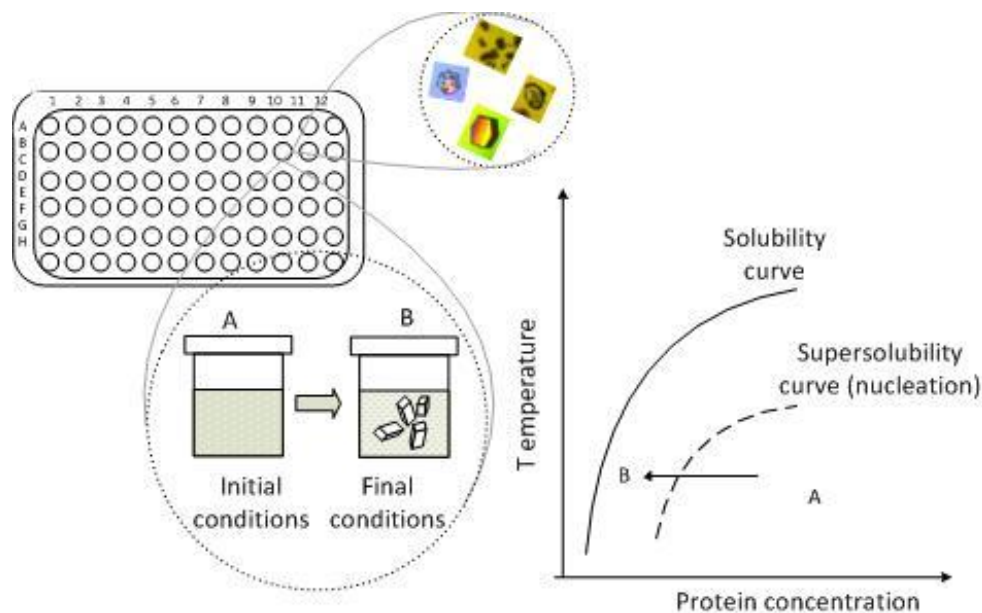


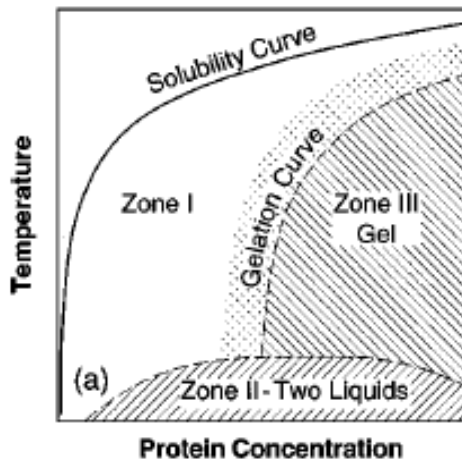
**Figure 4-1:** Scheme of 96-well plates used for the crystallization screening tests. A “micro-batch crystallization” (100  $\mu$ L volume) takes place [Dia10a] in each of the wells.

On the right side of Figure 4-1 a hypothetical solubility diagram is shown, on which the initial conditions (A) of the screening tests were approximated to be within the supersaturated region and the ideal final conditions (B) would belong to the region appropriated for crystal growth. A phase diagram in a rigorous definition, maps out equilibrium states as a function of the system variables. Nevertheless, also kinetic factors must be considered which determine the nucleation of the crystals, since the history of the process can be as important as the instantaneous values of the parameters [Dur96].

For this reason, although the phase diagram is a rigorous starting point, it has been useful to alter the concept somewhat and construct pseudo-phase diagrams representing experimentally obtained results, which give information on the concentration range over which the crystallization can occur.

So, once the final solutions are investigated, it is possible to locate the conditions of the system in a pseudo-phase diagram, regarding to the quality of the solids produced. If these solids were well shaped crystals and had a significant size, the conditions should belong to the metastable region (between nucleation and solubility curve). If no crystals were observed probably the initial solution was undersaturated and if large crystals are accompanied with very tiny ones, the solution probably passed the upper limit (nucleation curve) of the metastable zone.

In order to have a better visualization of the construction of pseudo-phase diagrams, the generic phase diagram for globular proteins is here once more cited in Figure 4-2.



**Zone I:** A region of supersaturation where well formed Lysozyme crystals form.

**Zone II:** A region where the Lysozyme solution undergoes a rapid liquid-liquid phase separation, with the resulting concentrated Lysozyme phase quickly transforming to the more stable crystalline form. Crystals formed in zone II are of poor quality.

**Zone III:** A region characterized by gel formation, unsuitable for crystal growth.

**Figure 4-2:** Generic phase diagram for globular proteins [Mus97].

To establish an analogy to the diagram shown in Figure 4-2, the zone I would be the metastable zone, and the curve delimiting the Zone I and Zone II would be the nucleation curve.

In order to verify the supersaturation level for crystal growth, 5 mL of the supersaturated protein solutions were also observed by time lapse microscopy at 4, 1, -3 and -7 °C. The crystallization was carried out within a microscope cell in which the temperature has been controlled by the use of a thermostat F8 (Fa, Haake), see Figure 4-3.

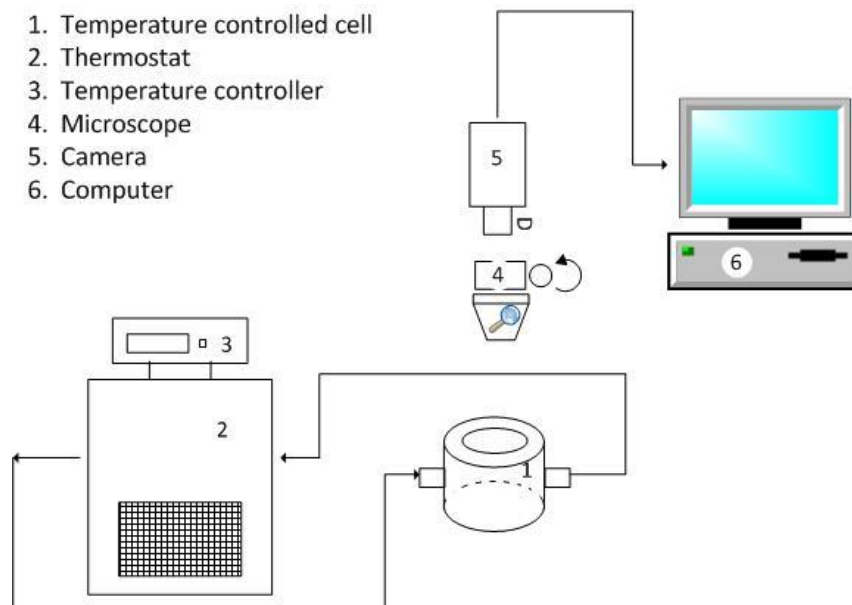


**Figure 4-3:** Set up for microscopy observations of a cell in which the supersaturated protein solution is contained [Dia10a].

At the moment in which the presence of crystals was detected by the microscope observation, a sample of 20  $\mu\text{L}$  of the solution was taken. Then the sample was analyzed by UV light absorption at 280 nm to determine the protein concentration and subsequently the supersaturation value in the solution by the use of Eq. 4.4.

With the information on the solubility and the region appropriated for crystal growth, it is possible to describe a phase diagram of the protein system. This phase diagram, also called pseudo-phase diagram [Ryu10a] is actually the solubility diagram accompanied by the upper limit of the metastable zone which is an approximation to the nucleation curve. In former research [Ryu10a], these data was collected for lysozyme-sodium chloride systems in sodium acetate buffer pH 4.4 with protein concentration between 2 and 12 mg/mL (eventually up to 15 mg/mL) and salt (NaCl) concentrations of 2, 5 and 7 wt. %

In order to complete the study in regard to the effect of the salt concentration on the crystallization of lysozyme, the missing concentrations of 3, 4 and 6 wt. % have been investigated in the present work.

#### **4.2.3 Turbidity Measurements for Determination of Nucleation and Solubility Curves**

In chapter 4.2.2, the microscopic observation methods were introduced for the identification of the limits of the metastable zone for different lysozyme-salt systems. In order to verify and complement this information, the turbidity measurement method is additionally used. This method is based on fact that changes in the turbidity of protein solutions, caused by the formation of the crystals or by their dissolution, could be detected while variations of the temperature were applied.

Protein and solutions with determined composition were prepared and cooled down while an IR signal was continuously passed through the solution and detected afterwards. The turbidity of the solution and consequent scattering of the IR signal indicated the formation of particles within the solution. The corresponding temperature was recorded as the nucleation point. Then the temperature of the protein solution has been increased and the temperature at which the IR signal passed without being scattered was recorded as the solubility point. This procedure is sketched in Figure 4-4, left.

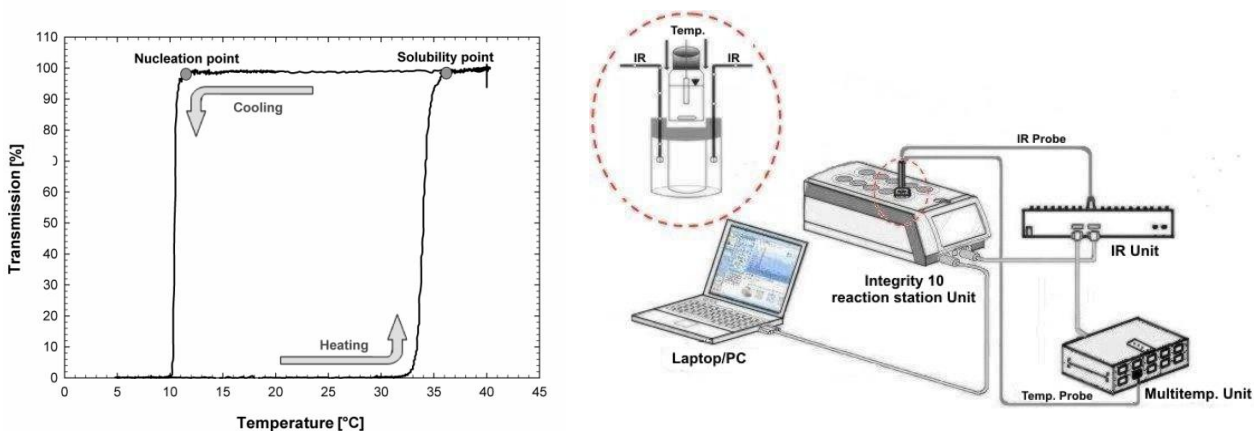


**Figure 4-4:** Left: Change of the transmission with the temperature in a turbidity measurement experiment, from which information on the nucleation and solubility points are obtained. Right: A STEM Integrity 10 system (Electro Thermal) used for the turbidity measurements and furthermore, the acquisition of nucleation and solubility data [Mao12].

A STEM Integrity 10 system (Electro Thermal) has been used to carry out the turbidity measurements (Figure 4-4, right). For this, 1 mL of the lysozyme solution to be tested was added into a sample glass of 1.5 mL volume.

The sample tube has been inserted into a non intrusive IR probe (part code ATS10360) placed in a compartment of the STEM Integrity 10 reaction station. The temperature sensor was then immersed through the cap of the glass into the glass containing the solution. A Multi-Temp 10 module was used to control the temperature of the system (part code ATS 10001), to this part the temperature sensor is connected.

Information on the turbidity in real time was collected by the connection of the non intrusive IR probe to a Multi-IR box (IR Unit). Both, the IR unit and the Multi-Temp 10 module have been connected to a computer through the STEM Integrity 10 reaction station block.

In this work the range of temperatures studied for the determination of the nucleation points corresponded to higher lysozyme concentrations (between 25 and 50 mg/mL) than in the screening tests (micro batch crystallizations). The concentrations of salt applied were 3 and 4 wt. %. The protein and salt were treated in sodium acetate buffer with a pH value of 4.4.

### 4.3 Solvent Freeze Out Process

The basic experimental equipment is described on the right side of Figure 2-4. Double walled beakers with volume of either 100 mL or 1000 mL have been set at constant temperature ( $T_w$ ) by the use of a programmable thermostat (either Haake C25 or Julabo F25). A single tube heat exchanger, named -cooled surface or cold finger- with determined length ( $L_{CF}$ ), has been placed

concentrically into the beakers and its temperature profile was controlled by the use of a thermostat (either ThermoHaake C30P or Julabo F32). In the former solvent freeze out process the temperature of the cooled surface used to be just decreased at one cooling rate in one step from an initial temperature to a final one [Ryu10a, Ryu10b]. However, in this work a new kind of temperature profile was applied to the cooled surface, which has been dynamic in order to control the actual conditions of the system. The temperature profile consisted on steps of cooling ( $dT/dt$ ) and constant temperature ( $T_{CT-CF}$ ) for a time ( $t_{CF-CT}$ ). The duration of a temperature profile which goes from an initial temperature ( $T_{CF}$ ) to a final one ( $T_{FT-CF}$ ), and takes into account cooling and constant steps, corresponds to the total crystallization time of a SFO process. The protein solution is occasionally stirred by the use of an axial glass impeller.

As mentioned before, in the laboratory a basic SFO process for protein crystallization is carried out in a double walled beaker containing a supersaturated protein-salt solution. The supersaturation of the protein solution is determined by the salt ( $C_S$ ) and protein ( $C_P$ ) concentrations. The low and high levels of salt and protein concentrations have been chosen based on the information obtained from the results of the experiments described in chapter 4.2. Once the crystallization time is reached, the cooled surface is removed out of the solution and the ice is molten and recovered for further analysis.

#### 4.3.1 Protein Crystallization from Pure Solutions

The kind of lysozyme crystallization from which lysozyme was separated out of solutions only composed of lysozyme and the crystallizing agent (NaCl) was denominated crystallizations from pure solutions. These crystallizations were carried out in the 1000 mL double walled beaker. The solutions were prepared by mixing double concentrated protein and salt solutions in a proportion 1:1 to reach a desired final composition. Then the SFO crystallization process was carried out as described in the previous chapter. The detailed technical sketch of the equipment can be found in the appendix I.

#### 4.3.2 Protein Crystallization from Mixture

The protein mixtures consisted of lysozyme, ovalbumin and NaCl as crystallizing agent. The composition of the mixture varied depending on the experimental aim. The individual solutions were prepared in such a concentration that the final mixtures lysozyme/ovalbumin/salt were in the ratio of 1:1:1 or 0.5:2:0.5 (for high ovalbumin concentrations). The mixtures prepared with varied compositions were then transferred into the 100 mL double walled beaker and the SFO

crystallization process was accomplished according to the general procedure. A detailed technical sketch of the corresponding equipment can be found in the appendix II.

#### 4.4 Evaluation and Characterization of the Crystals

As mentioned in chapter 4.3, once the final crystallization time has been reached, the cooled surface was immediately removed from the solution. In order to melt the ice layer, the temperature of the cooled surface was then increased to 4 °C.

The solution containing the formed protein crystals (mother liquor) were filtered through pre-weighed filter papers (particle retention 2 µm) and recovered for further analysis. The filter papers with the collected crystals were air dried and weighed in order to calculate the crystallization yield, expressed as the ratio of crystals produced per initial amount of lysozyme in solution.

The volumes of molten ice ( $V_{ICE}$ ) and remaining mother liquor ( $V_{ML}$ ) were recorded. Samples of 50 and 100 µL were taken to be analyzed by photometry and microscopy, respectively.

Based on the Lambert-Beer Law equation, the total concentration of protein was calculated after measuring the UV light absorbance of the samples at 280 nm. Furthermore, the size and morphology of the crystals were qualitatively analyzed by a microscope.

The size distribution of the crystals was measured in a Mastersizer-Hydro2000S (Malvern). For the measurements, 10-30 mg of dried crystals were suspended in a 12 wt. % NaCl solution with pH 6.0 sodium acetate.

Moreover, in order to confirm the nature of the crystals, they are characterized by SDS-PAGE (sodium dodecyl sulfate polyacrylamide gel electrophoresis) analysis and activity tests. The activity is determined by measuring the turbidity decay in a suspension of *Micrococcus lysodeikticus* resulting from their cell walls lysis in presence of lysozyme [Shu52]. For this test, lysozyme powder and crystals are treated in phosphate buffer pH 7.0 and the turbidity measurements are carried out at a wavelength of 450 nm by the use of a spectrophotometer (Specord 40, AnalytikJena). The activity of the HEWL powder is used as reference for a 100 % of activity and the activity of the crystals is compared to the reference to determine the remaining activity within the crystals.

#### 4.5 Optimization Strategy

For the process optimization in terms of yield, quality (morphology and size), activity of the crystals, minimal protein loss and efficiency, an iterative optimization path was followed. It



started with the reproduction of the crystallization process SFO using as setting parameters KPI those reported as optimal in a previous research [Ryu10a]. Followed by the evaluation of the results and then a respective feedback was applied, to get a new process design. The iterative path is shown a flow diagram in Figure 4-5.

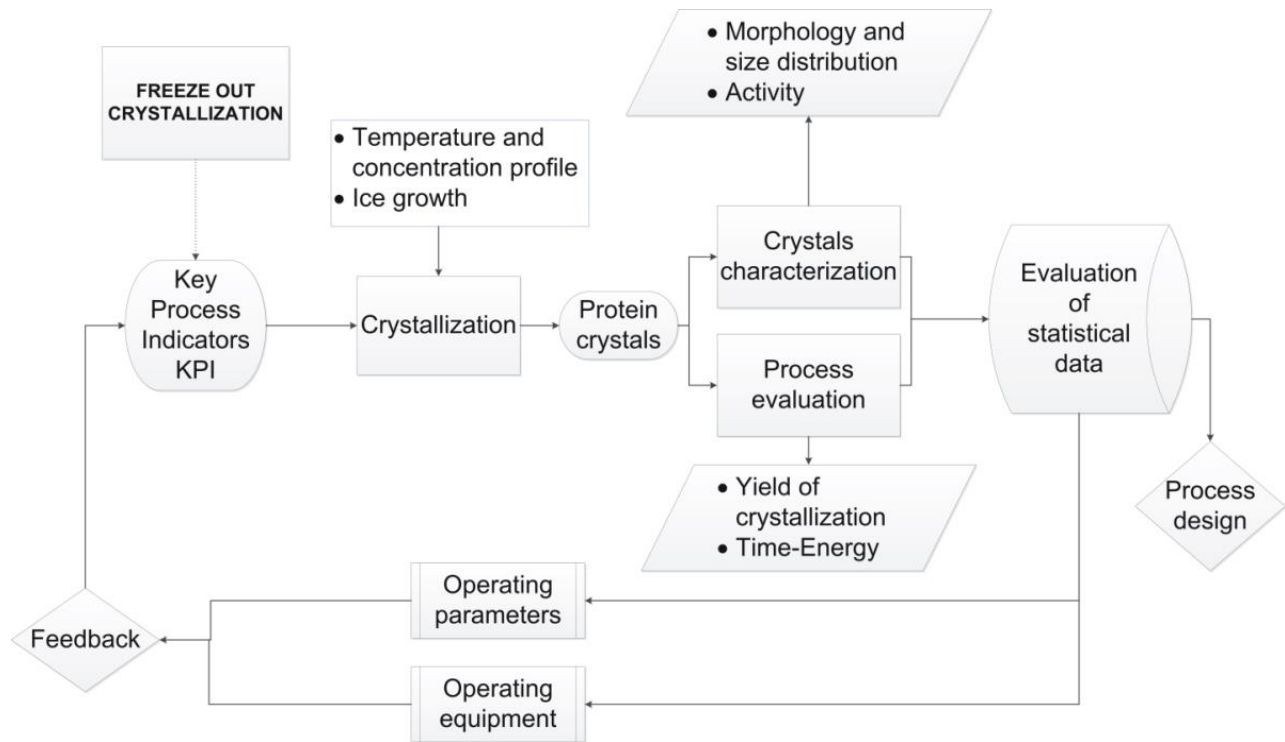


**Figure 4-5:** Optimization flow chart for the solvent freeze out protein crystallization technology [Dia10b].

In this general way the strategy consisted of the operation of a number of SFO crystallization processes with a systematic variation of the parameters values (factors). The process responses were analyzed with respect to these variations. The software STATISTICA [Sta02] was used to design the experiments (DOE e.g. [Haa89]) and to extract the relevant information such as magnitude of effects. Even although the Key Process Indicators -KPI are as the name says it, the key parameters of the process, several other parameters are interacting in a crystallization process (see chapter 2.1.2). These are the geometry arrangement of the device or the presence of agitation, within others. With the aim to identify the parameters to be included with more detailed in the advanced optimization strategy small design of experiments were initially carried out. Based on the preliminary results an advanced optimization strategy was carried out in two stages. In the first one, a fractional factorial design  $2^k$  (8-4) with two center points was accomplished in 18 runs. The lists of evaluated factors and responses are shown in Table 4-2.

**Table 4-2:** Factors and process responses evaluated in the  $2^8(8-4)$  fractional factorial design.

Factors	Process Responses
Initial protein concentration, $C_p$ [mg/mL]	Mean size
Salt concentration, $C_s$ [wt. %]	
Final temperature of cooled surface, $T_{CF-FT}$ [°C]	Yield of crystallization, [%]
Cooling rate of cooled surface, $dT/dt$ [K/min]	
Temperature of the wall, $T_w$ [°C]*	Volume of Ice, $V_I$
Length of the cooled surface, $L_{CF}$ [cm]	
Stirring [rpm]	Protein loss in the ice layer, [%]
Time at constant temperature, $t_{CF-CT}$ [min]	

In the second stage of the strategy a central composite design was carried out in 16 runs in order to find optimal values for the most influence parameters. Furthermore, this information was used to generate surface responses for the variable yield. This strategy has also been carried out by other researchers in the optimization of their products or processes, e.g. [And96, Yan95].

#### 4.5.1 Fractional Factorial Design

The first step of the advanced strategy was the implementation of a fractional factorial design  $2^8(8-4)$  with two center points. This design was carried with the aim to rule out the factors that had no significant impact on the different responses. The factors evaluated in all of the runs are shown in the columns on the Table 4-3. The combinations of the factors for each of the 18 runs are expressed by levels in the lines of the Table 4-3.

**Table 4-3:** Run numbers and level of the 8 factors in the fractional factorial design  $2^8(8-4)$ , 2 center points.

Run	$t_{CF-CT}$	$T_w$	$dT/dt$	$C_p$	Stirring	$C_s$	$L_{CF}$	$T_{FT-CF}$
1	-1	-1	-1	-1	-1	-1	-1	-1
2	1	-1	-1	-1	-1	1	1	1
3	-1	1	-1	-1	1	-1	1	1
4	1	1	-1	-1	1	1	-1	-1
5	-1	-1	1	-1	1	1	1	-1
6	1	-1	1	-1	1	-1	-1	1
7	-1	1	1	-1	-1	1	-1	1
8	1	1	1	-1	-1	-1	1	-1
9	-1	-1	-1	1	1	1	-1	1
10	1	-1	-1	1	1	-1	1	-1
11	-1	1	-1	1	-1	1	1	-1
12	1	1	-1	1	-1	-1	-1	1
13	-1	-1	1	1	-1	-1	1	1
14	1	-1	1	1	-1	1	-1	-1
15	-1	1	1	1	1	-1	-1	-1
16	1	1	1	1	1	1	1	1
17	0	0	0	0	0	0	0	0
18	0	0	0	0	0	0	0	0

There are three kinds of levels of the factors arranged in the different combinations through the number of runs: high level (1), center point (0) and low level (-1) (see values in Table 4-4).

**Table 4-4:** Values of low, center and high levels of factors in the fractional factorial design  $2^4$  (8-4).

$t_{CT-CF}$	-1	30.0 min	$T_W$	-1	274.0 K	$dT/dt$	-1	0.050 K/min	$C_P$	-1	10 mg/mL
	0	37.5 min		0	274.5 K		0	0.075 K/min		0	13 mg/mL
	1	45.0 min		1	275.0 K		1	0.100 K/min		1	16 mg/mL
Stirring	-1	0 rpm	$C_S$	--	3.0 %	$L_{CF}$	-1	10.5 cm	$T_{FT-CF}$	-1	266 K
	0	115 rpm		0	3.5 %		0	11.8 cm		0	267 K
	1	230 rpm		1	4.0 %		1	14.0 cm		1	268 K

The relevant factors influencing the response were identified as those with the highest effect on the response and were picked out to be analyzed in a center composite.

#### 4.5.2 Central Composite Design

In the second stage, a central composite design  $2^4$  (3) with 8 center points, was carried out in order to generate the response surface maps. The evaluated factors were stirring, final temperature of the cooled surface ( $T_{CF}$ ) and the duration of the cooled surface at constant temperature ( $t_{CF-CT}$ ). The effects of the independent variables on the responses yield, volume of ice and protein loss, were considered. The central composite design consisted of 16 runs, with 2 center points in the cube and star portions of the design, 8 cube points and 6 star points. The alphas for orthogonality and rotatability displayed by the program (STATISTICA) were 1.7638 and 1.6818, respectively. The course of the experiments with different combinations of the factors' levels is shown in Table 4-5.

**Table 4-5:** Course of the runs in the central composite design  $2^4$  (3) with 8 center points.

Run	Stirring	$T_{CF}$	$t_{CF-CT}$
1	-1	-1	-1
2	-1	-1	1
3	-1	1	-1
4	-1	1	1
5	1	-1	-1
6	1	-1	1
7	1	1	-1
8	1	1	1
9 C	0	0	0
10	-1.76	0	0
11	1.76	0	0
12	0	-1.76	0
13	0	1.76	0
14	0	0	-1.76
15	0	0	1.76
16 C	0	0	0

Five different levels can be recognized in the Table 4-5, these correspond to the values of the high, low, star and center points. The values of the factors corresponding to each level are shown in Table 4-6.

**Table 4-6:** Values of star, low, center and high levels of factors in the fractional factorial design  $2^4$  (8-4).

Stirring	-1.76	70 rpm	$T_{CF}$	-1.76	265 K	$t_{CT-CF}$	-1.76	24.3 min
	-1	110 rpm		-1	266 K		-1	30 min
	0	150 rpm		0	267 K		0	37.5 min
	1	190 rpm		1	268 K		1	45 min
	1.76	230 rpm		1.76	269 K		1.76	50.7 min

## 5. Results

In agreement to the section of materials and methods, the results of this work are presented by three approaches, which are:

- determination of the conditions for the formation of the crystals,
- reproduction of these conditions in the SFO, and
- optimization of the crystallization by this method.

### 5.1 Determination of Solubility Curves of Lysozyme

Since the solubility or equilibrium data of a system corresponds to the fixed limit of the metastable zone, it is the first approach to the knowledge of the crystallization conditions because this phenomenon only takes place in supersaturated conditions (see chapter 4.2). The knowledge of solubility or equilibrium data in the range of the operation temperatures of the solvent freeze out (between 266 and 277 K) is of relevant importance for the calculation of the supersaturation. Therefore, the transformed van't Hoff equation (Eq. 4.3) has been used to calculate the solubility of lysozyme at the operating conditions of the SFO and with concentrations of 3, 4 and 6 wt. % of NaCl. The different enthalpy data corresponding to the crystallization of lysozyme are obtained from literature [Sha96]. These values are reported in Table 5-1.

**Table 5-1:** Enthalpy data for experimental conditions of solvent freeze out. Lysozyme systems [Sha96].

Experimental condition	Enthalpy $\Delta H$ (kcal/mol)	Enthalpy $\Delta H$ (J/mol)
3 % wt NaCl pH=4.4	12.5	52250
4 % wt NaCl pH=4.4	14.8	61864
6 % wt NaCl pH=4.4	15.5	64790

The application of the transformed van't Hoff equation can be interpreted as an extrapolation of the solubility data at higher temperatures [For99] to raise awareness of the data at low temperatures. The obtained solubility data for lysozyme systems with a pH value of 4.4 and contents of 3, 4 and 6 wt. % of NaCl are shown in Table 5-2.

**Table 5-2:** Solubility data for experimental conditions of solvent freeze out. Lysozyme systems at pH 4.4 [For99].

Experimental condition	Solubility $C_{eq}$ (mg/mL)	Temperature (K)
3 % wt NaCl pH=4.4	2.20	283.75
4 % wt NaCl pH=4.4	1.24	278.25
6 % wt NaCl pH=4.4	0.71	283.75

The solubility data for the lower temperature ranges have, therefore, been estimated by replacing the enthalpy values (Table 5-1) and equilibrium data (Table 5-2) in the transformed

van't Hoff equation (Eq. 4.3) as described in chapter 4.2.1. The results of the solubility curves of lysozyme with 3, 4 and 6 wt. % of NaCl, in the range of temperature between 266 and 277 K and pH value of 4.4, are presented in Figure 5-1.

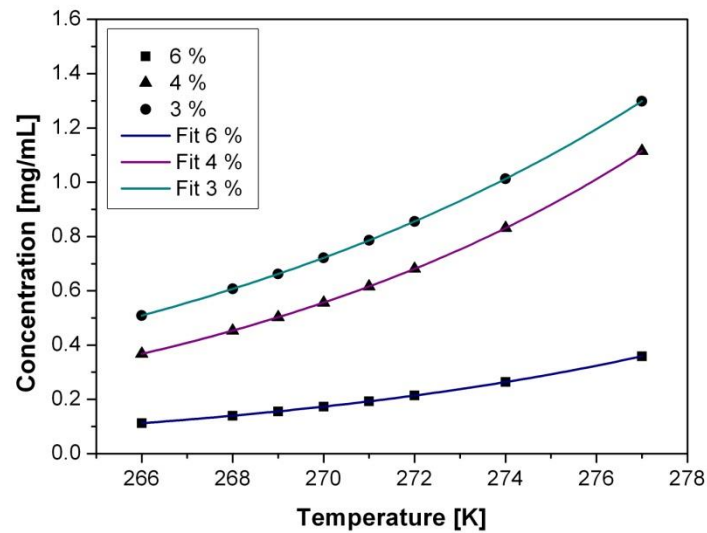


**Figure 5-1:** Solubility curves of lysozyme and 3, 4 and 6 wt. % NaCl in sodium acetate buffer at pH 4.4. Data obtained from extrapolation of literature values [For99].

The solubility data for pH value of 5.0 and salt concentrations of 3 and 4 %wt. are shown in Table 5-3.

**Table 5-3:** Solubility data for experimental conditions of solvent freeze out. Lysozyme systems at pH 5.0 [FOR99].

Experimental condition	Solubility $C_{eq}$ (mg/mL)	Temperature (K)
3 % wt NaCl pH=5.0	1.99	280.15
4 % wt NaCl pH=5.0	1.12	278.25
6 % wt NaCl pH=5.0	1.29	283.55

The results of the solubility curves for pH 5.0 are presented in Figure 5-2.

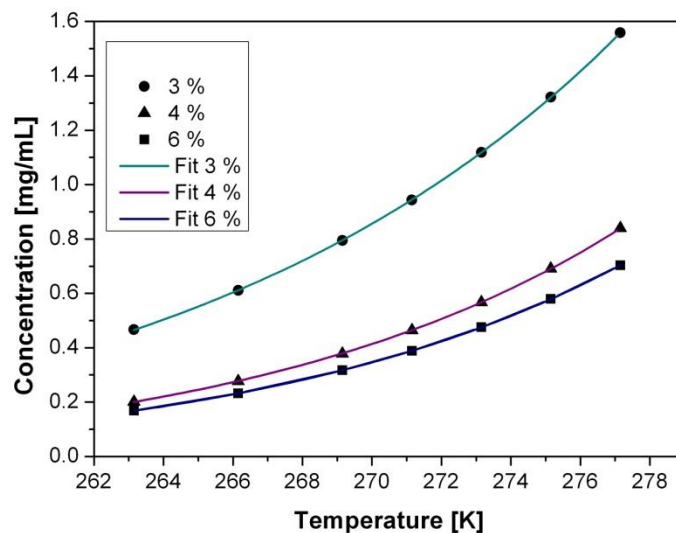


**Figure 5-2:** Solubility curves of lysozyme and 3, 4 and 6 wt. % NaCl in sodium acetate buffer at pH 5.0. Data obtained from extrapolation of literature values [For99].

From the diagrams presented in Figure 5-1 and Figure 5-2 it is possible to observe the increase of the solubility with increasing temperature and lower concentrations of salt.

Moreover, in these diagrams it is possible to observe that lysozyme presents a higher solubility at pH value of 5.0 than at pH value of 4.4 (for 3 and 4 % of NaCl).

## 5.2 Screening Test for Lysozyme Crystallization

In order to cover the whole range of conditions studied, several protein solutions were investigated. The complete imaging of the results is not shown in this work due to the extension but the information extracted from those is used in the following chapters.

The results from the screening tests described in chapter 4.2 were used for identification of the limits of the region under which formation of good quality lysozyme crystals takes place. This region is described by supersaturation values reported for pure lysozyme systems in the Table 5-4, Table 5-5 and Table 5-6 in the subchapter 5.2.1. Furthermore, this region is also represented in solubility diagrams accompanied with nucleation curves (pseudo-phase diagrams) in chapter 5.3, for pure lysozyme systems and lysozyme-ovalbumin systems.

### 5.2.1 Pure Lysozyme Solutions

The crystallization phenomenon has been investigated in micro-titer plates as described in the chapter 4.2.2.

The results presented in this chapter are mainly a sample of the complete results of the screening tests with duration time of 24 hours. Further detailed results from the screenings carried out in 24 hours as well as those performed in 5 hours are presented in more detail in a former work [Dua10].

Samples of the crystals obtained in the pure lysozyme solutions with a concentration of 12 mg/ml of lysozyme and 3 wt. % of salt (NaCl) are shown Figure 5-3.

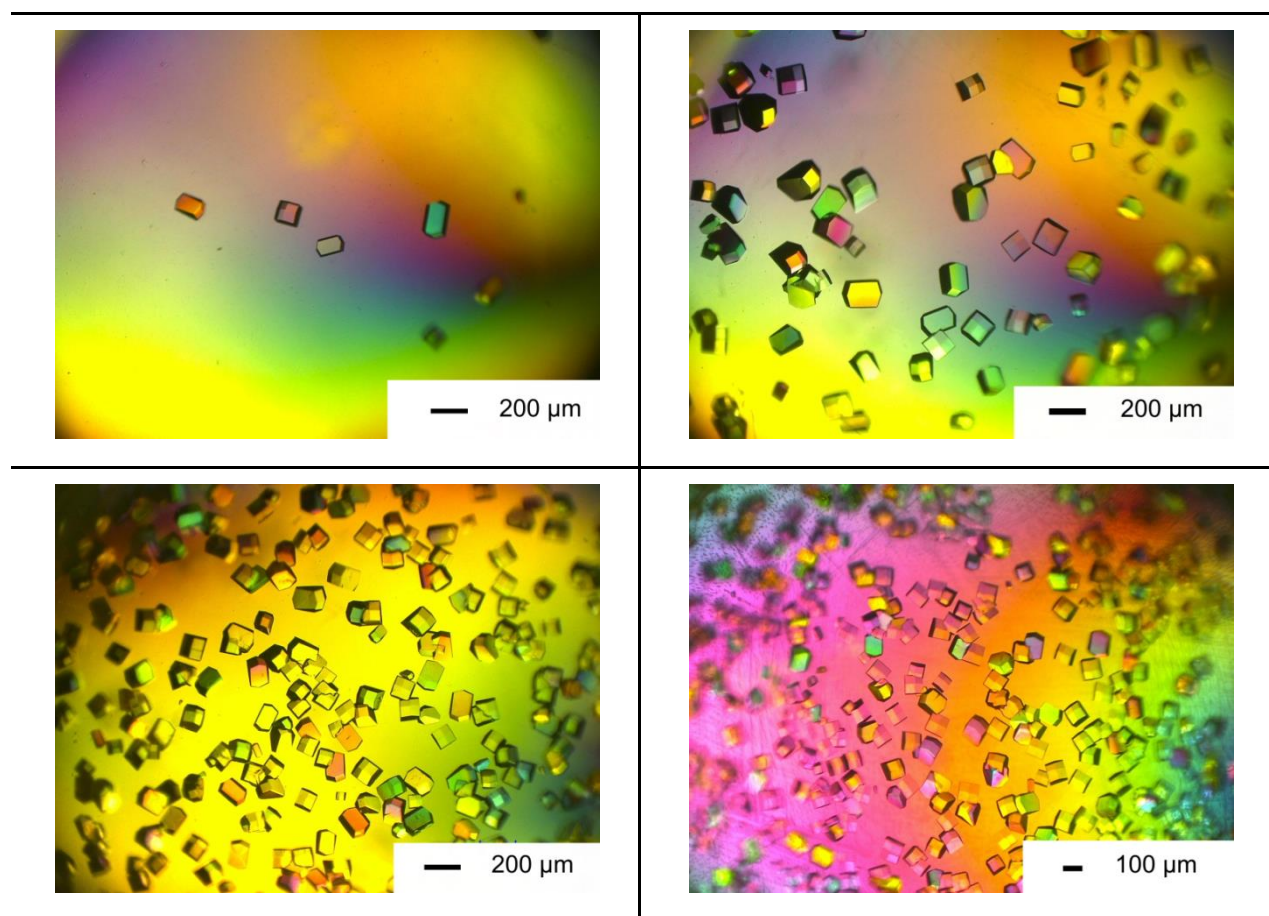


**Figure 5-3:** Lysozyme crystals obtained in micro-titer-plates according to screening tests. The initial composition of the solution was 12 mg/mL lysozyme and 3 wt. % NaCl. Top: 277 and 274 K. Bottom: 271 and 268 K.

The amounts of crystals seem to increase with decreasing operating temperature level. Independently of the temperatures, the crystals seem to grow up to similar sizes during the 24 hours of experimentation as it can be observed in Figure 5-3.

The supersaturation levels were calculated according to Eq. 4.4, by the use of the solubility data reported in the previous chapter and the initial conditions of the tested systems. The supersaturation values for the systems with 3 % wt are reported in Table 5-4.



As the crystals shown in Figure 5-3 present a good morphology and a good size distribution, it has been assumed that their production conditions belong to the region appropriate for crystal growth. In a similar way all the produced crystals were studied and the supersaturation conditions of the solutions were classified to belong to the region below of the solubility line (no crystals), above of the solubility line (crystals with good morphology) and close to the upper limit of the metastable region (crystals with irregular morphology or with heterogeneous size distribution). The location of the supersaturation values regarding to the quality of the crystals are respectively non-highlighted, highlighted in light blue (grey) or in dark blue (grey), for the three conditions mentioned above, in the Table 5-4, Table 5-5 and Table 5-6.

Therefore, values highlighted in light blue (grey) color correspond to the supersaturation values under which well shaped (tetragonal) lysozyme crystals were obtained, independently of the size or the amount, e.g. see crystals on Figure 5-3 (a) and supersaturation value of 9.24 in Table 5-4.

**Table 5-4:** Identification Zone I for 3 wt. % NaCl.

$C_{\text{PROT}}$	277 K	275 K	274 K	272 K	271 K	270 K	269 K	268 K	266 K
	$C_{\text{EQ}}=$	$C_{\text{EQ}}=$	$C_{\text{EQ}}=$	$C_{\text{EQ}}=$	$C_{\text{EQ}}=$	$C_{\text{EQ}}=$	$C_{\text{EQ}}=$	$C_{\text{EQ}}=$	$C_{\text{EQ}}=$
	1.30	1.10	1.01	0.86	0.79	0.72	0.66	0.61	0.51
2	1.54	1.82	1.97	2.34	2.54	2.77	3.02	3.30	3.93
3	2.31	2.72	2.96	3.51	3.82	4.16	4.53	4.95	5.90
4	3.08	3.63	3.95	4.67	5.09	5.54	6.05	6.60	7.87
5	3.85	4.54	4.94	5.84	6.36	6.93	7.56	8.24	9.83
6	4.62	5.45	5.92	7.01	7.63	8.32	9.07	9.89	11.80
7	5.39	6.36	6.91	8.18	8.91	9.70	10.58	11.54	13.76
8	6.16	7.27	7.90	9.35	10.2	11.09	12.09	13.19	15.73
9	6.93	8.17	8.88	10.52	11.4	12.48	13.60	14.84	17.70
10	7.70	9.08	9.87	11.68	12.7	13.86	15.11	16.49	19.66
11	8.47	9.99	10.86	12.85	14.0	15.25	16.62	18.14	21.63
12	9.24	10.90	11.85	14.02	15.3	16.63	18.14	19.79	23.60
13	10.01	11.81	12.83	15.19	16.5	18.02	19.65	21.43	25.56
15	11.55	13.62	14.81	17.53	19.1	20.79	22.67	24.73	29.49

The values marked with dark blue (grey) correspond to the supersaturation values of the solutions from which irregular crystals were formed or small crystals accompanied the bigger ones.

Lysozyme crystals formed within solutions with a composition of 12 mg/mL of lysozyme and 4 wt. % of NaCl are shown in Figure 5-4. These are samples of crystals obtained at 277, 274, 271 and 268 K from left to right.

It is possible to observe that the crystals obtained at 277 and 274 K have a good tetragonal morphology and sizes around 200  $\mu\text{m}$ . Therefore it is considered that the production conditions belong to the region for crystal growth.

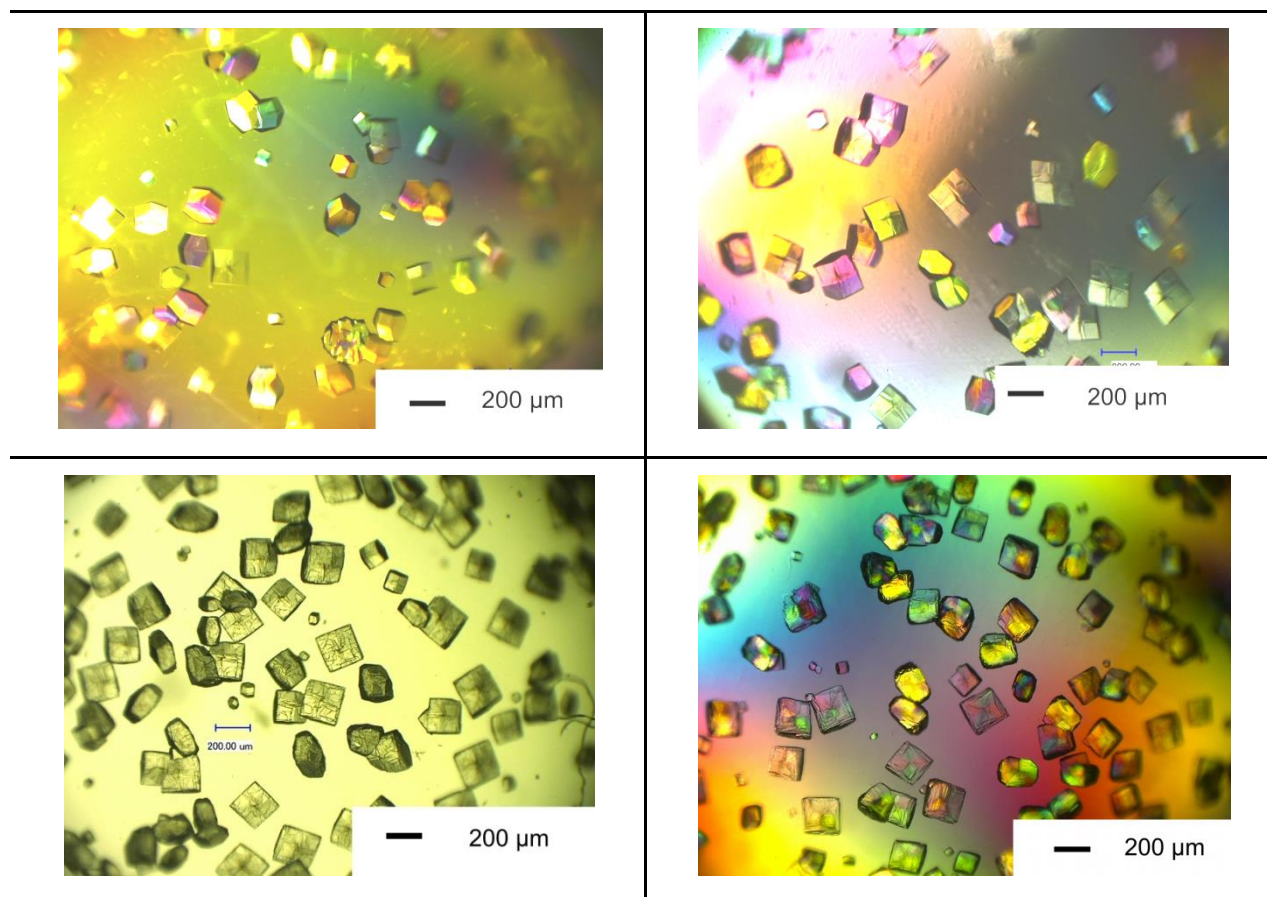


**Figure 5-4:** Lysozyme crystals obtained in micro-titter-plates according to screening tests. The initial composition of the solution corresponds to 12 mg/mL lysozyme and 4 wt. % NaCl. Top: 277 and 274 K. Bottom: 271 and 268 K.

The crystals obtained at 271 and 268 have slight irregularities in the tetragonal shape and crystals with sizes of around 200  $\mu\text{m}$  are accompanied of tiny crystals of around 20-50  $\mu\text{m}$ . Therefore it is assume that those crystals were obtained under conditions which belong to the vicinity of the upper limit of the metastable region, their corresponding supersaturation values should be marked in dark blue (grey) as following.

The supersaturation values corresponding to the studied solutions and determined by the temperature, lysozyme and salt concentrations of 4 % wt of NaCl are listed in Table 5-5. As in the case of 3 % wt NaCl (Table 5-4), the values highlighted in light blue (grey) and dark blue (grey) color correspond to values which led to well formed lysozyme crystals or crystals with varied size distributions, respectively.

**Table 5-5:** Identification Zone I for 4 wt. % NaCl.

$C_{\text{PROT}}$	Supersaturation								
	277K	275 K	274 K	272 K	271 K	270 K	269 K	268 K	266 K
	$C_{\text{EQ}}=$ 0.92	$C_{\text{EQ}}=$ 0.83	$C_{\text{EQ}}=$ 0.68	$C_{\text{EQ}}=$ 0.62	$C_{\text{EQ}}=$ 0.62	$C_{\text{EQ}}=$ 0.56	$C_{\text{EQ}}=$ 0.50	$C_{\text{EQ}}=$ 0.45	$C_{\text{EQ}}=$ 0.37
2	1.79	2.18	2.41	2.94	3.25	3.60	3.98	4.42	5.44
3	2.69	3.27	3.61	4.41	4.87	5.39	5.98	6.62	8.16
4	3.59	4.36	4.81	5.87	6.50	7.19	7.97	8.83	10.88
5	4.48	5.45	6.02	7.34	8.12	8.99	9.96	11.04	13.60
6	5.38	6.54	7.22	8.81	9.75	10.79	11.95	13.25	16.32
7	6.28	7.63	8.42	10.28	11.37	12.59	13.94	15.46	19.04
8	7.17	8.72	9.62	11.75	12.99	14.38	15.93	17.66	21.76
9	8.07	9.81	10.83	13.22	14.62	16.18	17.93	19.87	24.48
10	8.97	10.90	12.03	14.69	16.24	17.98	19.92	22.08	27.20
11	9.86	11.99	13.23	16.15	17.87	19.78	21.91	24.29	29.92
12	10.76	13.08	14.44	17.62	19.49	21.58	23.90	26.50	32.64

In the screening tests for crystallization of lysozyme, the salt concentration of 6 wt. % was also taken into account, even although the aim has been the use of low amounts of salt in future applications of the solvent freeze out.

Samples of those produced lysozyme crystals are shown in the pictures of Figure 5-5. The concentration of lysozyme has been 12 mg/mL and the tested temperatures were 277, 274, 271 and 268 K, in order to compare the quality of the crystals with the other amounts of salt 3% and 4% (results shown earlier).

The quality of the crystals in terms of morphology is decreased with the increasing amount of salt as it can be observed in Figure 5-5. Moreover, the crystals described an almost unrecognizable tetragonal shape, some of them present a size of about 200  $\mu\text{m}$  and some a size lower than 100  $\mu\text{m}$ . Moreover, there is a significant presence of sea urchin or espherulites.

This is observed for the crystals formed in the solutions with a composition of 12 mg/mL already at 275 K. The presence of irregular crystals and sea urchin or espherulites is observed for the solutions for which the supersaturation values are remarked with dark blue (grey) color in Table 5-6.

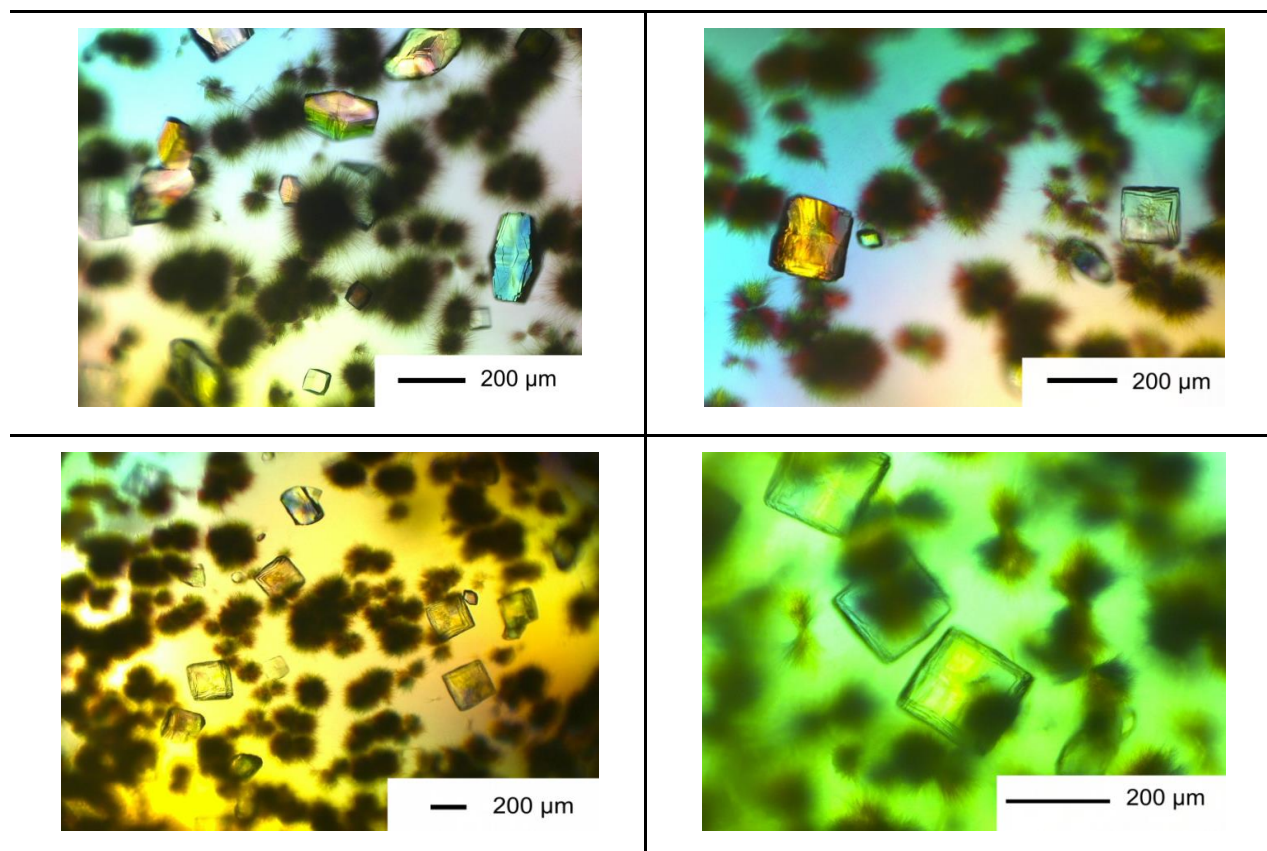


**Figure 5-5:** Lysozyme crystals obtained in micro-titter-plates according to screening tests. The initial composition of the solution corresponds to 12 mg/mL lysozyme and 6 wt. % NaCl. Top: 277 and 274 K. Bottom: 271 and 268 K.

It can be observed that the region (dark blue or grey color) unsuitable for formation of regular and good quality tetragonal crystals is dominating in Table 5-6 in comparison to the supersaturation values that lead to regular crystals (marked with light blue or grey color).

**Table 5-6:** Identification Zone I for 6 wt. % NaCl.

$C_{\text{PROT}}$	277 K	275 K	274 K	272 K	271 K	270 K	269 K	268 K	266 K
	$C_{\text{EQ}}$	$C_{\text{EQ}}$	$C_{\text{EQ}}$	$C_{\text{EQ}}$	$C_{\text{EQ}}$	$C_{\text{EQ}}$	$C_{\text{EQ}}$	$C_{\text{EQ}}$	$C_{\text{EQ}}$
	0.369	0.301	0.271	0.220	0.198	0.178	0.160	0.144	0.115
2	5.42	6.65	7.37	9.08	10.09	11.23	12.50	13.92	17.32
3	8.13	9.97	11.05	13.62	15.14	16.84	18.74	20.88	25.98
4	10.84	13.29	14.74	18.16	20.19	22.45	24.99	27.84	34.64
5	13.54	16.62	18.42	22.70	25.23	28.07	31.24	34.80	43.30
6	16.25	19.94	22.11	27.24	30.28	33.68	37.49	41.76	51.96
7	18.96	23.26	25.79	31.79	35.33	39.29	43.74	48.72	60.61
8	21.67	26.58	29.48	36.33	40.37	44.90	49.98	55.68	69.27
9	24.38	29.91	33.16	40.87	45.42	50.52	56.23	62.64	77.93
10	27.09	33.23	36.85	45.41	50.47	56.13	62.48	69.60	86.59
11	29.80	36.55	40.53	49.95	55.51	61.74	68.73	76.56	95.25
12	32.51	39.88	44.22	54.49	60.56	67.36	74.98	83.53	103.91



Within the experimental conditions of the screening tests, the supersaturation values appropriated for formation and growth of lysozyme tetragonal crystals is larger when 3 wt. % of NaCl is applied. This region is smaller in the case in which 4 % of NaCl is used and even smaller for the use of 6 % NaCl.

In order to compare the morphology of the lysozyme crystals produced at different salt compositions, images of crystals produced in solutions with similar lysozyme composition and temperature level are presented in Figure 5-6.

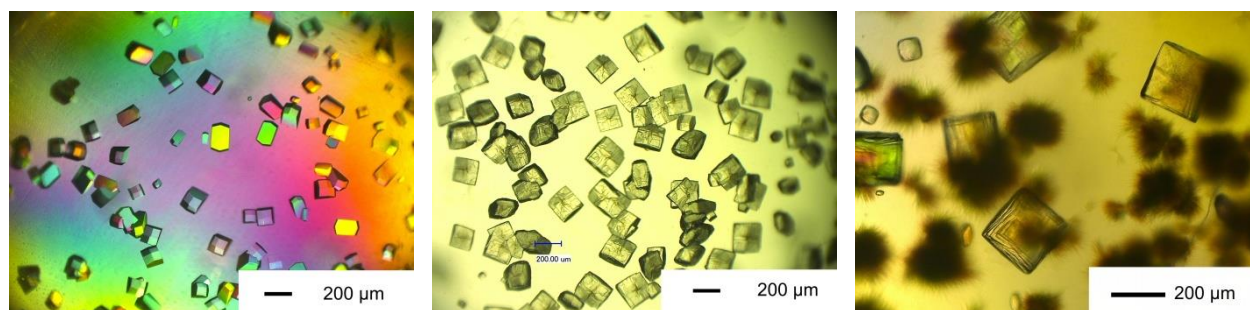


**Figure 5-6:** Lysozyme crystals from pure lysozyme solutions with 12 mg/mL of lysozyme, micro-titter plate at 272 K during 24 h. 3% NaCl (left), 4 % NaCl (middle) and 6 % NaCl (right).

It is possible to observe in Figure 5-6 that the quality of the crystals is decreased when the concentration of salt (NaCl) is increased.

Crystal growth observations have been carried out during 5 hours as described and sketched on Figure 4-3. Several protein systems were investigated such as those with salt concentrations of 3 and 4 % of NaCl, lysozyme concentrations of 2 to 15 mg/mL and temperature of 266, 268, 269, 270, 274 and 277 K.

Due to the large amount of images it is not possible to report the complete package of observations in this work, but only some examples are shown below. Samples of the images taken at different times of the protein solutions contained in the cell and the eventually grown crystals are shown in Figure 5-7. The tested conditions correspond to crystals formed within solutions at 277 K, with a content of 4 and 3 wt. % of NaCl and lysozyme concentrations of 10, 12 and 15 mg/mL.

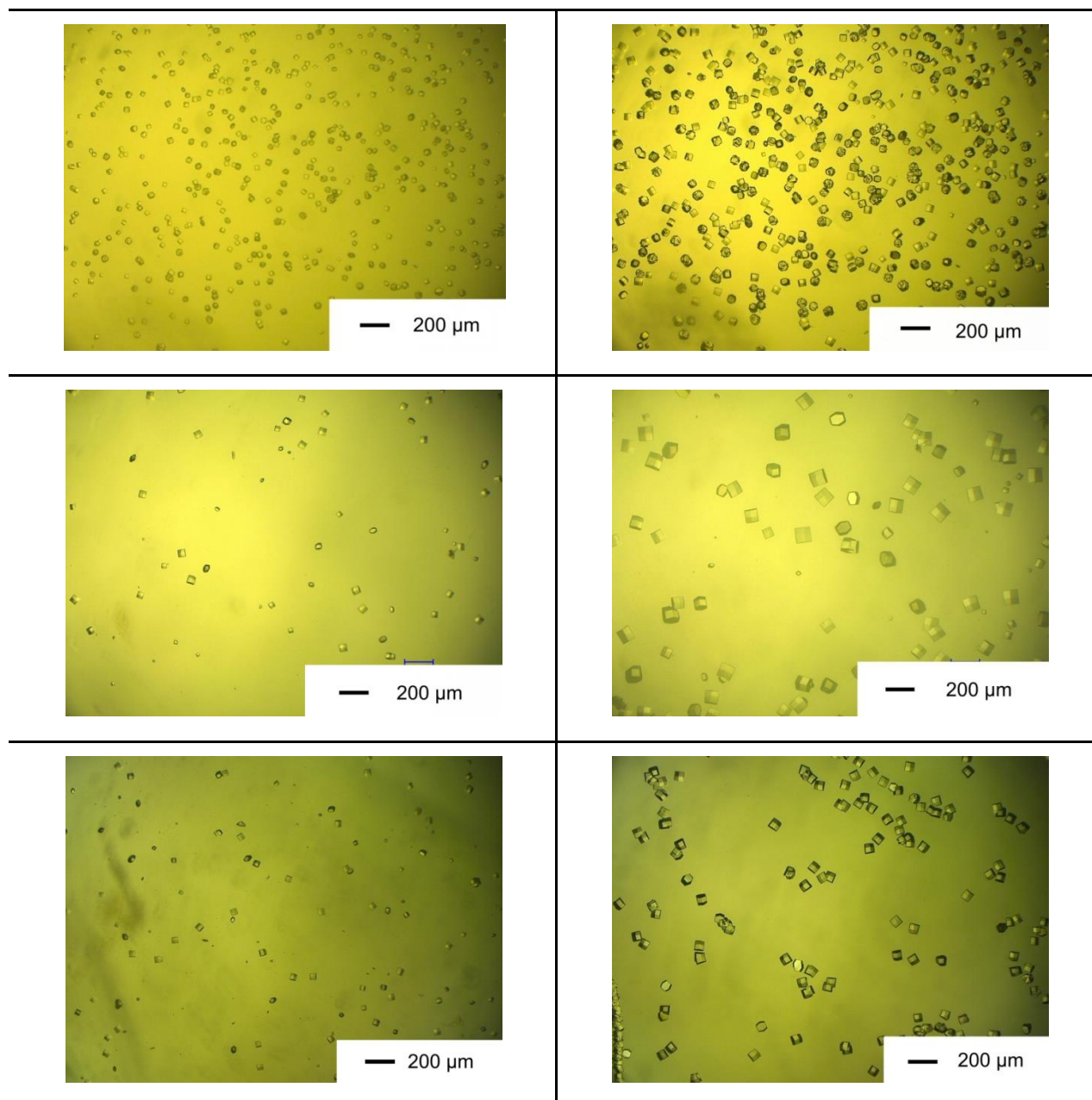


**Figure 5-7:** Lysozyme crystallization in cell. Top: 10 mg/mL of lysozyme and 4 wt. % NaCl, 150 min (left) and 300 min (right). Middle: 12 mg/mL of lysozyme and 4 wt. % NaCl, 105 min (left) and 300 min (right). Bottom: 15 mg/mL of lysozyme and 3 wt. % NaCl, 140 min (left) and 300 min (right).

In the solutions shown in the first lines, the concentration of salt was the same 4 %, but the concentration of lysozyme was 10 mg/mL in the first line and 12 mg/mL in the second one. The solution shown in the third line presented a concentration of 3 % of NaCl and 15 mg/mL of lysozyme.

In general, the first visible crystals were detected after the 15<sup>th</sup> and 20<sup>th</sup> minute for higher protein concentrations. Pictures of crystals after about 100 min are shown in the left column of

Figure 5-7. The size of the crystals was approximately 50  $\mu\text{m}$ , which increased to about 100  $\mu\text{m}$  or more after around 200 min, as it can be observed in the right column of Figure 5-7.

As the initial supersaturation and the actual temperature of the system are known, the appropriated conditions for the formation and growth of the crystals could be known as well. These conditions are recorded not just for the systems showed above, but also for all tested systems. This information has been used for the location of the conditions for ideal growth of the crystals in the pseudo-phase diagrams presented in the following chapter (5.3.1).

### 5.2.2 Lysozyme Ovalbumin Mixtures

Several crystallization screenings for lysozyme from lysozyme-ovalbumin mixtures have been done according to the description on chapter 4.3.2.

Samples of the results from the experiments carried out at 271, 269 and 266 K and with 4 wt. % are shown in Figure 5-8. In these pictures it is possible to observe the different morphologies of the crystals produced at pH values of 4.4 and 5.0. It is possible to observe that the crystals produce at pH 5.0 had better defined edges and homogeneous shapes. While for the crystals formed at pH 4.4 presented more rounded edges and diverse morphologies.

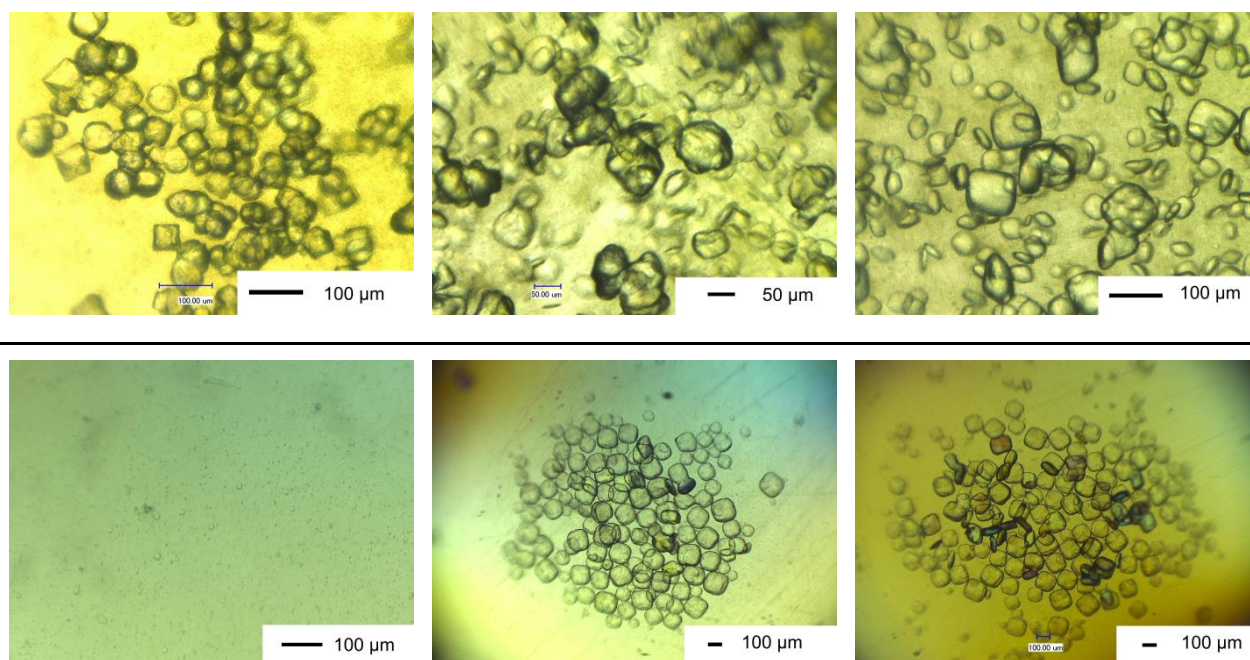


**Figure 5-8:** Lysozyme crystals from lysozyme-ovalbumin mixture (11 mg/mL of lysozyme, 2 mg/mL ovalbumin and 4 wt. % NaCl). Top: pH 4.4, 271 K (left), 269 K (middle) and 266 K (right). Bottom: pH 5.0, 271 K (left), 269 K (middle) and 266 K (right).



The crystals produced at a pH value of 4.4 have grown to around 50  $\mu\text{m}$  at 271 K, while the crystals produced at pH value of 5.0 are hardly visible at the same temperature. The quality of the crystals seems to get worse with decreasing temperature when the pH is 4.4. The crystals reached a maximal size of approx. 100  $\mu\text{m}$  under both conditions of pH 4.4 and 5.0.

Crystals obtained by the use of 3 wt. % of salt (NaCl) are shown in Figure 5-9, on the left at pH 4.4 and on the right at pH 5.0.

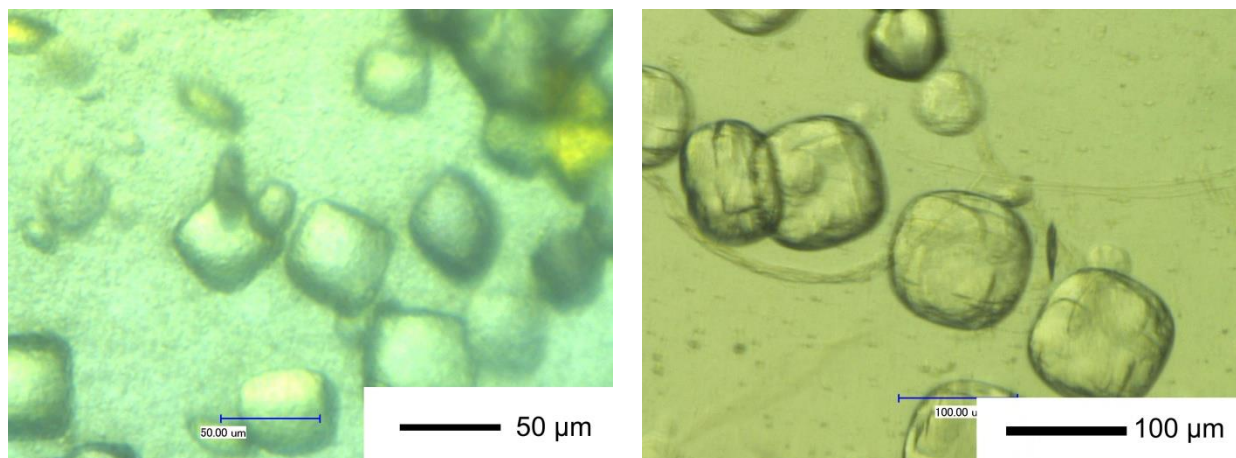


**Figure 5-9:** Lysozyme crystals from lysozyme-ovalbumin mixture (11 mg/mL of lysozyme, 2 mg/mL ovalbumin and 3% NaCl. Left: pH: 4.4 and Right: pH 5.0.

In Figure 5-9 it is possible to observe that the crystals produced with a pH of 5.0 had larger sizes than those produced at pH 4.4. Unlike the crystals produced with a salt concentration of 3 wt. %, those crystals presented similar sizes for both pH values.

In a similar way as it has been done for the screening tests analysis of the pure lysozyme solutions, the observations of the crystallizations of lysozyme from the ovalbumin-lysozyme mixtures were used for the location of the ideal crystal growth region within the phase diagram.

### 5.3 Pseudo-phase Diagrams: Solubility and Nucleation

Information obtained from the experiments give the starting parameters of the process for protein crystallization, especially, when the phase diagram of the protein is known. The availability of a phase diagram is important in order to develop a crystallization process. Phase diagrams provide vital data on the possible phases crystallizing and the number of variables that may be utilized to control the process [Dav00].

The collected information from the screening tests (chapter 4.2) was used for the construction of the pseudo-phase diagrams. The observations of the protein solutions and solids formed after the micro batch crystallizations were classified qualitatively into different groups. These



three groups are described in Table 5-7, and they represent the regions that belong to a pseudo-phase diagram.

**Table 5-7:** Classification of obtained crystals into regions of the pseudo-phase diagram.

Set of conditions: Temperature, protein concentration and salt concentration		
Lower limit of the metastable region	Within metastable region	Upper limit of the metastable region
No visible crystals at low protein concentration	Well shaped crystals	Irregular shaped crystals Sea Urchin [Mus97] Large crystals accompanied with small ones

Furthermore, regarding to the group characteristics it was assumed that the initial conditions of the solution (T, C<sub>pr</sub>) belong to the respective zone of the generic protein phase diagram (Figure 4-2).

The conditions, under which the wanted crystal quality was produced, were located within the pseudo-phase diagrams presented in the following chapters. This has been possible since the temperature and concentration were measured when the first crystal or crystals were observed under a microscope observation.

### 5.3.1 Lysozyme in Pure Solutions

The pseudo-phase diagrams for pure lysozyme solutions with a pH value of 4.4 are shown in the figures below. The crystallization of lysozyme from pure solutions was only investigated at the pH value of 4.4, because it has been reported as optimal parameter in the former work [Ryu10a]. Therefore, the influence of the pH on crystallization has not been neglected, but its influence on the crystallization of lysozyme has not been considered in the screening tests of pure solutions.

The pseudo-phase diagram for a lysozyme system in sodium acetate buffer, pH 4.4 and with a salt concentration of 3 wt. % is shown in Figure 5-10. The source data for the construction of this diagram has been presented in Table 5-4.

A concentration of salt of 3 wt. % has been chosen not just with the aim of reducing as much as possible the amount of salt, but also because the crystals obtained by the use of this amount described well shaped forms and larger sizes in the screening tests (see Figure 5-3). The possibility of using a small amount of salt and at the same time of getting good crystals quality, is of important value for the translation of this conditions in a step forward such as the SFO (Solvent Freeze Out process).

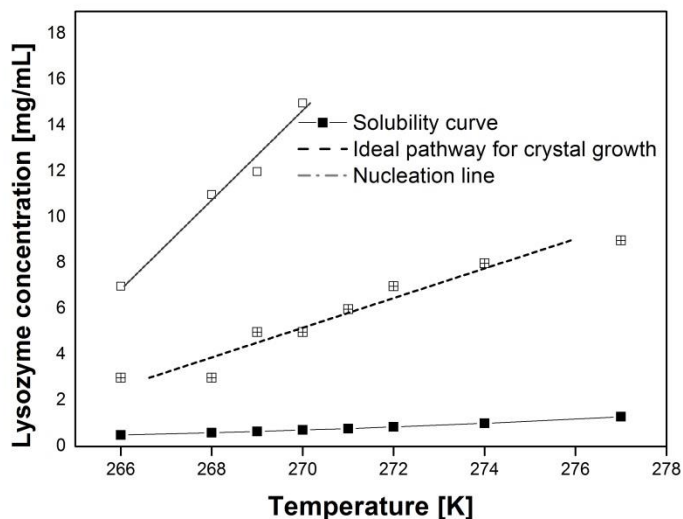


**Figure 5-10:** Pseudo-phase diagram for lysozyme in sodium acetate buffer pH 4.4 and 3 wt. % NaCl.

The values of protein concentrations investigated were between 2 and 15 mg/mL. The formation of lysozyme crystals (first visible threshold) was observed already at 277 K for the solutions with a concentration of 15 mg/mL. The nucleation points were linear fitted to represent the upper limit of the metastable zone, which once overcome would lead to the formation of new nuclei and consequently crystals of small mean size.

The ideal pathway for crystal growth is also obtained by fitting the points in which well shaped crystals were observed with regular size distributions (qualitatively).

Based on the data presented in Table 5-5, the pseudo-phase diagram for a lysozyme system pH of 4.4 with a salt concentration of 4 wt. % has been build and it is shown in Figure 5-11.

In this case the supersaturation value suitable for the formation of well shaped crystals was passed already at temperatures lower than 274 K with a concentration of 12 mg/mL. Therefore, higher concentrations of lysozyme have not been studied and presented in the pseudo-phase diagram since the range of temperature in the SFO is demanded to be between 277 and 266 K. In this case the control of the process would become difficult since the width of the metastable zone is decreased when the temperature is decreased, by increasing salt concentration from 3 to 4%. It can be observed in Figure 5-4 that at 271 and 268K the large crystals were already accompanied by smaller crystals and that the quality (shape) of the crystals was deteriorated.

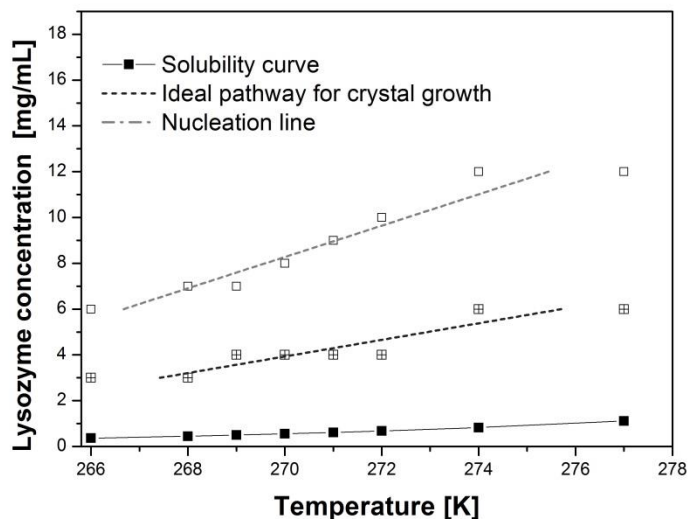


**Figure 5-11:** Pseudo-phase diagram for lysozyme in sodium acetate buffer pH 4.4 and 4 wt. % NaCl.

The pseudo-phase diagram built for the lysozyme system in sodium acetate buffer, pH 4.4 and with a salt concentration of 6 wt. % is shown in Figure 5-12. The original data on which this phase diagram was obtained can be found in Table 5-6.

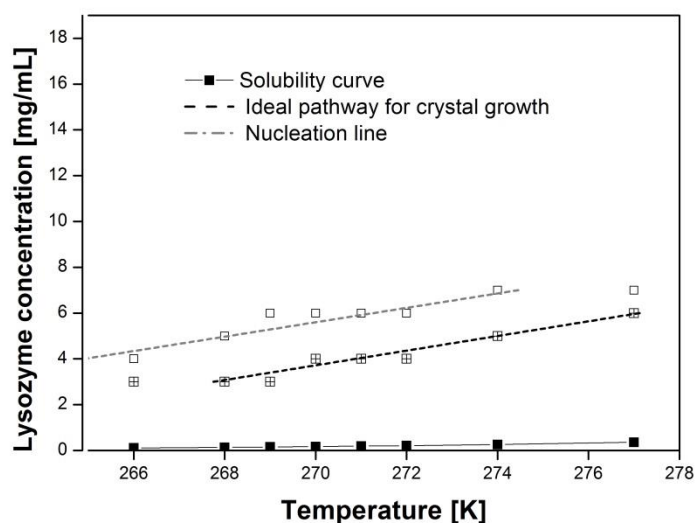


**Figure 5-12:** Pseudo-phase diagram for lysozyme in sodium acetate buffer pH 4.4 and 6 wt. % NaCl.

In this system, the narrowing of the metastable zone by the use of higher amounts of salt was even more evident. The possibility of applying concentrations of protein higher than 7 mg/mL could not be considered without decreasing the quality of the lysozyme crystals and without

avoiding the presence of new nucleation or irregular solids. These details can be observed in the pictures of the crystals obtained at 277, 274, 271 and 268 K with just 12 mg/mL of lysozyme.

Running a further SFO experiment with this pseudo-phase diagram as guide and applying a concentration of 6 wt. % of NaCl would be very difficult for the control of the process since the ideal pathway for crystal growth is too close to the limit of the zone I, or metastable zone.

Until this point the nucleation and solubility points were fitted in linear curves due to the relative small range of temperature investigated in the screening tests. Therefore, it has been desired to amplify the range of temperature and lysozyme concentrations in order to improve the analyses the phase diagrams. The nucleation data determined in the screening tests were coupled with the nucleation data obtained by the turbidity method as described in chapter 4.2.3. The coupled data was then fitted into a curve which would be interpreted as the nucleation curve and is represented in the pseudo-phase diagrams in Figure 5-13 (3% NaCl) and Figure 5-14 (4% NaCl). The salt concentration of 6 wt. % was not taken into account for the construction of these phase diagrams due to the poor performance described in the production of the crystals.

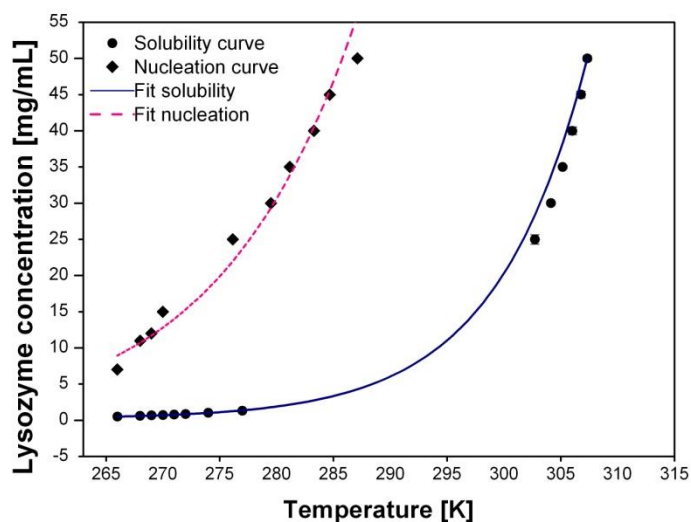


**Figure 5-13:** Pseudo-phase diagram for lysozyme in sodium acetate buffer pH 4.4 and 3 % NaCl. Coupling of solubility data obtained from literature [For99] (266 to 277 K) and turbidity tests (>277 K). Nucleation data obtained from screening tests (266 to 277 K) and turbidity tests (>277 K).

The pseudo-phase diagram shown in Figure 5-13 offers information on solubility and nucleation data for 3 wt. % of NaCl in a broader range of temperature as in the diagram shown in Figure 5-10. There is a good fit of the solubility data obtained by extrapolation of literature data and

those collected from the turbidity measurements. In a similar manner, the nucleation points observed during the screening tests could be fitted with those from the turbidity measurements in a single nucleation curve.

In regard to the pseudo-phase diagram corresponding to the 4 wt. % of NaCl, the solubility and nucleation curves are also well fitted by the coupling of the data obtained from literature, turbidity measurements and screening tests (Figure 5-14).

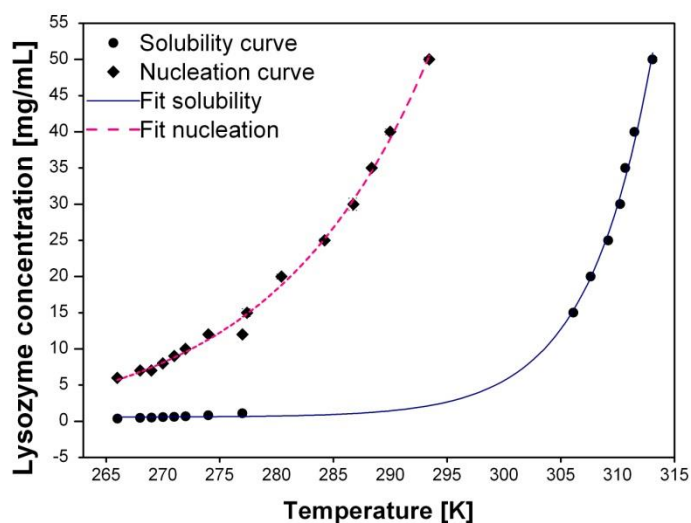


**Figure 5-14:** Pseudo-phase diagram for lysozyme in sodium acetate buffer pH 4.4 and 4 % NaCl. Coupling of solubility data obtained from literature (266 to 277 K) and turbidity tests (>277 K). Nucleation data obtained from screening tests (266 to 277 K) and turbidity tests (>277 K).

As mentioned in chapters above, the metastable zone described by the lower (solubility curve) and upper limits (nucleation curve) seems to be narrowed by the use of higher amounts of salts and by decreasing temperatures. This phenomenon can be better observed if Figure 5-13 and Figure 5-14 are compared.

These two diagrams present significant advantages for the control of the crystallization process, regarding to range of temperature, since the crystallization processes can start at standard room temperatures. This would offer the possibility of controlling the process from very early stages, such as preparation and mixing the protein solutions.

### 5.3.2 Lysozyme-Ovalbumin Mixture

The regions for crystallization were described in diagrams based on the information acquired from the screening tests. The quality of the crystals, regarding to the morphology, was better

when they were produced in pH values of 5.0. Therefore, the pseudo-phase diagrams were created for systems with 3 and 4 wt. % NaCl in sodium acetate buffer with pH 5.0

Only when crystals had regular shape and large sizes ( $> 10 \mu\text{m}$ ), were the conditions (T, C) of the wells located in the pseudo-phase diagrams (Figure 5-15 and Figure 5-16). These diagrams are named pseudo-phase diagrams since only the solubility curve represents a thermodynamic equilibrium. The located crystallization conditions are influenced by thermodynamics and by the kinetics of the process, and they are bind to the history of the crystallization process.

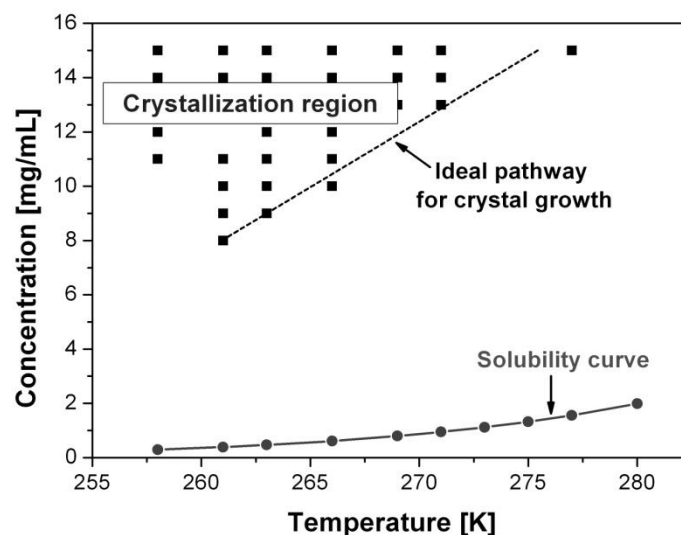


**Figure 5-15:** Pseudo-phase diagram for lysozyme in sodium acetate buffer pH 5.0, 3 wt. % NaCl and 2 mg/mL of ovalbumin.

From approximately 275 K well shape crystals were already obtained and the good quality was enhanced also when the temperatures were decreased down to about the 260 K. There is still presence of suitable crystallization conditions by the application of the high concentrations of lysozyme investigated in the screening tests, up to 15 mg/mL.

In the case of the application of 4 wt. % of NaCl, the range of temperature suitable for the crystallization is slightly decreased. The ideal pathway for crystal growth was shifted closer to the equilibrium curve, compared to the ideal pathway for 3% of salt (Figure 5-15).

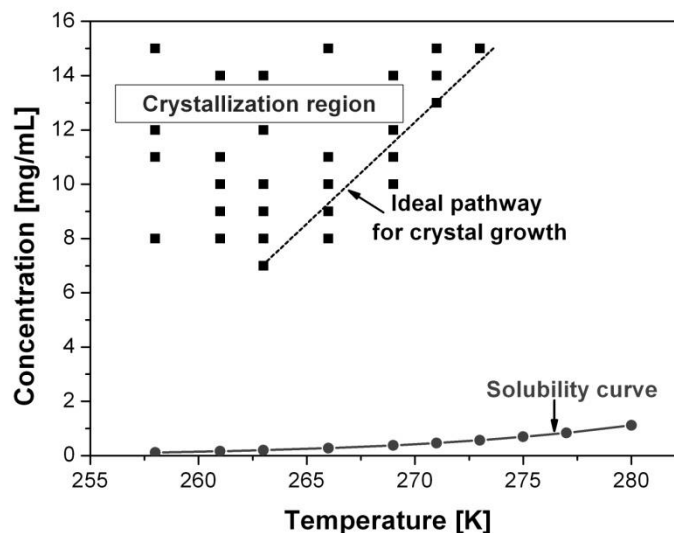


**Figure 5-16:** Pseudo-phase diagram for lysozyme in sodium acetate buffer pH 5.0, 4 wt. % NaCl and 2 mg/mL of ovalbumin.

In the range of the conditions tested, either formation or no formation of crystals was observed, but not precipitation. The upper limit of the metastable zone is not described in these diagrams, since within the range of the evaluated conditions the quality of the produced crystals were classified to belong to the metastable zone.

The line delimiting the region suitable for crystal formation in this work has been taken as the ideal pathway of conditions for crystal growth. It would be a kind of middle region of the metastable zone. Therefore, it is possible that the metastable zone width is also decreased by increasing the concentration of salt and by decreasing the temperature, similar to the behavior of the pure lysozyme solutions.

Once the adequate conditions for crystallization were found, it has been possible to use them as guide map in different solvent freeze out processes. The corresponding results to the next application are shown in the following chapter.

#### 5.4 Crystallization of Lysozyme by Solvent Freeze Out

In the previous chapters it has been described how the conditions for crystallization were found and how they were represented in pseudo-phase diagrams. These pseudo-phase diagrams are used as guide to select the initial conditions in the solvent freeze out process. Furthermore, this information has been also used to control the actual conditions of the system in order to keep

them within the metastable zone. This procedure is presented in the following subchapters for the crystallization of lysozyme in pure solution as well as in a protein mixture.

#### 5.4.1 Crystallization of Lysozyme from Pure Solutions

The crystallization of lysozyme by the SFO process from pure solutions was carried out in general as described in chapter 4.3.1. The obtained crystals were characterized according to the description presented in chapter 4.4.

The first crystallization of lysozyme was done using previously reported conditions [Ryu10a]. The process conditions were  $T_w = 274$  K,  $T_{CF0} = 274$  K, cooling at  $dT/dt = 0, 1$  K/min to  $T_{CF1} = 266$  K and crystallizing at  $T_{FT-CF} = 268$  K for 23 hours. The salt concentration was 5 wt. % and the protein concentration 4 mg/mL of lysozyme. Images of the crystals produced under these conditions are shown in Figure 5-17.

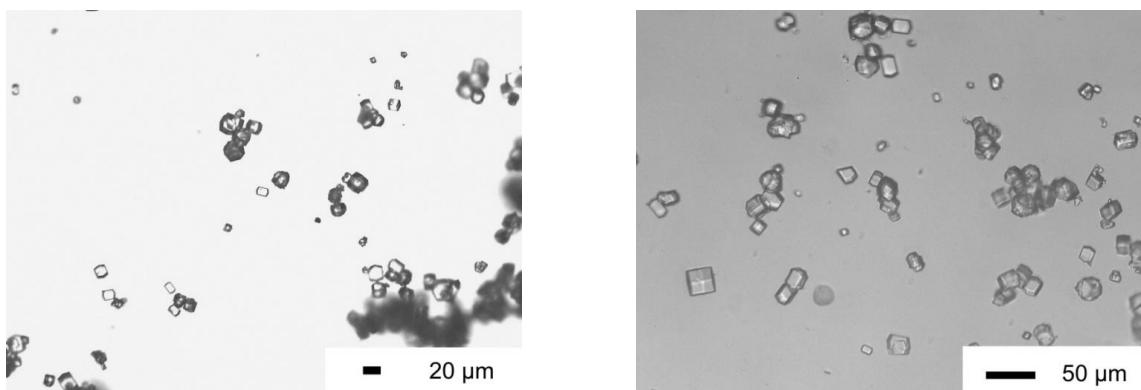


**Figure 5-17:** Lysozyme crystals obtained by the application of the KPI previously reported as optimal [Ryu10a].

The crystals produced by the use of these conditions presented small sizes, not larger than 20  $\mu\text{m}$ . Moreover, the crystallization yield was quite low, since it was not possible to get a significant amount of crystals after filtration. The measurements of the yield were based on the mass balance, in which the concentrations of the protein in the residual solution and in the ice were measured.

The amount of protein in the mother liquor at the end of the process corresponded to the 70% of the initial protein and the protein loss in the ice was of 22%. Therefore, it can be deduced that the yield of crystallization was of 8%.

In order to increase the crystallization yield and at the same time increase the size of the crystals, the process parameters were changed arbitrarily. Instead of cooling from an initial temperature to a final one in one step, it was done in different steps of cooling and constant temperature. The time at constant temperature was also varied with the aim of giving time to



the system for the transfer of material to the crystals surfaces. Stirring was also added in some experiments. From the basics that the crystal growth takes place within the metastable zone, the conditions of the system were tracked on time with the aim to identify how far or close they were to the ideal conditions for crystal growth.

For these preliminary experiments protein solutions with 6 to 15 mg/mL of lysozyme with 3 and wt. % of NaCl were investigated. Here just four representative examples of the experiments are presented. The parameters of the processes, named as KPI key process indicators are listed in Table 5-8.

The temperature of the cold finger was set at the same value as the double walled beaker in examples I and III (275 K). In the case of example II and IV, the temperature of the cold finger was higher than the one of the beaker, in order to moderate the temperature difference of the protein solution in the near of the cold finger. The final temperature of the cold finger was the same in the four examples (268 K), but the cooling profile of the cold finger was varied.

The concentration of salt (NaCl) corresponded to 4 wt. % in the first three examples and to 3wt. % in the example IV.

**Table 5-8:** Different KPI Key Process Indicators applied to four SFO crystallizations.

<b>KIP Key Process Indicators</b>	<b>Example I</b>	<b>Example II</b>	<b>Example III</b>	<b>Example IV</b>
$T_w$ [K]	275	273	275	273
$T_{CF0}$ [K]	275	283	275	279
$T_{CF1}$ [K]	268	268	268	268
$C_s$ [%]	4	4	4	3
$t_{cry}$ [min]	260	320	280	310
Agitation [-]	no	yes	yes	no

These conditions were chosen based on the successful results described in the screening tests by the application of 3 and 4 wt.%. The advantage in the SFO compared to the screening tests is that the temperature profile in the protein solution can be varied and therefore, the conditions of crystal growth.

In Figure 5-18 and Figure 5-19 the results of the four representative processes are shown. In the first line of these figures, the temperature profiles applied to the system and the measured actual temperatures in the melt (solution) are shown in diagrams of temperature vs. time.

In the second line, the actual conditions of temperature and concentration are presented, and located within the pseudo-phase diagrams. In the third line sample pictures of the obtained crystals are shown.

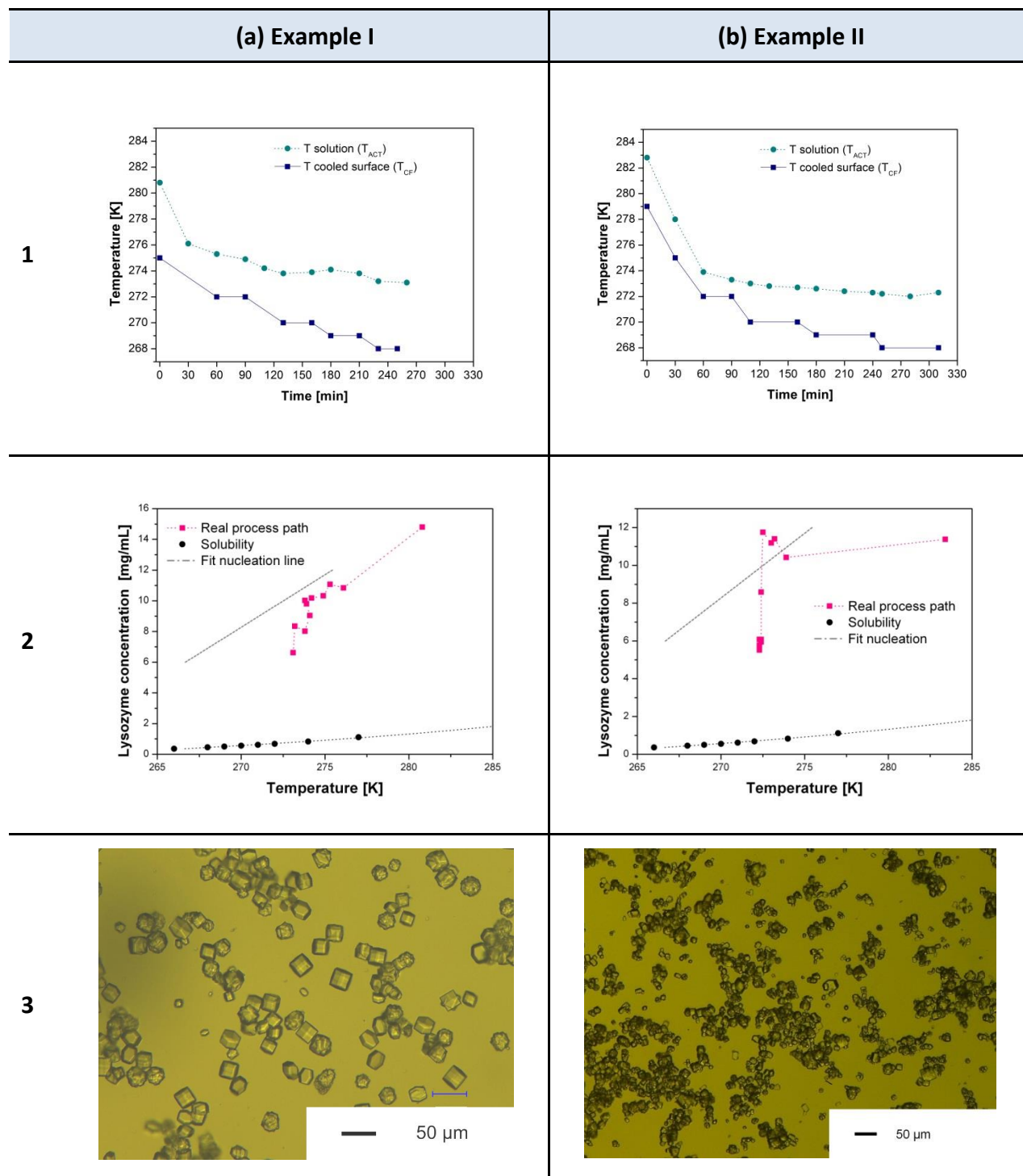


**Figure 5-18:** Line 1: Temperature profiles of cooled surface and actual temperature of the melt in time. Line 2: Concentration profiles of the melt during crystallization. Line 3: Lysozyme crystals from the solvent freeze out process.

The crystals shown in the column (a) of Figure 5-18 show a size of around 50  $\mu\text{m}$ , which is common to the most of the crystals appreciated in the picture. It can be observed that the actual conditions of the melt (solution) were located under the upper limit of the metastable zone in the pseudo-phase diagram (Figure 5-18 (a), line 2). While the tracking of the actual conditions in a different process showed that the limit of the metastable zone was passed (see Figure 5-18 (b), line 2). As a result, the crystals present relative smaller sizes, around 20  $\mu\text{m}$  and this size was not common to the most of the crystals. Moreover, they tended to group together (agglomerate) due to their smaller size. The two processes present a difference in the operation conditions. The most radical difference is the addition or not addition of agitation. The process on the left (a) was carried out without agitation, while the process on the right had an agitator with a speed of approximately 100 rpm. The concentration of protein was 15 mg/mL for the process (a) and 10 mg/mL for the process (b). The salt concentration was 4 wt. % in both of the processes. Another relevant difference between the processes was the initial temperature, which was of 2°C for (a) and 0°C for (b).

There is recognizable difference between the products of both crystallization and this gives precious information on adequate operation parameters for crystal growth and the quality of the crystals. Nevertheless, the yield of crystallization was still rather small and therefore for these four examples is not discussed. The preliminary search on optimal conditions by these random variations of conditions was continued and two further examples are similarly presented in Figure 5-19.

In a simple view at the Figure 5-19 (a), it is possible to recognize a large amount of crystals with a size of approximately 20  $\mu\text{m}$ , accompanied with a small amount of crystals with sizes of around 10  $\mu\text{m}$ . This process counted with agitation of approx. 100 rpm, an initial concentration of 11 mg/mL of lysozyme and an initial temperature of 2 °C.

Crystals produced with initial concentration of 16.8 mg/mL of lysozyme, 3% of NaCl and an initial temperature and temperature of the wall of 0 °C are shown in the third line of Figure 5-19 (b). Some of the crystals present a not that well defined tetragonal shape and some of them can be just identified as irregular solids.

If the two diagrams on the second line of Figure 5-19 (b) are compared, it can be observed that the conditions of the process (b) were totally over the limit of the metastable zone. While the conditions of the process (a) remained under the upper limit, but still too close to that limit.

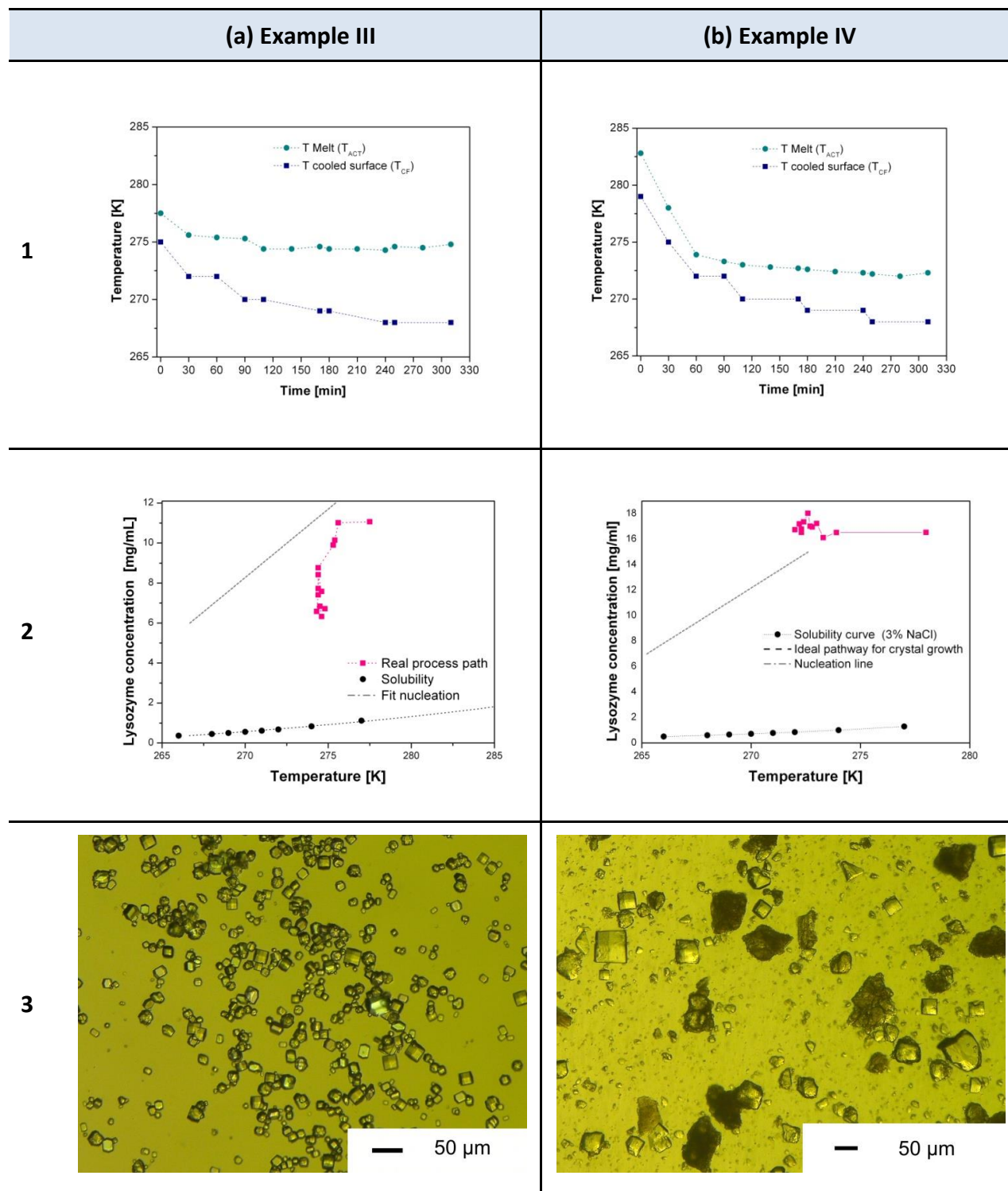


**Figure 5-19:** Line 1: Temperature profiles of cooled surface and actual temperature of the melt in time. Line 2: Concentration profiles of the melt during crystallization. Line 3: Lysozyme crystals from the solvent freeze out process.

It can be observed from these results that a change on the combination of the KPI (key process indicators) has a direct influence on the quality of the crystals. Therefore, this can be used as a

tool to control the process and influence it to get an optimal response of the process. By changing the parameters arbitrarily does not lead to precise information on how and which one of the parameters influences the responses. That is the reason why it has been necessary to call upon tools for experimentation and optimization of processes which were introduced in chapter 4.5 and whose results are reported in the chapter 5.5.

#### 5.4.2 Crystallization of Lysozyme from Lysozyme-Ovalbumin Mixtures

The first approaches to the crystallization of lysozyme from mixtures of this protein with ovalbumin (albumin from egg white) were made throughout the screening tests, whose results can be found in chapter 5.2.2. The collected information has then been used for the construction of the pseudo-phase diagrams which were presented in chapter 5.3.2.

With this information it has been possible to set the parameters in the solvent freeze out process in order to separate the lysozyme from the mixture by crystallization. Several runs have been done with the aim of getting high yields and good quality of the crystals in short operation times. Here two examples (see chapters 5.4.2.1 and 5.4.2.2) are presented as representation of several trials carried out toward the development of this process. The detailed steps taken in between can be found in two former works [Rüd11, Lei11].

##### 5.4.2.1 Preliminary Crystallization of Lysozyme by SFO

An example of one of the first crystallization of lysozyme from a lysozyme-ovalbumin mixture by the solvent freeze out SFO is presented in this subchapter. The SFO process was carried out according to the description presented in chapter 4.3.2. The key process indicators KPI of this experiment are shown in Table 5-9.

**Table 5-9:** Process parameters as KPI for a first preliminary crystallization of lysozyme from a mixture by the SFO.

KPI	pH	$C_p$ [mg/mL]	$C_s$ [wt. %]	$C_{Oval}$ [mg/mL]	$T_w$ [K]	$T_{IT-CF}$ [K]	$T_{FT-CF}$ [K]	dT/dt [K/min]	Total time [h]
	5.0	15	4	1.7	275	278	266	0.1	19

The KPI were chosen guided by the pseudo-phase diagram of lysozyme in the ovalbumin-lysozyme-NaCl system shown in Figure 5-16. Regarding to the pseudo-phase diagram, the investigated initial conditions of concentration and temperature,  $C_p = 15$  mg/mL of lysozyme at 278, lead to successful crystallization of lysozyme. It has been expected that by setting the KPI the system follows the ideal path way for crystal growth. In this process, the initial temperature of the cooled surface ( $T_{IT-CF}$ ) was set constant at 278 K during 10 min, unlike in the process for crystallization of lysozyme from pure solutions. In those experiments the initial temperature of

the cooled surface ( $T_{IT-CF}$ ) has been the same as the temperature of the vessel [ $T_W$ ]. The detailed temperature profile of the cooled surface is shown in Figure 5-20.

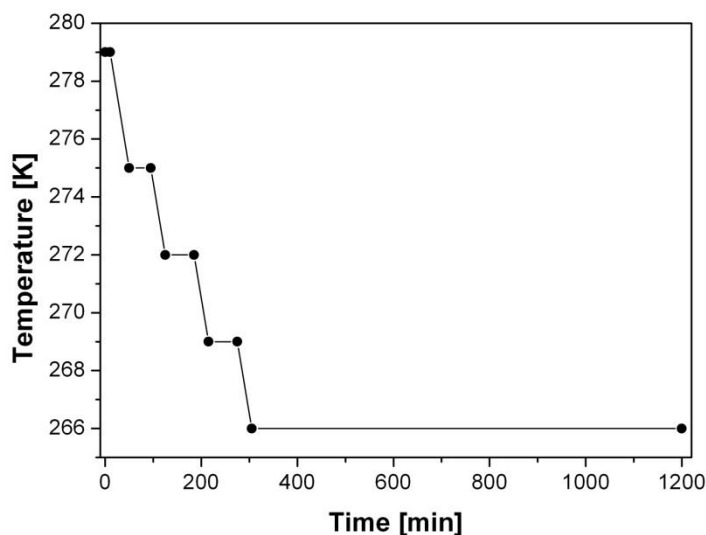


**Figure 5-20:** Temperature and cooling rate profile of the cooled surface in a solvent freeze out process for the crystallization of lysozyme from a lysozyme-ovalbumin mixture.

Once the process has ended up, the crystals were characterized as described in chapter 4.4. The crystals were analyzed by microscopy, activity test and SDS PAGE, but the yield of crystallization in this case was not investigated. Images of the crystals taken from the microscopic observations are shown in Figure 5-21.

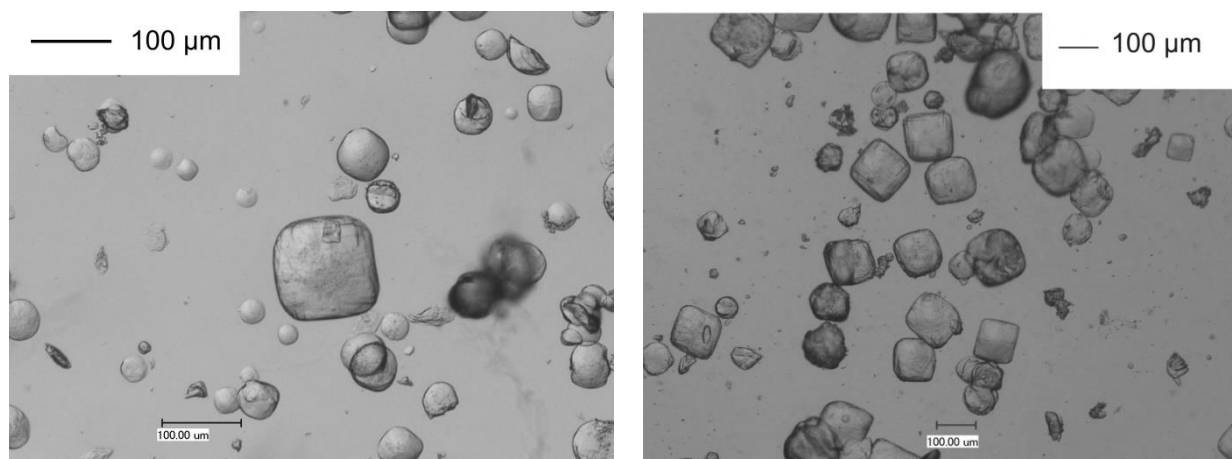


**Figure 5-21:** Lysozyme crystals from a mixture lysozyme-ovalbumin, 15 mg/mL lysozyme, 1.7 mg/mL ovalbumin and 4wt. % NaCl.

The obtained crystals with a size of approximately 100  $\mu\text{m}$  present a tetragonal shape with slightly rounded edges. There is a good similarity of the morphology of the crystals produced by



SFO and those produced by the micro batch crystallizations during the screening tests (see Figure 5-8 and Figure 5-9).

That the crystals present a similar morphology compared to the crystals produced in the screening tests is, however, not sufficient evidence that they are composed by lysozyme. Therefore, the crystals were subjected to a SDS Page analysis to confirm their nature. The obtained SDS PAGE Gel is shown in Figure 5-22.

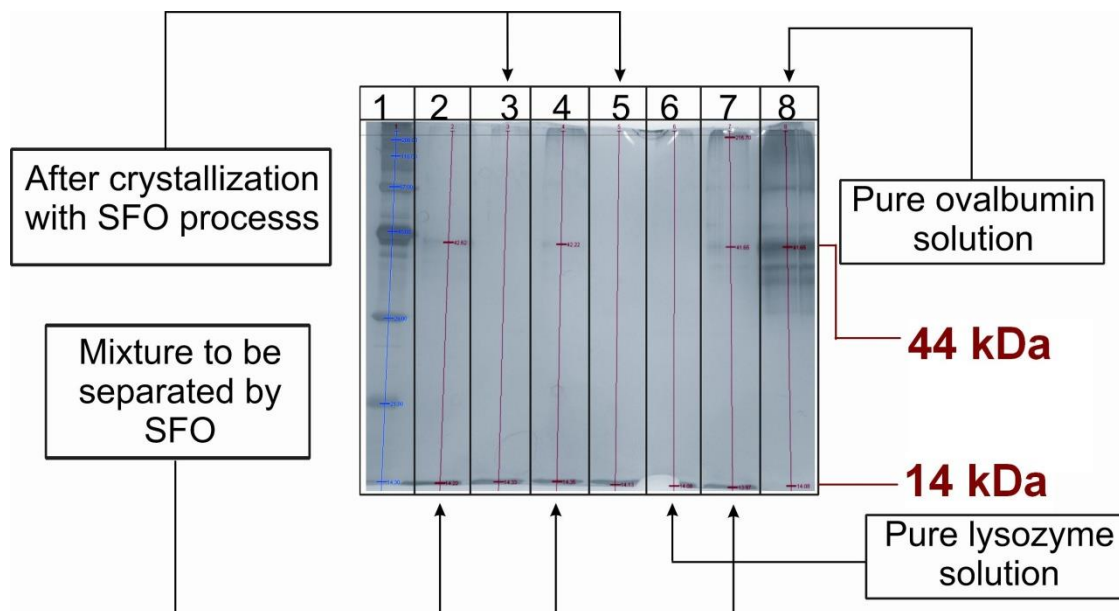


**Figure 5-22:** Gel from a SDS-PAGE analysis of ovalbumin solution, lysozyme solution, lysozyme-ovalbumin mixture and dissolved lysozyme crystals produced in a preliminary test of the SFO process.

The gel presented in Figure 5-22 counted with 8 lanes, from those the first one was filled with a solution of the marker sample. The mixture to be separated by SFO, which is the initial solution poured into the double walled glass, was tested in lane 2, 4 and 7. In these lanes bands of about 44 and 14 kDa can be recognized. A pure solution of lysozyme and a pure solution of ovalbumin were tested in lanes 6 and 8, respectively. On the lane 6 where the pure lysozyme solution was poured, a strong band about the 14 kDa can be observed. Although the gel had some defect at this point. The produced and further diluted crystals were tested in lane 5, in which a band by the 14 kDa is present. As there is an absence of a mark on the line of the 44 kDa, it can be here affirmed that the crystals produced are composed of lysozyme.

Once the nature of the crystals was proven, the activity test has been held as explained in chapter 4.4.

The extinction decay of the *micrococcus lysodeikticus* solution by the addition of the dissolved lysozyme crystals can be observed in the diagram shown in Figure 5-23.

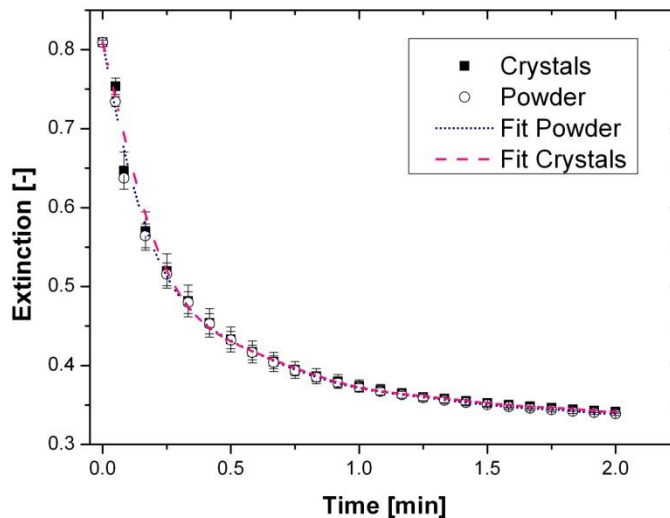


**Figure 5-23:** Absorption decay of a *micrococcus lysodeikticus* suspension due to the addition of dissolved lysozyme (commercial powder ○ and SFO crystals of a preliminary test ■). Results from activity test as described in chapter 4.4.

The activity of the commercial lysozyme powder which was used as solute in the protein solutions has been also tested and this result was used as reference. The fitted extinction decay of the bacterial solution due to the addition of the powder sample is shown in Figure 5-23 as solid line. The measured decay of the extinction produced by the addition of the dissolved crystals is shown as dotted line. There is an identical behaviour of the extinction decay for both of the samples. Based on this result it can be affirmed that the lysozyme conserved the enzymatic activity after being subjected to the crystallization by the SFO.

#### 5.4.2.2 Advanced Crystallization of Lysozyme by SFO

The KPI of the process have been set in different combinations with the aim of achieving a significant amount of crystals and therefore, to have the possibility of a yield evaluation. Here one example of the processes with the best performance is presented and nominated as an advanced crystallization process of lysozyme from the lysozyme-ovalbumin mixture. In this process the same composition of the system was evaluated, but the total time of crystallization has been reduced, according to new settings of the temperature profile. The KPI of this process can be found in Table 5-10.



**Table 5-10:** Parameters as KPI for an advanced crystallization of lysozyme from a mixture by the SFO.

KPI	pH	$C_p$ [mg/mL]	$C_s$ [wt. %]	$C_{Oval}$ [mg/mL]	$T_w$ [K]	$T_{IT-CF}$ [K]	$T_{FT-CF}$ [K]	dT/dt [K/min]	Total time [h]
	5.0	15	4	1.7	275	276.5	266	0.1	15.1

The dynamic temperature profile applied to the cooled surface can be observed in the diagram temperature vs. time on Figure 5-24. As explained in the chapters above, the temperature profile in steps of constant temperature and cooling helps the control of the actual conditions of the system and it determines the total crystallization time in a SFO run.

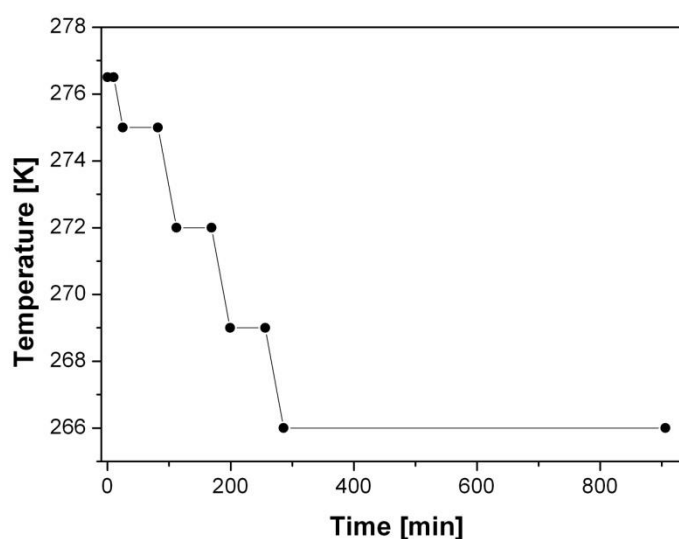


**Figure 5-24:** Temperature and cooling rate profile of the solvent freeze out process for the crystallization of lysozyme from a lysozyme-ovalbumin mixture.

In this case the duration of the process was of 15.1 h, this significant reduction of the time compared to the preliminary test presented in the subchapter 5.4.2.1 (time=19 h).

Moreover, due to the improved performance of the process it has been possible to carry out in more detail the characterization of the process and of the crystal product.

The solution with the initial conditions  $C_p$ ,  $C_s$  and  $C_{Oval}$  described in Table 5-10 belongs to the region of conditions suitable for crystal growth, which are also presented in a previous chapter (4.3.2). This also can be identified in the phase diagram from Figure 5-16. Therefore, a successful production of tetragonal lysozyme crystals took place as it was expected if the temperature profile was the appropriate as well. The data obtained from the characterization of the process, which in turn correspond to the final responses, are listed in Table 5-11.

**Table 5-11:** Responses of an advanced SFO process for lysozyme crystallization from a mixture (KPI in Table 5-10).

Crystallization time [h]	V <sub>ICE</sub> [mL]	V <sub>ML</sub> [mL]	Weight of crystals [g]	Crystallization yield [%]
15.1	26	34	0.62	69

From the initial 60 mL of the solution, 26 mL of the solvent were separated by the crystallization of the water (ice) on the cooled surface. In the 34 mL of the mother liquor (ML) the formation of 0.62 g lysozyme crystals took place.

An example of the obtained crystals can be observed on Figure 5-25. The crystals produced by this SFO crystallization also have a tetragonal shape with rounded edges, characteristic common to the crystals obtained in the screening tests (Figure 5-8 and Figure 5-11).

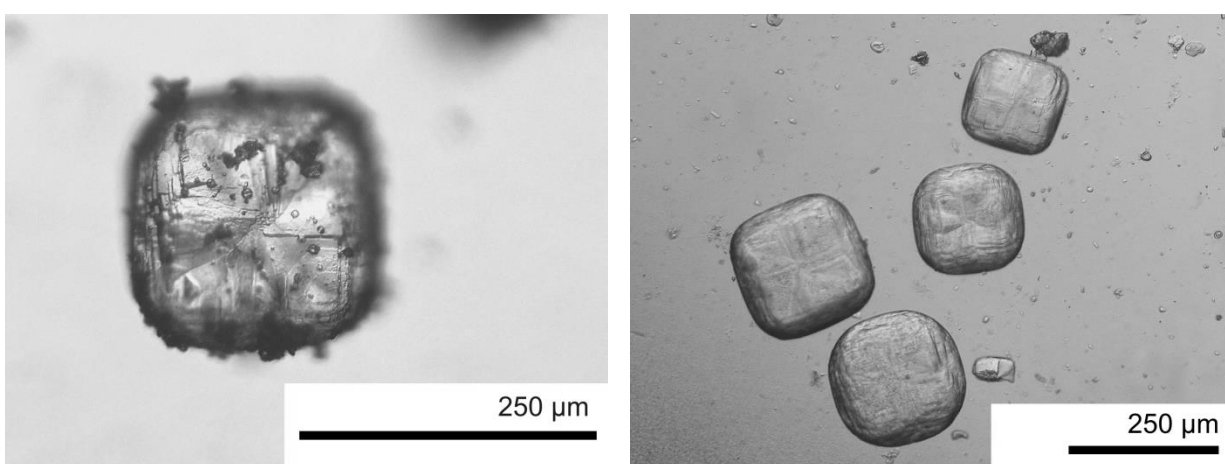


**Figure 5-25:** Lysozyme crystals obtained in an advanced SFO process. Solution conditions listed in Table 5-10. Left: dried crystals. Right: Crystals suspended in the mother liquor [Dia10c].

A further advantage of this improved crystallization has been the possibility of getting a higher amount of crystals to be used for the complementary analysis. Such an analysis is the measurement of the mean size distribution. The measured size distribution of the crystals is shown in Figure 5-26.

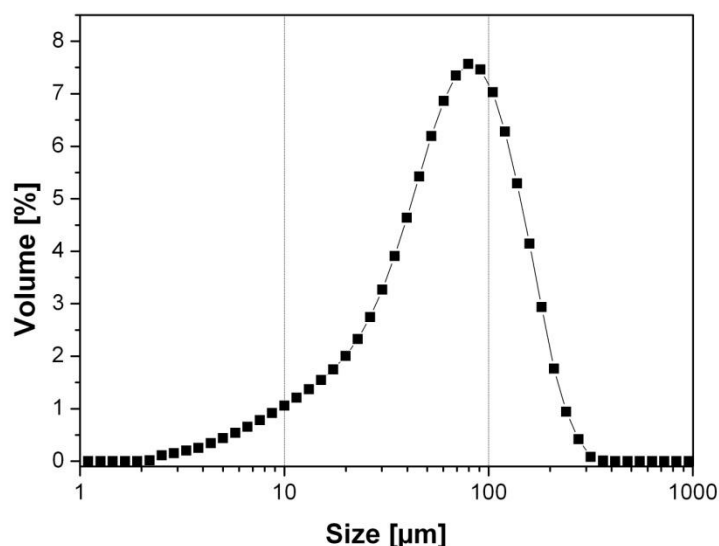


**Figure 5-26:** Crystal size distribution of lysozyme crystals obtained in an advanced SFO process. The mean size is  $75 \pm 5 \mu\text{m}$  [Dia10c].

The mono modal size distribution is shows the presence of a significant amount of crystals with a small size, between 2 and 30  $\mu\text{m}$ . If the left picture of the crystals on Figure 5-25 is thoroughly observed, it is possible to identify small crystals attached on the surface of the single crystal. The small crystals are also visible on the right picture (Figure 5-25), but they do not attach to the surface of the large crystals, because they were suspended in mother liquor.

The certainty that the crystals obtained were lysozyme and not ovalbumin is supported by the SDS PAGE and activity tests. In Figure 5-27, the gel from SDS PAGE is shown. On the lanes 1 to 4, lysozyme concentrations were tested, the intensity of the band is thus reduced with the decreasing concentration. On lanes 10 to 13, ovalbumin solutions were investigated, the intensity of the bands is also relative to the protein concentration. On the lanes 5, 6 and 7, diluted crystals of previous experiments (here not discussed) were tested. The diluted crystals discussed in this work were examined in lane 8. A sample of the studied mixture was analyzed in lane 9 (15 mg/mL lysozyme and 1.7 mg/mL ovalbumin).

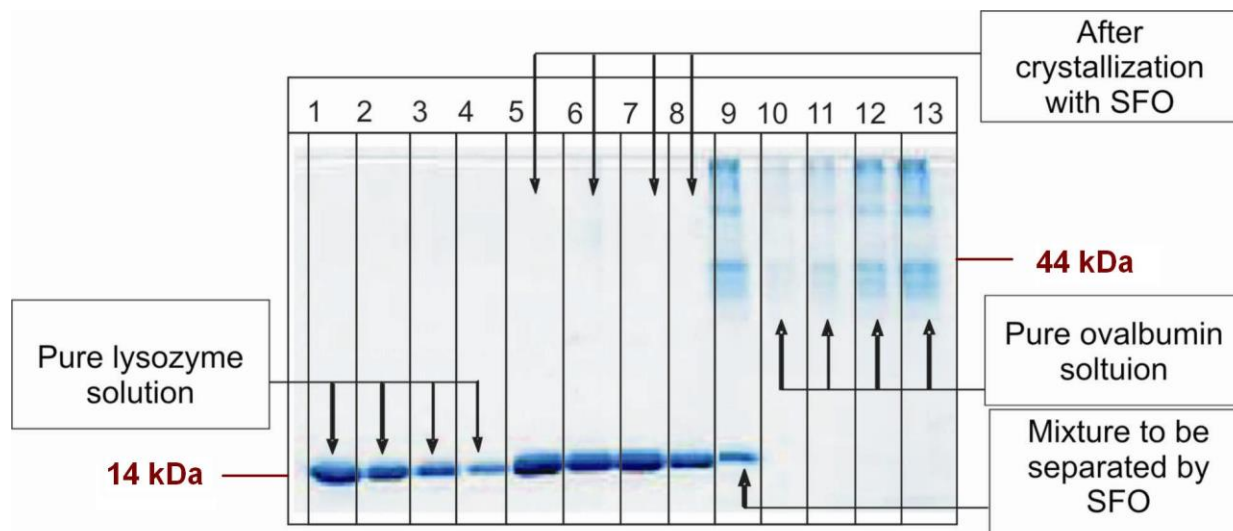


**Figure 5-27:** SDS-PAGE Gel. In slots 1, 2, 3 and 4 lysozyme solutions with decreasing concentrations are tested ( $M_w \approx 14$  kDa). In slot 5, 6 and 7 crystals from different SFO runs are tested. On lane 8 the crystals obtained in the advanced SFO were tested. The initial solution used for the SFO runs is tested in slot 9. Ovalbumin solutions with increasing concentration are tested in slots 10, 11, 12 and 13 ( $M_w \approx 44-45$  kDa) [Dia10c].

The bands obtained from the test of pure lysozyme solutions serve as a mark for this protein, since lysozyme has a molecular weight of 14 kDa [Can63, Bla65]. The bands of the ovalbumin solutions serve as mark for the  $\approx 44$  kDa ( $M_w$  of ovalbumin is around 45 kDa [Jud95] which is the average molecular weight of this protein. The band described by the tested crystals on lane 8 is at the same position as the pure tested lysozyme solutions (14 kDa). This result proves the lysozyme nature of the crystals and the absence of ovalbumin within them, since this is the only band (slots 5 to 8).

Once the purity of the lysozyme crystals was confirmed, the remaining activity of the crystals was quantified in the activity test as described in chapter 4.4. The absorption decay of the *Micrococcus lysodeikticus* measured in the activity tests for the lysozyme powder and the obtained crystals is shown in Figure 5-28.

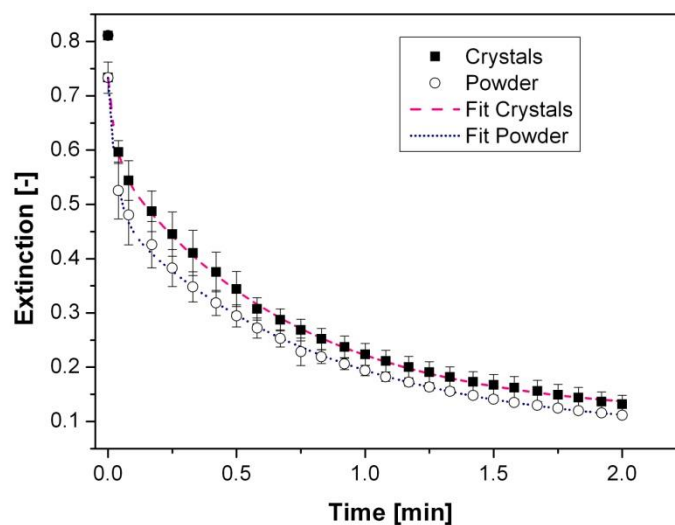


**Figure 5-28:** Decay of the absorption of a *Micrococcus lysodeikticus* solution after the addition of lysozyme in solution (commercial powder ○ and crystals ■ from an advanced SFO) [Dia10c]. Results of the activity test as described in chapter 4.4 [Dia10d].

The absorption was measured three times for each sample during 2 minutes with an integration time of 0.2 s. The decrease in the absorption was measured since the first second that the protein solution is dropped into the bacterial solution. At the beginning of the reaction the change of absorption occurs with high speed, inducing oscillations of the values measured and higher deviations as it can be observed in Figure 5-28.

The reaction tends to reach equilibrium by the second minute, therefore the region of interest of these curves is the linear part, in this case would consist on the first 3 points. The slopes of the lines were used for calculations of the activity. The remaining activity of the lysozyme within the crystals was 94 %.

## 5.5 Process Optimization

The general strategy for optimization of the process shown in Figure 4-5, p. 33 was followed by several times. Initially the process parameters were the key process indicators (KPI) reported as optimal by [Ryu10a]. Afterwards, the process parameters were varied randomly and some of these results have been shown in chapter 5.4.1, p. 56. In this way it was possible to identify the apparently relevant parameters of the process and the desired characteristic of the crystals or value of the responses. Nevertheless, the application of a design of experiments was necessary in order to have an organized structure of experimentation. This strategy is described in chapter 4.5 and in this chapter the results will be presented.

### 5.5.1 Fractional Factorial Designs

Even if the influencing and interacting parameters (see Figure 2-2) in a crystallization process are known, it is necessary to quantify those parameters in order to enhance the optimal responses. Also in the case of the SFO, when the KPI are known, it is still required to set the equipment parameters to optimal values. As described in chapter 4.5.1, the experiments realized based on the fractional factorial design correspond to the first part of the strategy toward finding the optimal values. The different combinations of these parameters or factors through the different runs can be visualized in Table 4-3. The temperature profile in the bulk of the solution is determined by the temperatures of wall, of the cooled surface and its cooling rate. How these three factors were combined in three runs is shown in Figure 5-29 as example.

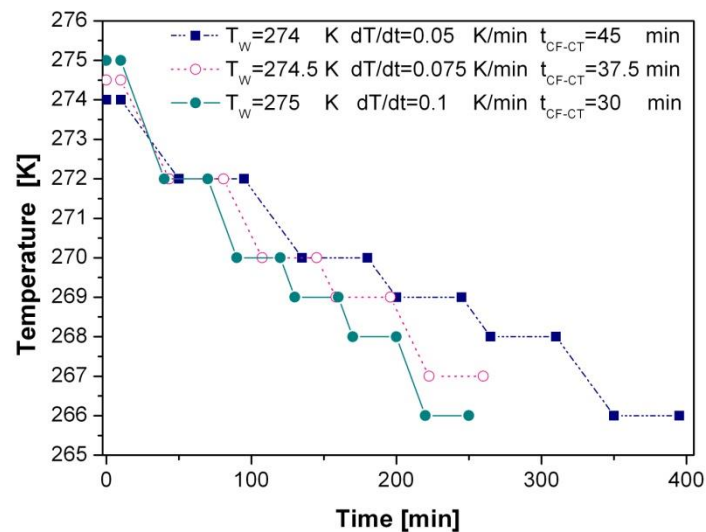


**Figure 5-29:** Three examples of temperature profiles of the cooled surface applied in the first stage of optimization strategy. Run 10 ■, Runs 17, 18 ○ and Run 15 ●. Temperature of the wall  $-T_w$  corresponds to the initial temperature of the cooled surface ( $T_{CF}$ ).

Therefore, in these three SFO processes the total operation times were different, 6h 35' for run 10. When the temperature of the wall, the final temperature of the cooled surface and the cooling rate were set at the center points, the duration of the processes was 4h 20' (center points: runs 17 and 18). And the duration of the process was 4h 10' in the run 15 in which all the parameters of the process were set at their low levels (see Table 4-4). The responses activity, yield, volume of ice ( $V_I$ ) and protein loss ( $P_L$ ) evaluated in the runs of the  $2^8$  (8-4) design are shown in the Figure 5-30.

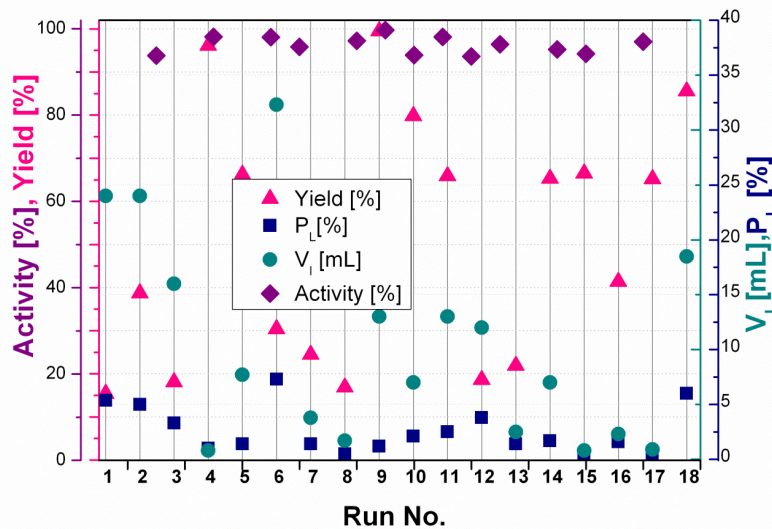


**Figure 5-30:** Responses evaluated in the 18 runs of the fractional factorial  $2^{(8-4)}$  experimental design.

The yield of crystallization obtained from the run 10 was 79.8 %, from the run 17 it was 65.2 % and from run 18 it was 85.5 %. From run 15, the yield was of 66.5 %. Here it is possible to observe that the highest yield of crystallization was not necessary described by longer crystallization times.

The highest yield was enhanced from the run 9, with a value of 99.5 %, run which had duration of 4 h 12'. A further high yield of 96.1 % was obtained from run 4, process carried out in 6 h 55'. The lowest yield was obtained in the run 1 with a value of 15.4 %. The run took place in 5 h 18'. A further low yield of 16.9 % was obtained from run 8, in a time of 5 h 25'. The runs 3 and 12 presented low yields as well, with 18.1 % and 18.6 % respectively (4h 30' and 5h 30').

The values of protein loss from this experimental design are in average bellow 10 %, which is a relative low value. Three runs did lead to high protein losses such as run 6 (7 %), run 18 (6 %) and run 1 (5 %). There was almost no protein loss in the runs 8, 15 and 17. Even when runs 17 and 18 have the parameters at the same values, the responses volume of ice and protein loss are markedly different.

The volume of ice varied significantly throughout the 18 runs. The highest amount of ice was formed after the crystallization in run 6 (32 mL). Volumes of molten ice under 1 mL were obtained in runs 4, 15 and 17.

It was possible to measure the activity of 14 runs, for which the remaining activity was between 94 and 99 %. It was not possible to measure the activity of the crystals for the runs 1, 3, 13 and 18 due to the low amount of material recovered.

If the results from the Figure 5-30 are analysed based on the parameters of each run, it is possible to identify, for example, at simple glance that higher yields are obtained when the temperature are constant temperature is higher. Nevertheless, it results very laborious to find a relation between the individual values of the parameters with the responses. This is the reason why it has been necessary to quantify the magnitude of the effects of the factors on the process responses. The analysis of the effects is shown in the following chapter 5.5.2.

Further characterizations of the produced crystals such as microscopy analysis or size distribution measurements are presented in the paragraphs below.

The samples of obtained crystals either dry or suspended in solution, were subjected to microscopic observations and pictures were recorded to be additionally analyzed. The amount, the shape and the size of the crystals differed from one run to the other. This is somehow evidently, since the parameters and the interactions might have a different effect on the quality of the crystals.

In order to present some pictures of the crystals obtained as example in a systematic way, those were grouped regarding to the cooling rate applied to the process in Figure 5-31 and Figure 5-33. These results, however, can not be compared only based on the effect of the cooling rate since the other factors were differently combined.

Samples of the crystals obtained in processes in which a cooling rate of 0.05 K/min was applied are shown in Figure 5-31. These pictures correspond to samples of crystals obtained in the runs 2, 3, 10 and 11, respectively.

Crystals with a large size of approximately 100  $\mu\text{m}$  accompanied by crystals with significantly smaller sizes (e.g.  $60 \pm 10 \mu\text{m}$ ) and a large amount of crystals smaller than  $20 \pm 2 \mu\text{m}$ , are observed in the picture (a).

The presence of large and tiny crystals together is also observed in pictures (b) and (c). The large crystals in this case had a maximal size of 50  $\mu\text{m}$ . Another difference between these pictures is that the crystals shown in (a) and (d) were still suspended in the mother liquor and those in (b) and (c) were already air dried. In the “dry” state the smaller crystals tend to attach to the surfaces of the larger crystals.



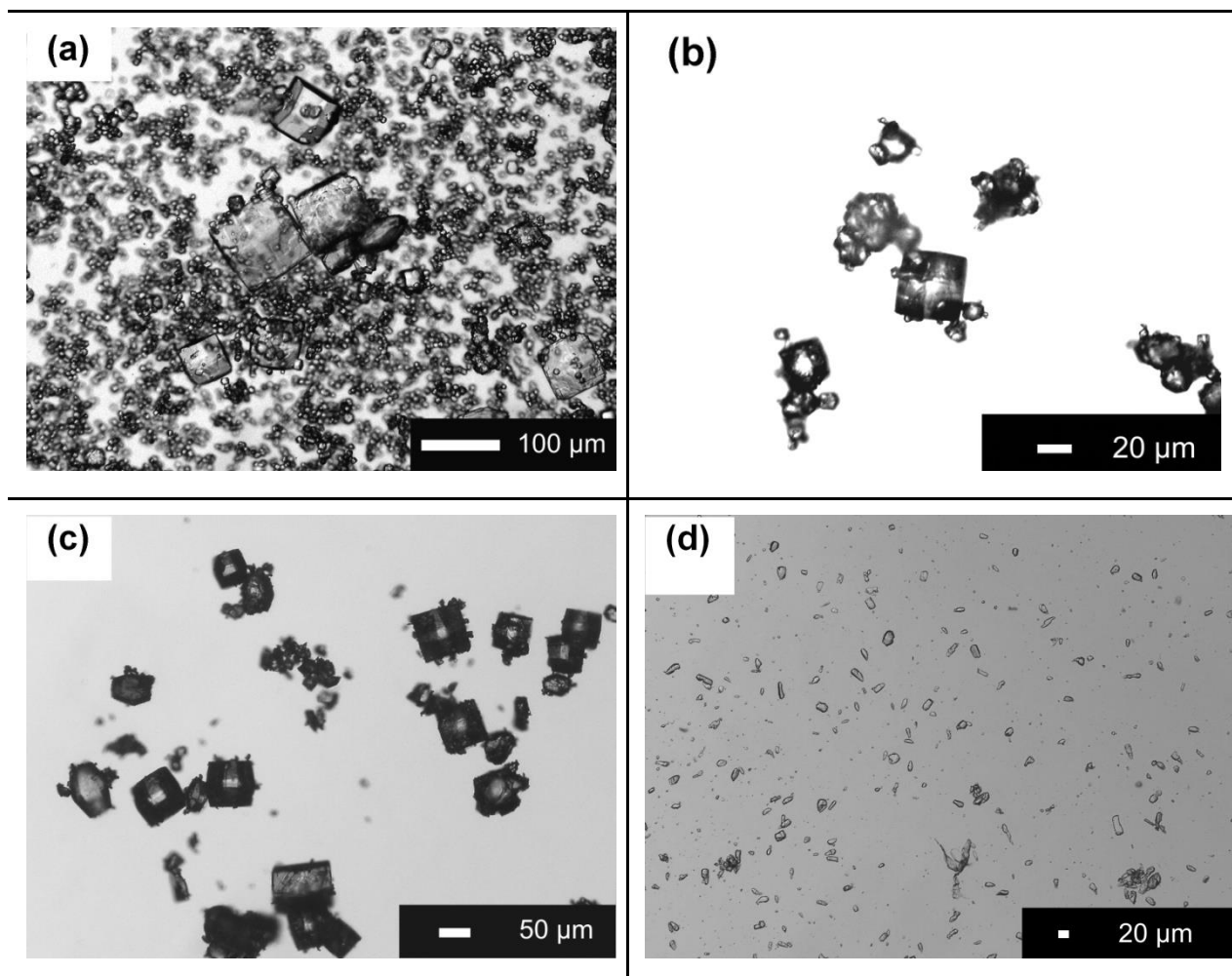


**Figure 5-31:** Crystals from four SFO crystallization processes with cooling rate of 0.05 k/min. Combinations of the parameters as determined in the fractional factorial design as runs 2 (a), 3 (b), 10 (c) and 11 (d).

The tetragonal shape of the crystals can be recognized in the pictures a, b and c, as difference to the picture (d), from which it is not possible to identify the morphology of the particles.

The size distributions of the crystal products of the runs in the fractional factorial design were measured as described in chapter 4.4. As example, the results from the runs 2, 3, 10 and 11 are presented in Figure 5-32.

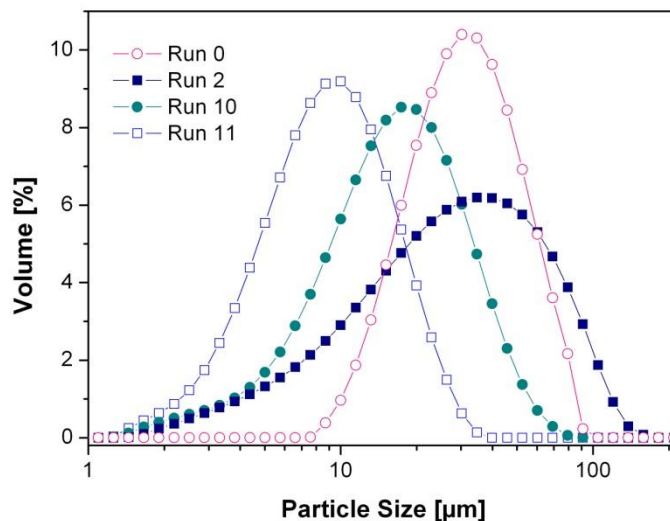


**Figure 5-32:** Mean size distributions of the crystals produced in runs 2 ■, 0 ○, 10 ● and 11 □.

The distribution of the crystal sizes in the run 2 was quite wide, describing sizes between 1 to 110  $\mu\text{m}$ , with a mean size about the 30  $\mu\text{m}$ . This result agrees with the picture of the crystals shown in Figure 5-31 (a). The mean size of the crystals in run 3 was about the 40  $\mu\text{m}$ , and described a narrower size distribution than in the case of the crystals in run 2. The sizes of the crystals are between 10 and 100  $\mu\text{m}$ . In the picture (b) of Figure 5-31, it is possible to observe that small crystals with sizes between 8 and 20  $\mu\text{m}$  are surrounding the larger crystals (of  $\cong 40\mu\text{m}$ ).

The distribution of the crystal sizes in run 10 is wide as well, with a significant amount of crystals with sizes below and above the mean size -10 to 20 $\mu\text{m}$ -. The sample of crystals representing this result was shown in Figure 5-31 (c).

The particles obtained in run 11 were distributed in a narrower way, with a mean size of around 9  $\mu\text{m}$ , as it can be confirmed in the Figure 5-31 (d).

Samples of crystals obtained from the processes in which a cooling rate of 0.1 K/min was applied are shown in Figure 5-33.

Dried crystals obtained under the conditions of run 8 are shown in Figure 5-33 (a). The main amount of crystals has a regular tetragonal shape with mean size of 46.23  $\mu\text{m}$ . A small number of tiny crystals are attracted to the surface of the large crystals are similar to the crystals from runs 1b and 1c.

The size distributions of the crystals from which the samples were presented in Figure 5-33 are shown in Figure 5-34.

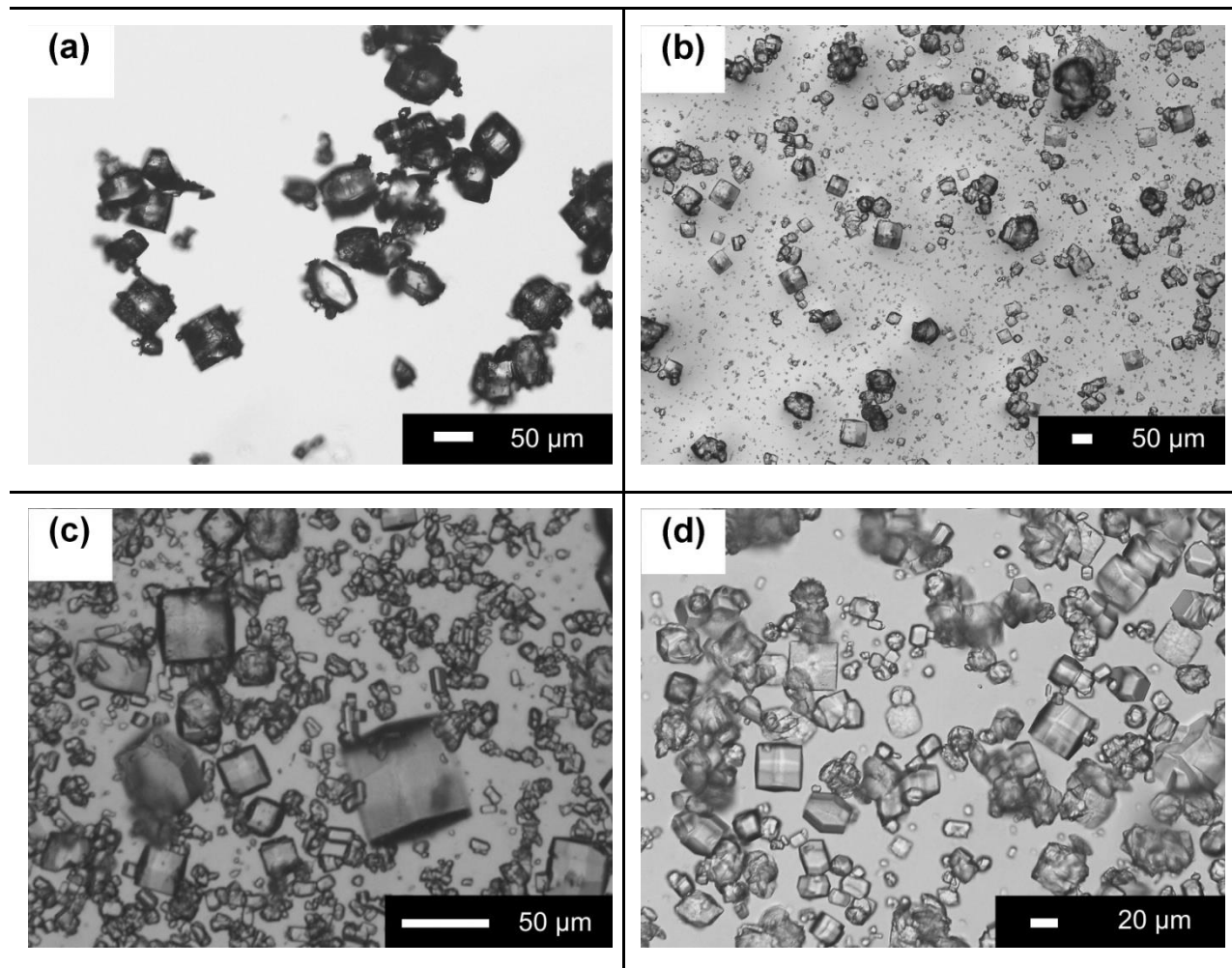


**Figure 5-33:** Crystals from four SFO crystallization processes with a cooling rate of 0.1 k/min. Combinations of parameters as determined in the fractional factorial design as runs 8 (a), 5 (b), 13 (c) and 16 (d).

In the image of the crystals produced in run 8 Figure 5-33 (a), it is possible to observe the presence of tetragonal crystals of around 50  $\mu\text{m}$  with small crystals with visible sizes of 10, 20  $\mu\text{m}$  as an example. This image agrees with the results from the measurement of the size distribution presented in Figure 5-34. The broad size distribution of the crystals sizes shows a significant presence of small crystals with sizes between 1 and 30  $\mu\text{m}$ .

A good example of crystals with a narrower distribution of the sizes and with a mean size of the crystals is about 35  $\mu\text{m}$  is presented in Figure 5-33 (b). These crystals obtained from run 5, have a recognizable but not that well formed tetragonal shape. There is a significant presence of small and large crystals, making the size distribution varying between 8 and 100  $\mu\text{m}$  as it can be observed in Figure 5-34.

It can be observed in the picture of the crystals shown in Figure 5-33 (c) that there is a marked difference of crystal sizes and shapes. The main size of the crystals was measured to be around 50  $\mu\text{m}$ , but this accompanied with a great number of crystals with sizes between 10 and 30  $\mu\text{m}$ . And with a relative significant amount of crystals with sizes larger than 70  $\mu\text{m}$  and up to 105  $\mu\text{m}$  (see below in Figure 5-34).

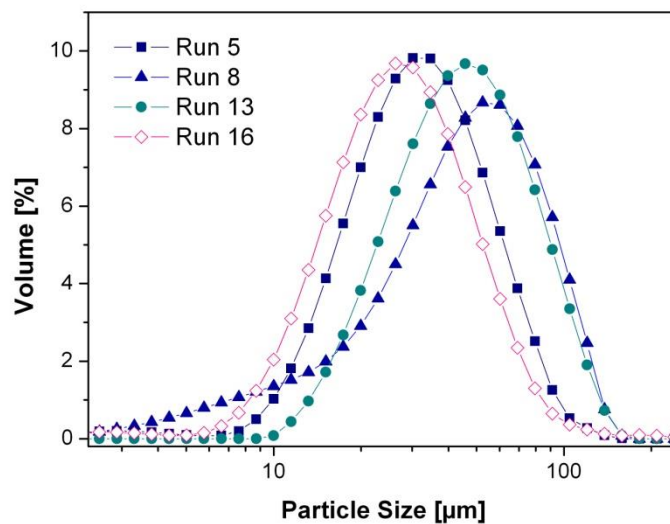


**Figure 5-34:** Size distribution of the crystals obtained in runs 8, 5, 13 and 16.

A better distribution of the crystals sizes is observed in the picture shown in Figure 5-33 (d). The crystals produced by the run 16 have a narrower distribution of the crystals with a mean crystal size of around 25  $\mu\text{m}$ .

The activity test, with three replicates, was carried out for the 16 runs for which the amount of crystals was enough for analysis. An average value of the extinction measured during the time of the test was obtained and represented in a diagram in Figure 5-35. The extinction decay curve obtained from the activity test of the commercial lysozyme is also shown in this diagram. The error bars correspond to the standard deviation of the measuring points.

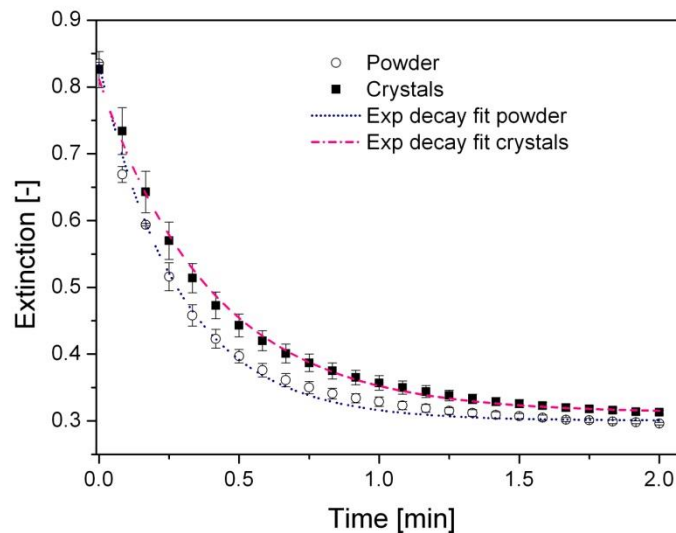


**Figure 5-35:** Decay of the extinction of a microbial solution by the addition of dissolved lysozyme crystals.

The average activity of the crystals describes a quite consistent behavior independently on the factors combinations. The specific activities were calculated based on the linear part of the exponential decay. Furthermore, the values were expressed in percent in regard to the 100 % value which corresponds to the lysozyme powder. The crystals conserved between 94 and 99 % of the activity compared to the pure commercial lysozyme.

### 5.5.2 Significant Effects

In order to set the parameters at an optimal value, it was first necessary to identify the parameters with the strongest influence on the responses. The effects of the eight parameters (Table 4-3) on the response size ( $L$ ), volume of ice ( $V_i$ ), protein loss ( $P_L$ ) and yield ( $\dot{M}$ ), were calculated by the statistical analysis of the results of the 18 experiments ( $2^{(8-4)}$  design). The Pareto charts of effects are shown in Figure 5-36.

The response size is influenced at most by the final temperature of the cooled surface ( $T_{CF-FT}$ ), the concentrations of salt ( $C_S$ ), of protein ( $C_P$ ), and the cooling rate of the cooled surface ( $dT/dt$ ). In fact, the listed set of conditions determines the actual supersaturation of the system.

Stirring has a significant influence on the three responses  $V_i$ ,  $P_L$  and yield, but a minimal effect on the size of the crystals.



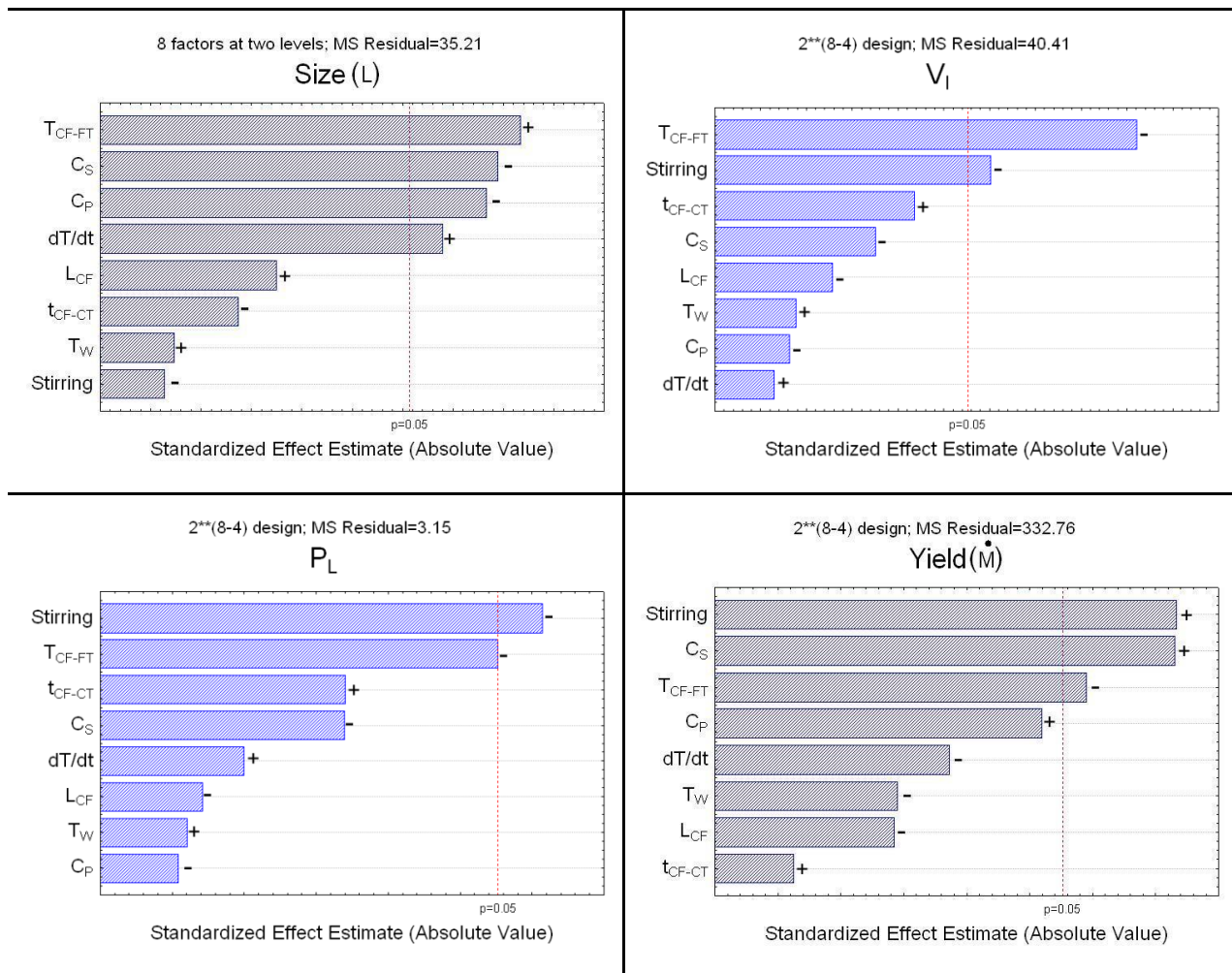


**Figure 5-36:** Standardized effects of the factors on responses: mean size, volume of ice, protein loss and yield. Analysis of the fractional factorial  $2^8(8-4)$  design [Dia10d].

Stirring has a negative effect on the amount of the ice layer ( $V_I$ ), but at the same time it has a positive effect on the purity of the ice. It is displayed in Figure 5-36 through the strong negative effect of stirring on the protein loss ( $P_L$ ). Moreover, the yield of protein crystallization increased proportionally with the addition of stirring as it can be observed in the Pareto diagram of effects on the response yield.

An increase in salt ( $C_S$ ) and protein ( $C_P$ ) concentrations lead to higher yields of protein crystals, but simultaneously leads to a lower volume of ice ( $V_I$ ). When the retention time of temperature of the cold surface was kept longer at constant values ( $t_{CF-CT}$ ), the formation of volume of ice was increased as well as the protein included in the ice-protein loss.

### 5.5.3 Central Composite

Together with the concentrations of protein  $C_P$  and salt  $C_S$ , the factors stirring, final temperature of the cooled surface and time at constant temperature showed the greatest effects on the four

responses evaluated in the fractional factorial design (previous chapter). Therefore, based on this result the three factors stirring,  $T_{CF-FT}$  and  $t_{CF-CT}$  were selected to be analyzed in the second stage of the strategy. The conditions of  $C_p$ ,  $C_s$ ,  $dT/dt$  and  $T_w$ , were fixed at the center values of the first stage (see Table 4-4). Mainly because of their good performance on the quality and morphology of the crystals (see Figure 5-37).

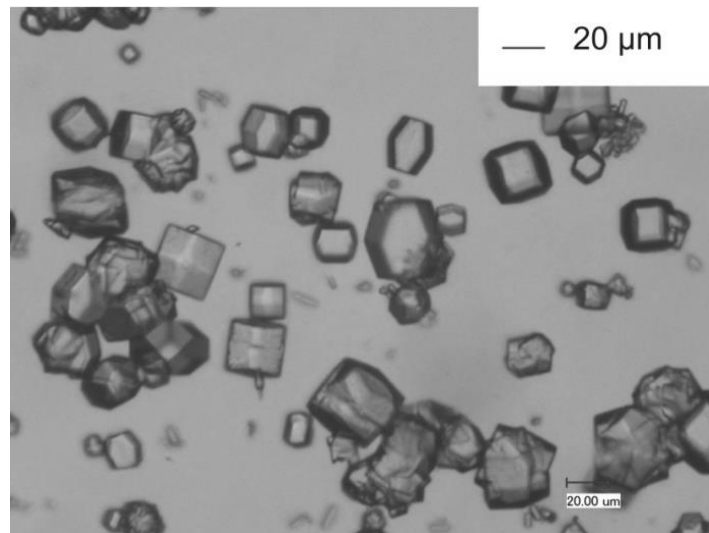


**Figure 5-37:** Crystals obtained with the parameters at center point of the previous fractional factorial design (see Table 4-3).

In this stage the experiments were designed in a central composite arrangement (see Table 4-5). It consisted of 16 runs with 2 center points, 8 cube points and 6 star points which values are shown in Table 4-6.

As the temperature of the wall was fixed at 274.5 K (1.5 °C), the initial temperature of the cooled surface was the same through the 16 runs. The final temperature of the cooled surface changed as well as the constant temperatures and times at those temperatures. Due to the interactions of the named parameters, the total time of the processes varied. Three temperature profiles are shown on Figure 5-38, which were applied in runs 2 and 6 (duration  $\cong 350$  min), 3 and 7 ( $\cong 220$  min), and in runs 9, 10 and 16 ( $\cong 260$  min). This has been done to evaluate if there is a directly relation between longer crystallization times and yields or crystal sizes.



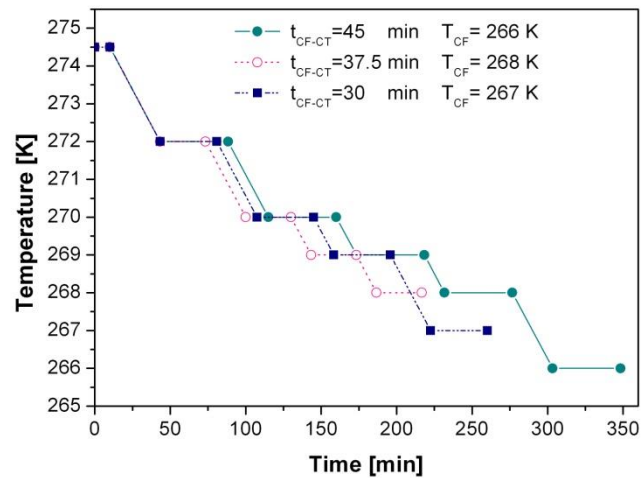


**Figure 5-38:** Three of the temperature profiles applied to the cooled surface in the central composite design (runs 2 and 6 ●, runs 3 and 7 ○ and runs 9, 16 and 10 ■).

The three evaluated responses yield, volume of ice ( $V_i$ ) and protein loss ( $P_L$ ), of the 16 runs are shown in the diagram of Figure 5-39. It can be observed that the values of the responses are closer to each other than in the previous  $2^{(8-4)}$  design.

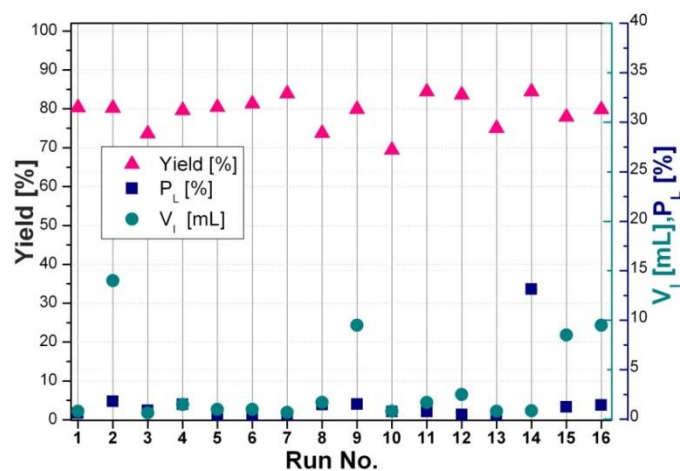


**Figure 5-39:** Values of three responses evaluated in the crystallization processes based on the central composite design.

The maximum crystallization yield of 84.4 % was reached in runs 11 and 14, followed by run 7 in which a yield of 83.9 % was obtained. The lowest crystallization yield was reached by run 10 with a value of 69.4 %, followed by the yields from run 3 and 8 with very close values of 73.6 and 73.7 %, respectively.

Very low volumes of ice were obtained in the most of the crystallization processes with exception of those obtained in runs 2, 9, 15 and 16. The protein losses of the processes had similar values in each case with exception of run 14 with a protein loss of 13.14%.

In order to show samples of the different kind of crystals obtained in the central composite design, four pictures are shown in Figure 5-40.

These crystals have tetragonal shape and present different sizes, the most visible are between 20 and 50  $\mu\text{m}$ . In these samples it is also possible to observe that the large crystals are accompanied by smaller ones. In some cases the small crystals are grouped, such as in Figure 5-40 (a), (b) and (d). At a first glance, the crystals produced in run 5 have the smallest size (see Figure 5-40 (c)).

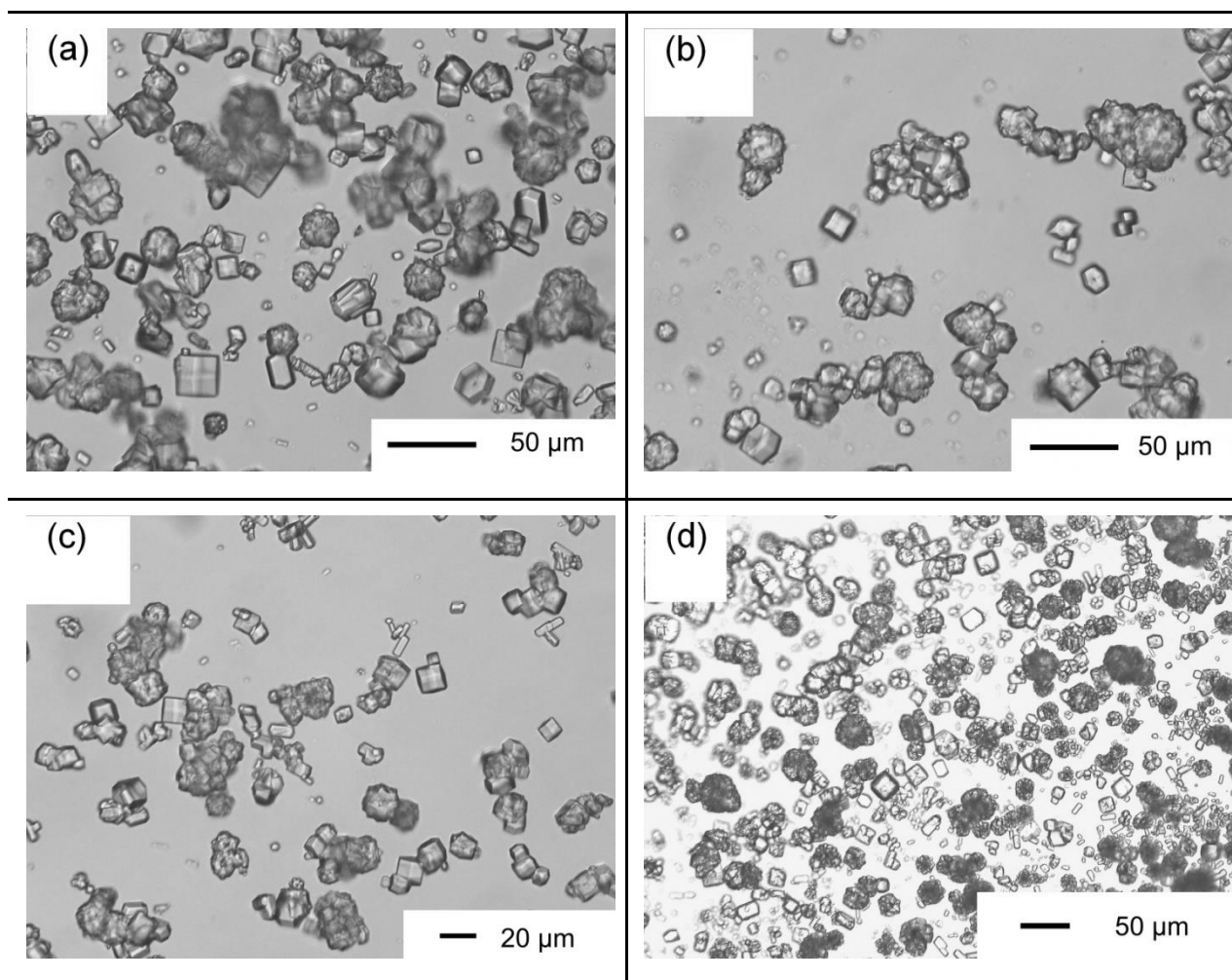


**Figure 5-40:** Lysozyme crystals obtained from runs 2 (a), 3 (b), 5 (c) and 11 (d).

The distribution of sizes of the crystals obtained in runs 2, 3, 5 and 11 are shown in Figure 5-41 as example of the results of the central composite.

The largest crystals were obtained in run 2 with a mean size of 25  $\mu\text{m}$ . Similar mean sizes were described by the crystals produced in runs 3 and 11. In agreement with the image of the crystals in Figure 5-40 (a), the smallest crystals were obtained from run 5 with a mean size of 18  $\mu\text{m}$ .

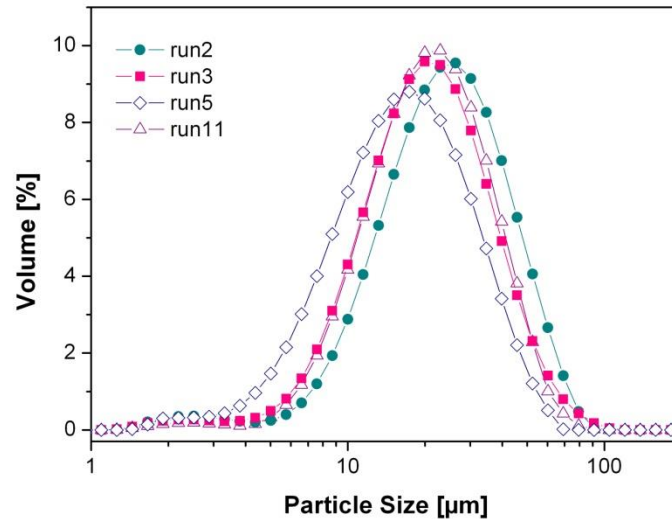


**Figure 5-41:** Size distributions of the crystals produced in four of the 16 runs of the series of experiment based on the central compositing.

For all four runs shown as examples here (Figure 5-41) in common, there is a presence of small crystals with sizes between 1 and 10  $\mu\text{m}$ . The small crystals can be described as a small pick beside the main picks of the larger crystals size distributions.

### 5.5.3.1 Surface Response

One advantage of the realization of the central composite design is the possibility of the optimization of a multivariable system for independent responses by the analysis of the collected information.

For this part of the optimization, the response yield has been chosen as target since it is an important criterion for the profit of industrial crystallization processes.

The surface and contour plots of the response “yield” have been obtained by the use of the “Response Optimization” function of the program STATISTICA [Sta02]. These results are shown on the right side of Figure 5-42 from top down. The pairs of conditions were:  $T_{CF-FT}$  - stirring (a),  $t_{CF-CT}$  - stirring (b), and  $t_{CF-CT}$  -  $T_{CF-FT}$  (c).

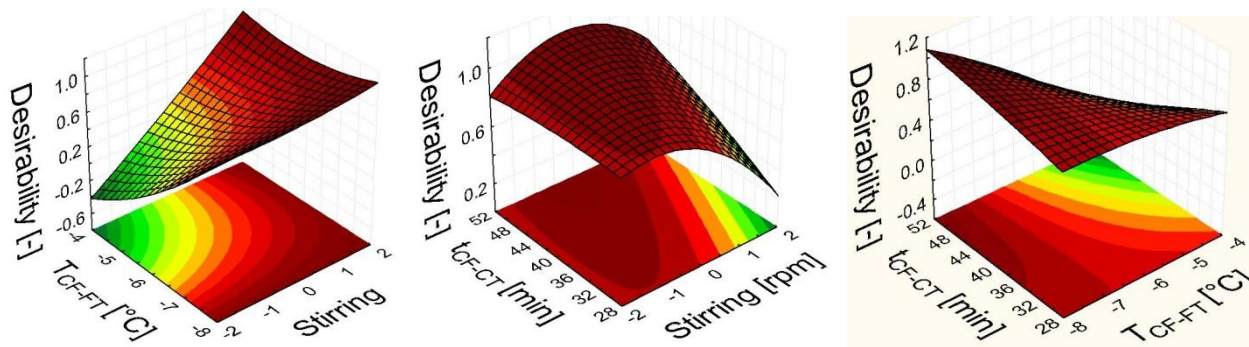


**Figure 5-42:** Response surfaces generated based on experimental results from the central composite design [Dia10d].

It can be observed that a broad range of values of time  $t_{CF-CT}$  lead to high yields (Figure 5-42, left). However, the  $T_{CF-FT}$  should be set lower than  $-5\text{ }^{\circ}\text{C}$  ( $268\text{ K}$ ) in order to get good yields, this in combination with stirring values between the center and high levels (values= 115 and 230rpm).

### 5.5.3.2 Desirability Profile

In the subchapter above, it can be seen that there is a broad range of stirring or time at constant temperature values ( $t_{CF-CT}$ ) that can be applied in order to get high yields. But these values should be also combined with the temperature of the cooled surface ( $T_{CF}$ ) in such a way that the other responses of the process are still within acceptable values. Therefore, it was necessary to complement the optimal value of the response yield with optimal values of responses volume of ice ( $V_I$ ) and protein loss ( $P_L$ ).

Therefore, in the second stage of the experimental strategy, the desirability function of the program STATISTICA [Sta02] was used to set optimal values for the dependent parameters  $V_I$  and  $P_L$ .

The values of maximum and minimum desirability are 1.0 (100%) and 0, respectively. The predicted values for these variables are related in that way that the response is set as close as possible to the optimal value. In the case of volume of ice  $V_I$  the optimal value is a maximum and for protein loss  $P_L$  the optimal is a minimum.

The suggested values of the independent variables can be observed in Figure 5-43. The optimal value at which the stirring variable should be set is 115 rpm. The final temperature of the cooled surface  $T_{CF}$  should go to  $-6.9\text{ }^{\circ}\text{C}$  and the time ( $t_{CF-CT}$ ) at which the temperatures of the cooled surface should be constant is of 44 minutes.

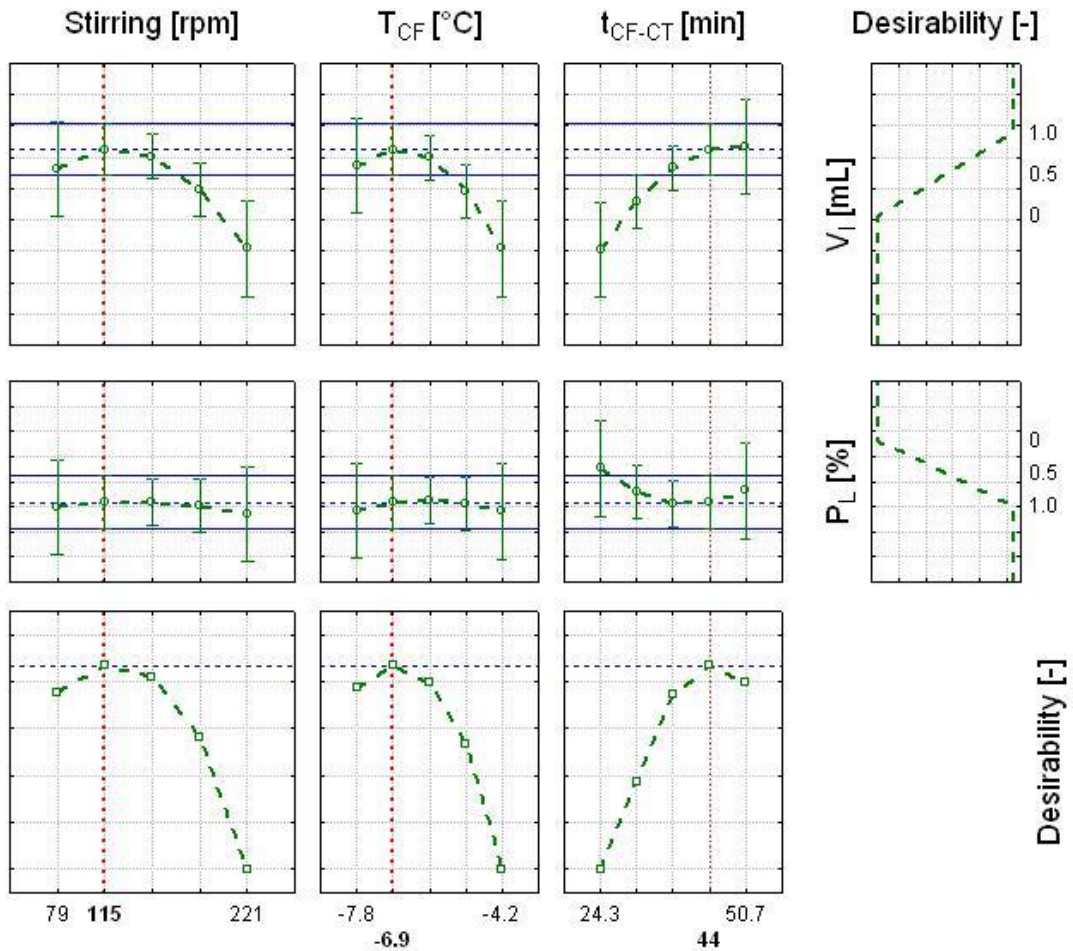


**Figure 5-43:** Profiles for predicted values and desirability for the responses "volume of ice" and "protein loss" [Dia10d].

The analysis by the desirability function and surface methodology (Figure 5-43) of the central composite experiment can be used to optimize, minimize or maximize any other response. This method allows the observation of how changes in the levels of the factors influence not only each of the dependent variables (responses)  $V_I$  and  $P_L$ , but also the overall desirability of both together.



## 6. Discussion

### 6.1 Determination of Pseudo-Phase Diagrams for Lysozyme

The pseudo-phase diagrams shown in chapters 5.3 and 5.4 were based on the data obtained from the screening tests (nucleation curve) and literature.

An exception are the pseudo-phase diagrams shown in Figure 5-13 and Figure 5-14, which were obtained by coupling literature data, and results from the screening tests and turbidity measurements. The estimation of the nucleation points in the screenings contains an uncertainty, due to the fact that they are detected by an optical method. The observed points of the nucleation curve found by this method showed a good agreement when fitted in one exponential curve together with those nucleation points measured by the turbidity method. This result reaffirms the validity of both methods for the construction of pseudo-phase diagrams to be used as process map, in the context of this work, in the solvent freeze out technology (SFO).

If all the built pseudo-phase diagrams are compared, it is possible to observe two common behaviors within them. The first one is that the width of the metastable zone decreases with the increase of the concentration of salt (NaCl). The second prevailing behavior is that the metastable zone becomes narrower as the temperature decreases which is quite frequent with good soluble compounds.

According to the definition of the pseudo-phase diagrams [Dre92], the description of the zone I or metastable zone width is strongly related to the kinetic properties of the crystallization and at the difference to the solubility region, they do not represent an equilibrium state.

It is possible to take advantage of these two phenomena in the application to the SFO technology. On one hand, as the width of the zone I (appropriated for crystallization) seemed to be wider if the salt concentration was decreased, the operating conditions of the system are also expanded which allows a better control of the process. On the other hand, the yield of crystallization can be increased since the use of higher protein concentrations is possible. Furthermore, the growth of the crystals can be supported by having the possibility of a better control of the conditions within the metastable zone.

A further significant advantage is that the use of less amounts of salt has a lower environmental impact, and this supports one of the aims of this research that is the minimization of the salt usage. The influence of the salt concentration on the metastable zone has also been observed and discussed in a further work [Mao12], in which the solubility and nucleation curves were

measured at ranges of temperature between 45 and 2 °C (318 and 275 K). The protein concentrations were between 4 and 50 mg/mL. The collected data are presented for pH values of 4.4 and 5.0, and these diagrams are in this work in Figure 6-1.

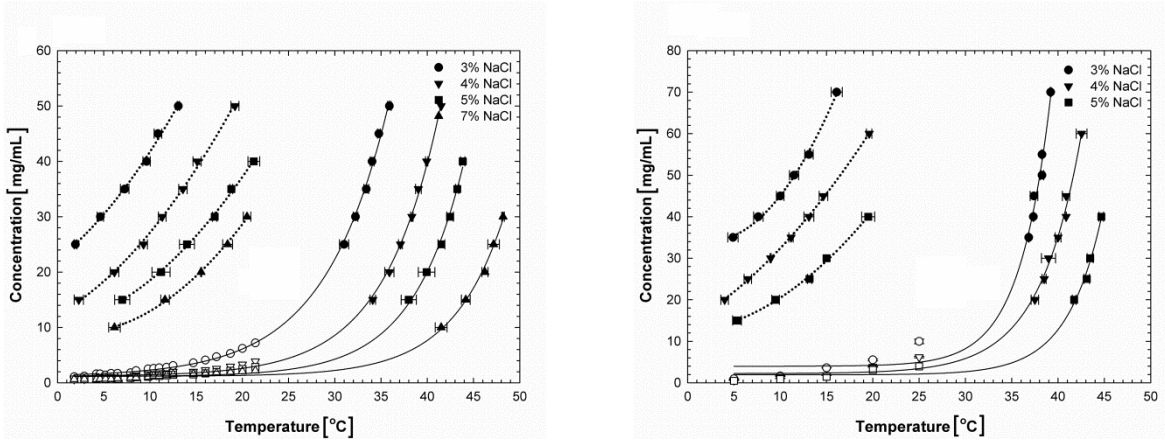


**Figure 6-1:** Phase diagrams [Mao12] of lysozyme in sodium acetate buffer. Left: pH 5.0. Right: pH 6.0.

It is possible to observe in the two diagrams presented in Figure 6-1, that there is a shifting of the solubility curves and of the nucleation curves by changing the concentration of salt to values of 3, 4, 5 and 7 %.

It is observed that there is a variation of the metastable width of each of the systems with the temperature. At low temperatures the metastable zone seems to be narrower than at higher temperatures. The change of the metastable zone with the increase of salt concentration can be better visualized in Figure 6-2.

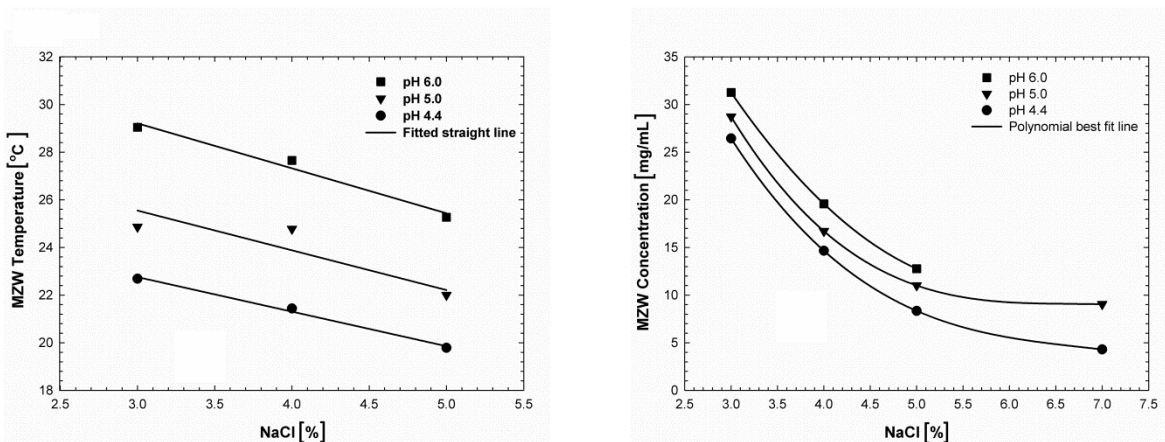


**Figure 6-2:** Left: Influence of NaCl concentration and solution pH on the MZW with respect to temperature level. Lysozyme concentration: 40 mg/mL. Right: Influence of NaCl concentration and solution pH on the MZW with respect to protein concentration at 5 °C [Mao12]



In order to support these results, the nucleation curve has been assumed to be the curve limiting the Liquid-Liquid metastable region (Zone II) of the generic phase diagram for protein crystallization (see Figure 4-2). Here it is useful to remark that the generic phase diagram is presented with inverted axis as T vs. C. In this work, it is assumed that the nucleation of the protein crystals takes place within the drops rich in protein presented in the L-L metastable region. The nucleation temperature in this study would then be similar to the cloud point temperature investigated for other protein systems, and reported by different authors, e.g. [Liu10, Mus97].

Due to the protein-protein interactions and salt-protein interactions, the crystallization conditions of a protein change with the composition of the system. The concentration of salt and therefore, the presence of ions can reduce the energy barrier of the diffusion of protein molecules from the bulk solution to the nuclei (more ions represent less protein – solvent interaction). Therefore, the attraction between molecules interaction is increased with increasing salt concentration.

The solubility is also affected by the protein-protein and protein-salt interactions. Therefore, the cloud point temperature (nucleation temperature) is shifted together with the solubility curve. To cite another example a literature reported phase diagram is shown on the left of Figure 6-3.

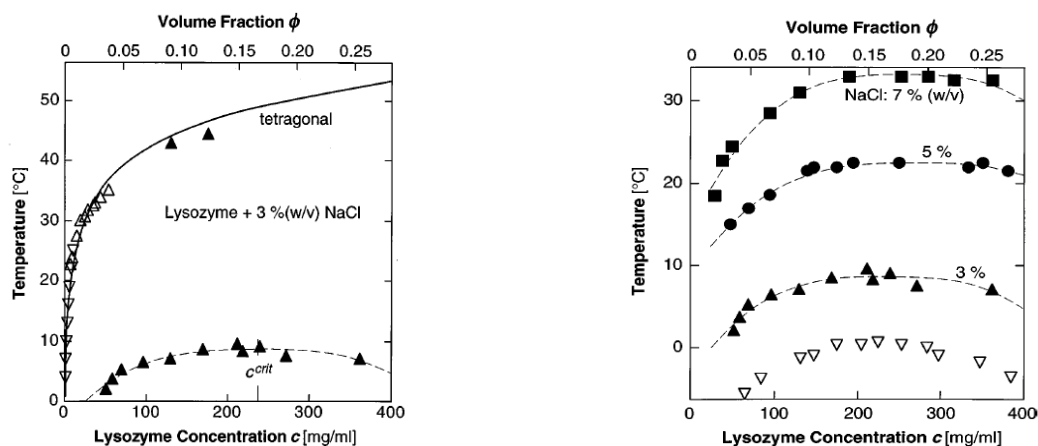


**Figure 6-3:** Left: Literature reported phase diagram for lysozyme with 3% NaCl pH=4.5. Right: Cloud point data for lysozyme at pH=4.5 and 6.0 [Mus97].

The position of the curve composed of the cloud points is shifted with the concentration of salt as it can be seen on the right of Figure 6-3. Therefore, the nucleation curve (cloud points) is approached to the solubility line narrowing the metastable region.

## 6.2 Crystallization of Lysozyme from Pure Solutions and Mixtures

### 6.2.1 Screening Tests

The observations of the protein solutions and solids formed during the screening tests were classified regarding the quality, into different groups as explained in chapter 4.2.2. The thermodynamic conditions which lead upon formation of an appropriated crystal were located in the presented pseudo-phase diagrams.

Crystals with good morphologies and sizes were formed in the screening tests carried out for pure lysozyme when the concentrations of the salt were 3% and for a large range of protein concentration. The sizes of the crystals were larger after the application of 3 wt. % of salt. Moreover, good morphology of the crystals was observed in a large range of protein concentrations, as it can be observed in the pictures of Figure 5-3.

Unlike the results obtained when the amount of salt used was 4 wt. %. The size of the crystals were smaller and the range of application of initial protein concentration was smaller because new nucleation was observed with an increase in the protein concentration and decreasing experimental temperature, see Figure 5-4. In the solutions with concentrations of 2 to 12 mg/mL of lysozyme with experimental temperatures between 280 and 266 K well shaped crystals were formed when the concentrations of salt was 4 % wt. But for the concentration of 6 % of salt, most of the crystals presented poor qualities.

The use of 6 wt. % of salt led to more irregular crystals, see Figure 5-5. The formation of spherulites and sea urchin were increased when the incubation temperatures were below 269 and the protein concentrations higher than 7 mg/ mL.

According to the chapter above the width of the metastable zone is decreased with increasing - salt concentration, which in turns means that the nucleation of the protein crystals occurs earlier and therefore in a less controlled way. The protein-protein interactions are significantly stronger and the conditions of the system enter once more into the Zone II where the formation of sea urchin takes place (see Figure 4-4).

In the screening tests for crystallization of lysozyme from the ovalbumin-lysozyme mixture, the crystals obtained at pH 5.0 describe a good defined shape and uniformity of the size and salt concentration in this case did not show a visible influence on the morphology and amount of crystals.

But if the crystals are compared with those produced in pure solutions, rounded edges on the crystals can be identified.

This phenomenon could be explained by the presence of ovalbumin as foreign substance. Impurities influence significantly crystal growth because they may affect the kinetics of crystal growth of each of the crystal faces and consequently the crystal habit [Dav00]. It is also possible that an uncontrolled supersaturation in the system lead to imperfections in the crystal lattices.

The supersaturation can be approached from two sides, the temperature and the composition. The possible influence on the composition by the addition of ovalbumin has been discussed in the paragraph above. With respect to the influence of the temperature on the supersaturation, and therefore on the crystal morphology, the crystals were cooled at the same rate as in the case of the pure lysozyme solutions where the crystals presented very well shaped tetragonal forms. Therefore, the influence of the temperature on the “uncontrolled supersaturation” can here be neglected.

### 6.2.2 Solvent Freeze Out -SFO

Running different SFO process varying the parameters arbitrary has been useful to get a preliminary insight to the influences in the crystal products. An overview of the results of the four examples is available in Figure 5-18 and Figure 5-19. The quality of the crystal products can be significantly influenced by changes in the temperatures of the cold finger or of the wall, by addition of stirring, by the cooling rates, among the other conditions. For these reason some conditions were constrained and investigated later in a systematic way in the optimization strategy which results were presented in chapter 5.5 and their respective discussion can be find by following (chapters 6.3 and 6.4).

In general, the growth of the crystals was enhanced not just by the application of adequate compositions, but also due to the permanent maintaining of the driving force for crystal growth. This driving force was provided by proper supersaturation values, cooling effects and by the effect of the salt (salting-out).

After the successful generation of crystals out of the protein mixture in the screening tests, the conditions for the SFO process were adjusted to lead successfully to the formation and growth of lysozyme crystals in the supersaturated solution. The mean sizes of the crystals were larger than those for the crystals obtained in pure protein solutions.

The time of crystallization for the mixture experiments was significantly larger than for the time of the pure solutions this might have allowed the growth of the crystals as well as the cooling effect and the effect of the salt (salting-out).

The crystals presented a similar rounded shape as in the screening tests, but in this case it is not possible to neglect the influence of the temperature in the control of the supersaturation. The geometry of the solvent freeze out SFO equipment used for the crystallization of lysozyme from mixtures differs to the geometry of the equipment used for the pure solutions. The distance between the cold finger and the wall of the vessel is shorter in the equipment 2 (see appendix II) used for the mixture trials. The contact between the cooled surface and the bulk solution is thus higher than the respective contact in the equipment 1 used for the crystallization of lysozyme in pure solutions. This is visualized in Figure 6-4, in which the heat transfer area in the equipments 1 and 2 (appendixes I and II) is corresponding to volume changes in the container as shown.

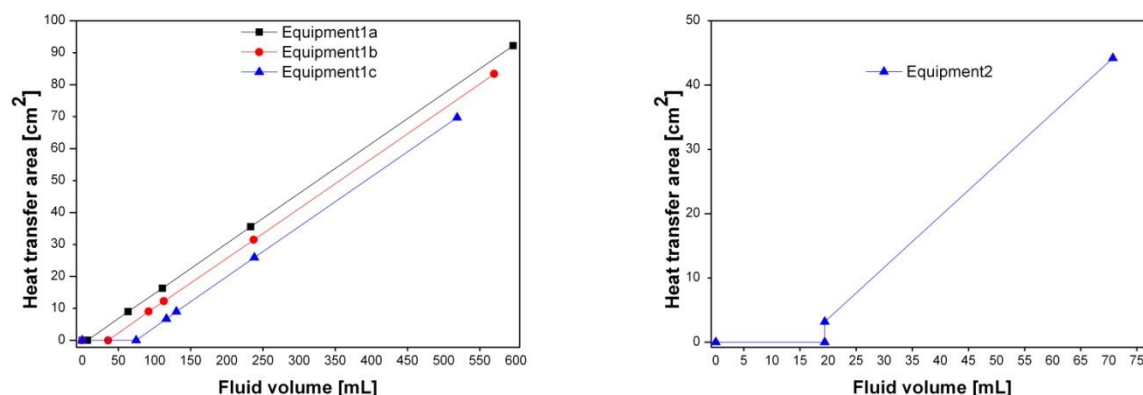


**Figure 6-4:** Diagrams of cumulative volume vs. wetted area of the cold finger in two kinds of SFO equipments. Left: equipment 1 with 3 lengths of cold finger a, b and c. Right: equipment 2. See appendixes I and II.

The ratio between the fluid volume and the heat transfer area is 0.1 in the equipment 1a and 0.58 in the equipment 2, a significantly higher value.

The homogeneity of the size distributions (Figure 5-26) is decreased by the presence of a significant amount of small crystals. If the crystals on left side of Figure 5-25 are carefully observed, it is possible to identify small crystals attached on the surface of a single crystal. The small crystals are also visible on the right picture (Figure 5-25), but in this case they are suspended within the mother liquor and far away from the single crystal. The small dried crystals have high electrostatic forces which attract them to the larger crystals (agglomeration phenomena).

During the drying (evaporation of the solvent) of the filtrated crystals, supersaturation could take place on the wetted surfaces of the small crystals and new crystals could have been formed or nuclei already present in the solution could have further grown. This phenomenon has been

also discussed by Müller in the studies of the nature of lysozyme crystals and their solubility behavior [Mül12].

Moreover, as mentioned above this crystallization process was carried out without stirring. It could be also possible that small crystals fall down to the bottom of the vessel and did not have enough transport of material on their surface to grow up to larger sizes.

With regard to the stepwise changed temperature profile of the cold finger, in the first 5 h the formation of a significant amount of ice took place. Once the solution was concentrated, it was kept at 266 K for 10 hours and the further growth of the crystals held (see Figure 5-24). It can be assumed that during this time, inclusions of protein solution within the ice migrated back to the mother liquor. It was possible to observe a change in the color during this time from milky to transparent. The migration of liquid inclusions occurrence has been observed in solid layer melt crystallization processes and its discussion can be found in literature [Hen01, Sch93].

### 6.3 Effects of Parameters and Interactions on Process Responses

The analysis of the results from the fractional factorial design revealed the effects of the process parameters on the responses in the first stage of the optimization strategy. The discussion on these effects is presented in the following paragraphs.

#### Response Size (L):

This response was influenced at most by the final temperature of the cooled surface ( $T_{CF-FT}$ ), the concentrations of salt ( $C_S$ ) and protein ( $C_P$ ), and the cooling rate of the cooled surface ( $dT/dt$ ) as presented in Figure 5-36 (a). In fact, this set of conditions determines the supersaturation of the protein solution at actual states, mainly the  $C_S$  and  $C_P$ .

At high supersaturation values the nucleation rate is faster than at low values [Oha73]. Therefore, the negative but strong effects of  $C_S$  and  $C_P$  and the positive effect of  $T_{CF-FT}$  are evidences that few nuclei could be formed at low supersaturation. Those could then grow to large sizes, if furthermore a driving force for crystal growth was continuously applied to the system, which means if the conditions were pushed in the middle region of the metastable zone. This is the reason why the supply of higher cooling rates ( $dT/dt$ ), in combination with the supersaturation values, enables the conditions of the system to remain in the region for crystal growth. The control of the crystal growth is lead as well by the subsequent cooling of the solution in a moderate rate at the front of the ice layer, besides to the removal of water.

Stirring showed a minimal influence on the size of the crystals in the results shown in Figure 5-36 (a). Here it is not neglected the influence of the fluid dynamics on the distribution of material, just that the effects of other parameters shown to be more significant.

#### Responses Volume of Ice ( $V_I$ ) and Protein Loss ( $P_I$ ):

The addition of stirring showed a major influence on these two responses (see Figure 5-36 (b) and Figure 5-36 (c)). Stirring had a negative influence on magnitude of the formed ice layer ( $V_I$ ) as it can be seen in the Pareto diagram in Figure 5-36 (b). At the same time stirring showed a positive effect on the purity of the ice (decreasing protein loss). In the Pareto diagram displayed in Figure 5-36 (c) the strong negative effect of stirring on the protein loss ( $P_I$ ) is observed.

The fluid mechanics of the suspension had an effect on the kinetics of nucleation and growth of the continuously forming ice layer. This positive effect of the stirring on the purity of the crystal layers was investigated by some authors (e.g. [Mee02]).

This phenomenon can be cleared by taking a look insight in the interfacial region. This region corresponds to the area between the cooled surface -later ice surface- and the bulk solution. This region is known as diffusion layer, as well as, temperature boundary layer. Both, the crystal layer and the interfacial layer are strongly related to the fluid dynamics, they decrease in thickness, but increase in purity, with increasing agitation [Mee02].

The negative effect of the stirring on the volume of ice shown on the Pareto diagram in Figure 5 35 (b) is therefore supported by the premise that thickness of the diffusion boundary is decreased with addition of convection. Therefore, the amount of impurities is consequently reduced in the front of the growing layer, which leads to ice layers with high purity, but lower magnitudes due to the better equalization of temperature.

#### Response Yield ( $\dot{M}$ ):

The yield of protein crystallization was increased proportionally with the addition of stirring as it is displayed in the Pareto diagram of effects corresponding to the response yield in Figure 5-36 (d). The presence of agitation in the crystallizer contributed to the homogeneous distribution of the material throughout the protein solution profiting the mass transfer.

Besides the mass homogenization, stirring increased the energy input in the system and as a consequence produced a reduction of the metastable zone width. The addition of stirring should be, therefore, moderated in such a way that the yield of crystallization is profited, but new nucleation do no take place. Under specific conditions this new nucleation could be detected by the presence of a certain amount of small crystals as it was observed in Figure 5-31

(a) or in Figure 5-33. When new nucleation took place there was a small pick was observed in the size distribution diagrams, response which is discussed as follows.

In Figure 5-36 it is also possible to observe that an increase in salt ( $C_s$ ) and protein ( $C_p$ ) concentrations lead to higher yields of protein crystals, but simultaneously lead to a lower volume of ice. As mentioned above, the initial and actual values of the supersaturation in the protein solution influence the size, number and quality of the protein crystals. Nevertheless, the crystallization of the water out of the melt (“the rest”) turns to more difficult as the concentration of impurities in the melt increase. Therefore, a binary phase diagram is used to explain this crystallization. If the sketch of the general melt phase diagram is observed on the left side of Figure 2-5, it is possible to recognize that if the fraction or composition of “the rest” in the melt is increased, the volume fraction of water is decreased and the temperature of the phase transition should be decreased as well.

#### Distribution of the crystals sizes:

As it has been mentioned the supersaturation values had a stronger statistical effect on the mean sizes of the crystals than stirring. However, the fluid mechanics in the suspension is relevant for the crystal size distribution [Gar95], hence it is expected that stirring in interaction with the other process parameters, influences the distribution of the crystals sizes.

The appearing of small peaks beside the main one in the size distribution was observed when high supersaturation values were applied (since the nucleation rates increase proportionally), and at the same time high speeds of stirring (high energy input induce nuclei production [Oha73]). Therefore the conditions of the system were moved out of the region appropriated for crystal growth (middle of metastable zone or Zone I).

When the retention time of temperature of the cold surface was kept longer at constant values ( $t_{CF-CT}$ ), the formation of volume of ice increased as shown in Figure 5-35 (b). The protein included in the ice is increased as well (protein loss), see Figure 5-35 (c). The impurities migrate from the crystal layer, back to the bulk material where the concentration or temperature equilibrium is then found [Hen01, Mee02, Sch93].

There is still a higher protein loss with the increment of ice when longer times at constant temperature are applied, because even in 45 min (high value) the migration of the protein from the ice layer to the mother liquor takes longer time than the uptake of protein into the ice layer.



#### 6.4 Optimization of the Process Parameters in the SFO Crystallization of Lysozyme

The importance of the first stage of optimization –fractional factorial design- was not only in the possibility of finding the most influencing factors, but also in that the addition of the 2 center points to the design. It allowed the possibility to evaluate the curvature of the model, this mean if the assumed linearity between response and factors was correct.

The linear effect of the process variable time at constant temperature ( $t_{CF-CT}$ ) was of great significance for the responses Vi and PL, as it can be observed in the respective diagrams on Figure 5-36. But it did not reveal a strong influence on the variables mean size (L) and yield ( $\dot{M}$ ). Nonetheless, information obtained from the statistical analysis revealed that the factor time might have a significant influence on the responses when it interacts with the other variables and it might describe a non linear effect. For instance predicted values by a linear relation were plotted against observed values to be compared with a non-linear relation, this results are presented in Figure 6-5.

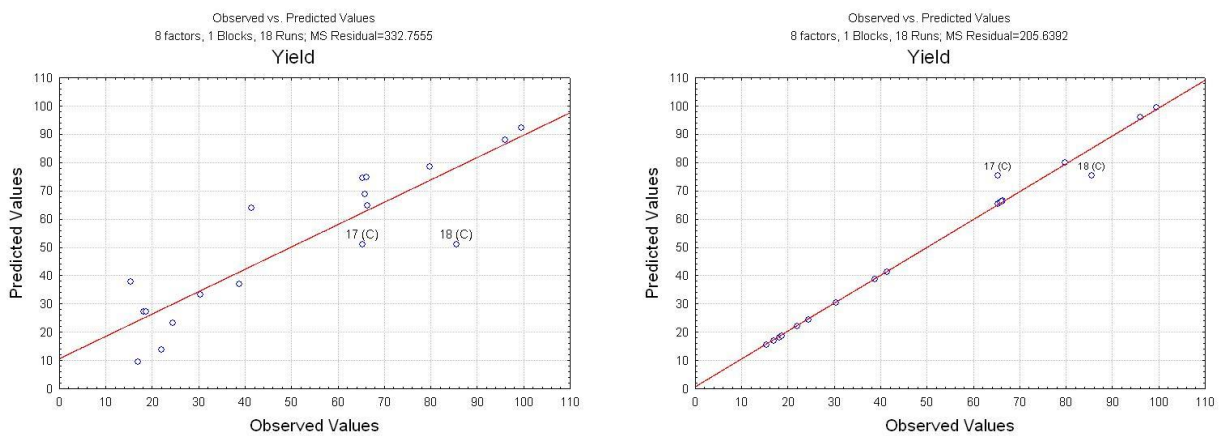


**Figure 6-5:** Diagram of predicted against observed values of the responses. Left: Linear model. Right: Quadratic model.

There is a better fit of the observed values and the predicted ones when a non-linear model is applied showing a better statistical significance. For this reason the independent variable ( $t_{CF-CT}$ ) was chose together with the variables stirring and final temperature of the cold finger ( $T_{CF-FT}$ ) to optimize the process in the second stage –the central composite-.

Once the central composite was carried out, it was possible to obtain the real model that adjusted the observed and predicted values with the best accuracy for the dependent variables yield. Therefore, it was possible to construct as an example the response surfaces for the dependent variable yield (Figure 5-42), with a desirability of 1.0 for 100%.

Consequently the desirability function to find the optimal responses of the process  $V_I$  and  $P_L$  by adjusting the independent parameters at optimal values (see Figure 5-43). These two responses should be optimized in parallel, to find the optimal set of conditions that lead to a desirability of 1 for maximum volume of ice and 1 for minimum protein loss. The rest of factors such as cooling rate,  $T_w$  and length of the cooled surface, were set at the center values.

### 6.5 Considerations on the Design of Solvent Freeze Out Process

This technology can be proposed as a good alternative for the production of industrial proteins. Some relevant aspects with regard to the protein activity and purity which should be considered at the moment of scaling up the process are shortly discussed here.

The nature and the purity of the protein crystals produced by the SFO technology was proven and shown in the results of the SDS Page tests presented in Figure 5-22 and Figure 5-27. The enzymatic activity of the proteins was retained after the crystallization processes with values between 90 and 99.9% (e.g. see Figure 5-30). This values were considered acceptable in the context of this work and therefore, further optimization of the retained activity was (to 100%) was not carried out. The losses of activity could be caused by the contact of the protein molecules in solution with the growing ice. Former investigations on the activity of lysozyme crystals founded in the ice layer, showed an inherent decrease of the protein activity [Ryu10a, Ryu10b]. The growth rate of the ice crystal and its influence on the activity of the proteins should definitely be taken into account in future research.

Beside this open question, the SFO technology describes further positive results such as those obtained in the application of 3 wt. % of salt. It can be affirmed that the required amount of salts has been minimized, together with the crystallization time. In the first column of Table 6-1, the main scope of this technology in the present investigation are listed and summarized. In the second and third column two of the alternative technologies for protein separation are also reviewed in an example for lysozyme.

**Table 6-1:** Performance of the SFO technology in comparison with two alterative methods.

SFO	IEC [Chi90]	Salting Out [Cha00]
Production capacity 1.0 g/h 3-5 h pH=4.4 (crystallization from pure solution) 17 h p.H=5.0 (crystallization from protein mixture*) (500 mL solution) 65 to 99* % yield	Production capacity 0.22 g/h 5-13 h (isolation from pre-treated egg white solution) (500 mL solution) 85 to 95 % yield	Production capacity 0.07 g/h 72-96 h pH=9.5 (isolation from egg white) 24 h p.H=5.0 (crystallization from pure supersaturated solution) <u>60 to 80 % yield</u>

It is important to remark that not all the three processes allow the obtaining of well shaped and active protein crystals. For instance, it is often necessary to subject the protein product of the IEC to a SEC (size exclusion chromatography) run for a better purification. In the case of salting out, the protein crystals describe a lost of the activity eventually [Mül12]. By SFO, crystals with high activity, good size distributions and good stabilities are obtained with great reproducibility from batch to batch if the conditions of the systems are well controlled. As counterexample, the yield and volume of ice obtained in 15 runs operated at the same conditions but with failures in the operating conditions are shown in Figure 6-6.

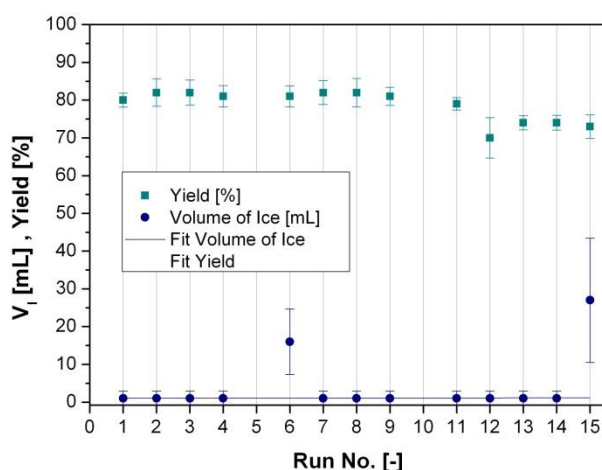


**Figure 6-6:** Yield and volume measured in 15 SFO batches with the parameters set at the same values.

The obtained volume of ice was about 1 mL in 13 runs, but it was 15 and 25 mL in two runs. In these two runs, the 6<sup>th</sup> and 15<sup>th</sup> a common problem during operation was identified.

The double walled beaker was not completely sealed and there was a significant influence on the temperature of the protein solution. Therefore the driving force for crystals growth was higher and therefore the volume of ice greater. This failure seemed to do not reflect an influence in the yield of crystallization as observed in Figure 6-6. It is possible that the crystallization yield was not significantly affected but the distribution of the crystals sizes. Pictures of a sample of crystals from the 15 runs is shown on the left side of Figure 6-7. They present recognizable tetragonal shapes but with diverse sizes.

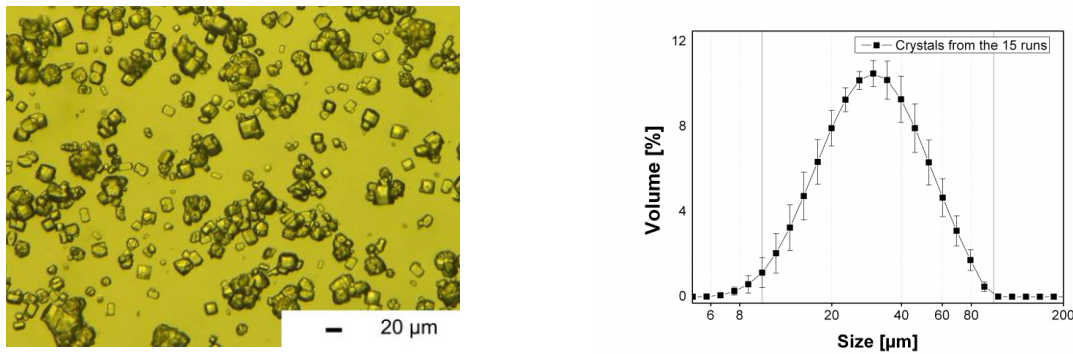


**Figure 6-7:** Left: Lysozyme crystals obtained in of the 15 runs. Right: Size distribution of the crystals from the 15.

On the right side of Figure 6-7, the size distribution is shown. The sizes of the crystals are mono modal distributed, but not homogenously. As it has been discussed in chapter Figure 6-3, the interaction between process parameters and their control have a strong influence on the process responses such as on the product size.

Due to the importance of the knowledge of the phase diagrams in crystallization processes, they were required for the development of the SFO technology. The temperature ranges of this process have been reported between 277 and 266 K. As there was a lack of solubility diagrams accompanied with nucleation data at certain conditions of interest in this study, these phase diagrams were constructed for lysozyme concentrations between 2 and 15 mg/mL, with salt contents of 3, 4 and 6 % (wt) of NaCl in sodium acetate buffer with pH value of 4.4. The use of results from screening tests and data collected from microscopy observations allowed the construction of the pseudo-phase diagrams, some of them where later complemented with data obtained from turbidity measurements.

In an early stage of this work it was possible to increase the size of the crystals up to 60-80 μm, that is approx. 30 % bigger compared to those obtained by the immediate previous investigation in which also salt concentrations of 5 % (wt) were applied [Ryu10a]. Several crystallization runs by the freeze out technology were carried out varying the temperature profiles of the system and by operation of the process under the guidance of the pseudo-phase diagram of 4 wt. % NaCl, with operation times within 5 and 6 hours. At this point it was observed that it is possible to control nucleation and crystal growth by controlling temperature of the cold finger and the improvement of mass transfer by implementation of a stirrer was observed. The production of crystals described good morphologies and crystal sizes of approximately 70 μm. Nevertheless, the yield of crystallization was low and had to be improved.

Therefore, the process had to be improved and even more, had to be proven not only for pure protein systems but also for mixtures of proteins.

In consequent the solvent freeze out technology was presented here as an alternative method for protein purification. Hen egg white lysozyme was purified by crystallization out of a lysozyme-ovalbumin mixture. The nature and purity of the lysozyme crystals was proven by SDS PAGE and there was an absence of contamination of ovalbumin within the crystals. The activity of the crystal was preserved up to 94 % of the original enzymatic activity. One valuable finding is that the crystals produced by the SFO process presented similar sizes (around 100  $\mu\text{m}$ ) and morphologies like those produced in micro-batch crystallizations during the screening tests. The duration of the SFO process was of 15 h in an advanced process, which is 9 h less than the duration of the screening tests, and the production of the crystals was in mass certainly higher. For this precise application, pseudo-phase diagrams were also built for systems containing lysozyme-ovalbumin and NaCl in 3 and 4%, with pH values of 4.4 and 5.0. By the use of this information it was possible to control and improve the process in terms of higher yields from a preliminary test to an advanced one. The use of the pseudo-phase diagrams was relevant when at the same time different temperature profiles were applied.

The optimization and reproducibility aspects of this technology were successfully achieved. Lysozyme crystals have been adequately obtained out of pure solutions and protein mixtures by the use of the technology. The activity of the protein was kept up to 99 % after the freeze out crystallization from pure solutions.

The most influencing factors on the responses were found by performing a multi-factorial design, from which the results gave valuable information for the application of modifications in the process toward a desired response.

It was possible to set the process variables at values which led to the desired response such as high yield, low impurity contents in the ice layer or larger crystal sizes and maximum volume of ice.

Moreover it was found that variations in the geometry of the equipment influenced significantly the responses of the process. For instance, an increase in the surface of the cold finger could lead to high yield of crystallizations if to increase the yield is a target.

The Solvent freeze out crystallization is conducted within 3.5 and 7 hours, which is a relative fast method and the amount of salt used has been reduced down to 3 % in consequence to the aim of having a less negative environmental impact.

In regard to the supersaturation values, the results from screening tests can be use with high reliability in the optimization of the solvent freeze out. Determined ranges of supersaturation values which lead to very good quality of the crystals in the screening tests were located as ideal path for crystal growth in pseudo-phase diagrams. The correct use of this information would ensure the same performance in the SFO. The points of attention in the solvent freeze out lay on the control of the temperature profiles of the cooled surface, time and the fluid dynamics.

The solvent freeze out (SFO) crystallization process has been proposed for protein crystallization, and additionally has been optimized for a maximal performance in the case study of lysozyme. This optimization was carried out by a systematic design and analysis of experiments, together with the application of essential information on supersaturation levels for protein crystallization. The optimization which can in principle be applied for SFO crystallization of any kind of protein from a pure protein solution or protein mixture consists of 6 general steps. These steps [Dia10d] are:

- Collect thermodynamic and kinetic information of the crystallization of the solvent and protein (phase diagrams).
- Identify the parameters governing each of both crystallization processes in SFO equipment.
- Identify and estimate the values of the responses to be optimized.
- Fix the range of the parameters values based on the information collected in the first two points.
- Design statistically the experiments for the identification of the most relevant parameters e.g. fractional factorial designs. Then, use the response surface methodology for finding the optimal values of parameters.
- Use the collected information to design the final process.

The results of the strategy agreed with the theoretical principles of mass crystallization. However, it has been crucial in order to quantify the parameters and allow the control of the crystallization process.

With regard to the performance of the solvent freeze out process, it would be desired to optimize the mechanic separation of the crystals. Some studies should be added to the retention times and the influence of capillarity effects. Furthermore, investigation on the use of

vacuum filtration would be of valuable interest, mostly for reducing filtration time. But they should consider effects on the activity of the crystals.

There is still an open question with regard to the roundness of the lysozyme crystals obtained from the protein mixtures. Just hypothetical answers have been proposed, but it is not clear if amorphous layers are present within the crystals, if the control on the supersaturation was not optimal or if this is an inherent result from the protein-protein interactions.

A further open question is if the reduction of the activity of the crystals is due to the direct contact with the ice. Crystallization trials with additives which inhibit the effect of the ice on the proteins would be desired.

Preliminary experiments on crystallization of lysozyme from ovalbumin and BSA protein mixtures have been done and proven in micro-batch experiments, but not reported in the context here. The crystallization of lysozyme is therefore suggested for SFO technology.

Preliminary experiments on crystallization of transglutaminase have been done, but not optimized [Rüd11, Lei11]. It is suggested to continue the research on the applicability of the SFO process for the crystallization of this protein. The use of the SFO equipment 3 is suggested because due to the low scale it is possible to save protein material and therefore the research efficiency can be increased. The technical sketch of this equipment is provided in appendix III,

The crystallization of lysozyme directly from the hen egg white would be a step further, perhaps with the addition of lyophilization step to reduce the amount of water in the egg.

Moreover, the addition of a second cold finger or processes in series could be a right decision if the mass production of process is considered necessary.



## 7. Conclusions

New pseudo-phase diagrams constructed based on experimental conditions are presented in this work, providing information on the nucleation conditions for different lysozyme systems.

The availability of the knowledge of suitable conditions for protein crystallization in pure solutions and mixtures permitted the operational guide in the solvent freeze out SFO crystallization process. By this process tetragonal lysozyme crystals were produced and additionally characterized in order to describe the process performance regarding the quality of the crystal product.

A path for the optimization of the SFO crystallization process applied to proteins with lysozyme as case study has been proposed. This path was based on three main steps, the identification of crystallization conditions, the statistical analysis of the process parameters and its optimization in two stages based on the design of experiments. Valuable results were obtained, as follows: maximization of volume of ice and minimization of protein loss on the ice layer and maximization of the crystallization yields.

The solvent freeze out technology is presented here as an alternative method for protein purification. The potential of the SFO for the purification of proteins has been introduced by proving the purification of lysozyme by its crystallization from a protein mixture lysozyme-ovalbumin as a test example. The possibility of application of this technology for protein purification on an industrial scale is given, since the amount of salt used has been minimized, together with the crystallization time. Additionally, the scale up of the process could be straightforward since the two composing processes of the SFO -the solution and the solid layer melt crystallizations- are well known industrial processes. The information concerning equipment and scaling up can be found in literature, (e.g. [Sch93, Ste03]).

For a hypothetical new protein system the proposed optimization strategy can be reproduced, since on laboratory scale the process requires only simple equipment. And if new information on the solubility and nucleation of the protein should be collected, some fast and efficient methods for their determination have been proposed here.

A very important fact that should be here addressed here is that the nature and purity of the lysozyme crystals was proven. In the case of the SDS PAGE analysis from the lysozyme crystals obtained out of the protein mixture, no contamination of ovalbumin was detected. Furthermore, the lysozyme crystals preserved up to 94 % of the original enzymatic activity in the trials performed with protein mixtures and up to 99% in those performed in pure solutions.

## 8. Summary

Proteins are macromolecules, present in and all around our life, in food, cosmetics, and medicaments and nowadays even in packing films. Therefore, Industry needs enzymes for the production of those fine chemicals, as reflected by the demand in the global market.

Current methods used in protein extraction such as chromatography, precipitation by salting or drowning out or evaporation, possess some disadvantages like such as requiring high investments and operation costs, long operation times and high temperatures or the use of large amounts of salt.

A good target process for protein extraction and purification on industrial scale is crystallization, because it offers the integration of purification, concentration and even in some cases formulation in one step.

Industrial crystallization processes must be efficient; they should possess good reproducibility and be environmentally friendly, meaning requiring low amounts of salts, energy and time.

The solvent freeze out SFO is a novel technology with great potential to fulfill industrial requirements. In this process, the crystallization of the proteins is enhanced by three effects, cooling, water removal and salting out. The advantage here is that by increasing the effects of cooling and water removal the salting out effect can be reduced.

This method is a combination of solid layer melt crystallization and solution crystallization. By means of the solid layer crystallization a protein solution is concentrated and a consequence supersaturated, giving the possibility for the protein crystals to be formed and grown within the solution.

The separation of the water from the melt is due to its phase change (liquid to solid) and a consequent growth of a crystal layer perpendicular to the cooled surface in direction to the bulk of the melt. Since it is possible to control the temperature of the cooled surface and therefore the temperature in the interface, the crystal growth rate can be controlled, which is around 1000 times faster than the crystal growth rate in suspension processes. Nonetheless, due to this high driving force, contaminated liquid melt can be entrapped in the solid layer.

In the solution, the protein crystals grow in the melt at very low rates leading to very pure products. In this process the control of the temperature and supersaturation is an important point of attention for nucleation and crystal growth, because new nucleation or dilution of the crystals should be avoided.

In order to take the best from the SFO technology, the before mentioned problems of melt and solution crystallization were minimized. The technology has been developed and further optimized in terms of product quality and yield. The amount of salt was minimized together with the time and energy.

Very relevant achievements were to define the region of conditions suitable for crystal formation and growth, and consequently the maintenance of those conditions during the crystallization process. It has been here, where the phase diagrams appeared directly related to the crystallization process.

Different phase diagrams were constructed based on experimental conditions, which consisted of solubility data accompanied by the nucleation ones. In this case study, lysozyme, the nucleation values were determined at low temperatures by screening tests conducted in micro-titer plates and analyzed by light microscopy. The solubility values were extrapolated from literature data. At higher temperatures, the solubility and nucleation data were measured by the use of turbidity measurement methods.

Despite the structural complexity of proteins their crystallization is still governed by thermodynamics and kinetics. Therefore, the knowledge of the appropriate conditions was used as a process guide in further crystallization processes of lysozyme by the SFO.

The parameters involved in the process and the crucial interactions which affected the characteristics of the final product the most were identified. The characteristics of the product concern the crystal size distribution, the total crystal mass which determines the yield of crystallization, the mean crystal size, the purity and the activity of the protein crystals.

The generation and maintenance of an adequate supersaturation in the crystallizer, together with the suspension fluid dynamics were identified as crucial parameters for the kinetics of the nucleation and growth of the crystals.

Moreover, an experimental strategy was carried out by use of pure lysozyme solutions as a model. As a result, a set of parameters was conformed in order to get high yields and by use of the desirability function, maximum volumes of ice and minimal protein loss were also achieved.

The potential of the SFO for the purification of lysozyme by crystallization was proven. Protein mixture lysozyme-ovalbumin was chosen as a case study. Lysozyme crystals were produced with high purity and enzymatic activity. This technology is therefore presented here as an alternative method for protein purifications since the amount of salt required is low, the crystallization time is short and the scaling up of the process might be straightforward.

## Nomenclature

$C_x$	Concentration	[mg/mL]
$C_{eq}$	Concentration of the protein solution in equilibrium	[mg/mL]
$C_p$	Concentration of lysozyme	[mg/mL]
$C_s$	Concentration of sodium chloride (NaCl)	wt. %
$C_{oval}$	Concentration of ovalbumin	[mg/mL]
$dT/dt$	Cooling rate applied to the cooled surface (cold finger)	[K/min]
$\Delta H^\circ$	Enthalpy of crystallization	[kcal/mol], [J/mol]
$k_{T_x}$	Equilibrium constant	[-]
$k$	Number of factors in an experiment	[-]
$L_{CF}$	Length of the cold finger	[mm], [cm]
$\dot{M}$	Yield of crystallization	[%]
$M_w$	Molecular weight	[g/mol], [kDa]
$n$	Number of replications of the experiments	[-]
$p$	Number of factors generated from interactions of a full factorial	[-]
$P_L$	Protein loss in the ice layer	[%]
$R$	Ideal gas constant	[J/mol·K]
$r$	Levels of each of the factors in an experiment	[-]
$s$	Supersaturation	[-]
$s_{cr}$	Thickness of the ice crystal layer	[mm]

$T_{CF}$	Temperature of the cooled surface (cold finger)	[°C], [K]
$t_{CF-CT}$	Time at constant temperature in the cold finger	[min]
$T_{CT-CF}$	Constant temperature value in the cold finger	[°C], [K]
$T_i$	Temperature in the interface (ice-bulk solution)	[°C], [K]
$T_{IT-CF}$	Initial temperature of the cold finger	[°C], [K]
$T_{FT-CF}$	Final temperature of the cooled surface (cold finger)	[°C], [K]
$T_{s(r)}$	Temperature profile in the crystal layer	[°C], [K]
$T_w$	Temperature of the wall	[°C], [K]
$T_x$	Temperature	[°C], [K]
$T_\infty$	Temperature in the bulk solution	[°C], [K]
$V_{ICE}$	Volume of the ice	[mL]
$V_{ML}$	Volume of the mother liquor	[mL]
$v_{cr}$	Crystal growth rate of the ice layer	[m/s]

## References

- [Ald46] Alderton, G., Fevold, H. L.: Direct Crystallization of Lysozyme from Egg White and Some Crystalline Salts of Lysozyme, *J. Biological Chemistry*, 164 (1946) 1, 1-5.
- [Ant06] Anton, M., Nau, F., Nys, Y.: Bioactive egg components and their potential uses, *Worlds Poultry Science Journal*, 62 (2006) 3, 429-438.
- [And96] Anderson, M. J., Whitcomb, P. J.: Optimize your process optimization efforts, *Chemical Engineering Progress*, 92 (1996) 12, 51-60.
- [Ash04] Asherie, N.: Protein crystallization and phase diagrams, *Methods Macromolecular Crystallization*, 34 (2004) 3, 266-272.
- [Ber07] Berg J.M., Tymoczko, J.L., Stryer, L., *Stryer Biochemie*, Elsevier GmbH, München, 2007.
- [Bla65] Blake, C. C. F., Koenig, D. F., Mair, G. A., North, A. C. T., Phillips, D. C., Sarma, V. R.: Structure of Hen Egg-White Lysozyme - a 3-Dimensional Fourier Synthesis at 2A Resolution, *Nature*, 206 (1965) 4986, 757-761.
- [Bie98] Bierwirth, J., Zur Trennwirkung von Schichtkristallisationsprozessen, Dissertation, der Universität Bremen (Shaker, Achen, 1998)
- [Ben02] Bennett, R.C., Crystallizer selection and design, in: A. S. Myerson (Ed.), *Handbook of Industrial Crystallization*, Butterworth-Heinemann, Boston, 2002, p. 115.
- [Box78] Box, G. E. P., Hunter, W.G., Hunter, J. S., *Statistics for experiments*, John Wiley & Sons, New York, 1978, p. 374-433.
- [Cac91] Cacioppo, E., Pusey, M. L.: The solubility of the tetragonal form of hen egg white lysozyme from pH 4.0 to 5.4, *Journal of Crystal Growth*, 114 (1991) 3, 286-292.
- [Can63] Canfield, R. E.: Amino Acid Sequence of Egg White Lysozyme, *Journal of Biological Chemistry*, 238 (1963) 8, 2698-2707.

- [Cha86] Li-Chan, E., Nakai, S., Sim, J., Bragg, D. B., Lo, K. V.: Lysozyme Separation from Egg White by Cation Exchange Column Chromatography, *Journal of Food Science*, 51 (1986) 4, 1032-1036.
- [Cha00] Chang, H.-M., Yang, C.-C., Chang, Y.-C.: Rapid Separation of Lysozyme from Chicken Egg White by Reductants and Thermal Treatment, *Journal of Agricultural and Food Chemistry*, 48 (2000) 2, 161-164.
- [Chi03] Chianese, A., Parisi, M., Fundamentals of nucleation and Crystal Growth, in: J. Ulrich, H. Glade (Eds.), *Melt Crystallization Fundamentals, Equipment and Applications*, Shaker Verlag, Aachen, 2003, p. 41-69
- [Chi90] Chisti, Y., Mooyoung, M.: Large-Scale Protein Separations - Engineering Aspects of Chromatography, *Biotechnology Advances*, 8 (1990) 4, 699-708.
- [Chv85] Chvapli, M., Eckmayer, Z.: Role of proteins in cosmetics, *International Journal of Cosmetic Science*, 7 (1985) 2, 41-49.
- [Cur06] Curtis, R. A., Lue, L.: A molecular approach to bioseparations: Protein-protein protein-salt interactions, *Chemical Engineering Science Biomolecular Engineering*, 61 (2006) 3, 907-923.
- [Dav00] Davey, R., Garside, J.: *From molecules to crystallizers: An Introduction to Crystallization*, Oxford University Press, New York, 2000.
- [DeM92] DeMattei, R. C., Feigelson, R. S.: Controlling nucleation in protein solutions, *Journal of Crystal Growth*, 122 (1992) 1-4, 21-30.
- [Dia10a] Díaz Borbón V. P., Ulrich J., Advances toward optimization of a novel freeze out protein crystallization technology, in: T. Stelzer, J. Ulrich (Eds.), *proceedings of BIWIC'10 (17th International Workshop on Industrial Crystallization)* Halle, Cuvillier Verlag Göttingen, 2010, p. 232-240.
- [Dia10b] Díaz Borbón, V.P., Ulrich, J.: Optimization of the novel technology: freeze out protein crystallization, in *proceedings of ISIC 18 (18th International Symposium on Industrial Crystallization)*, Zurich, edited by Biscans B., Mazzotti M., AIDIC, 2011, p. 496-497.



- [Dia10c] Diaz Borbon, V. P., Ulrich, J.: Solvent freeze out crystallization of lysozyme from a lysozyme-ovalbumin mixture, *Crystal Research and Technology*, 47 (2012) 5, 541-547.
- [Dia10d] Diaz Borbon, V. P., Ulrich, J.: SFO-solvent freeze out-technology for industrial proteins, *Journal of Crystal Growth*, 2012, 10.1016/j.jcrysgro.2012.09.031.
- [Dua10] Duan Z.: Determination of Pseudo Phase Diagrams for Solvent Freeze Out Protein Crystallization, Diploma Thesis, Martin-Luther-Universität Halle-Wittenberg, Halle (Saale), 2010.
- [Dre92] Drenth, J., Haas, C.: Protein crystals and their stability, *Journal of Crystal Growth*, 122 (1992) 1-4, 107-109.
- [Dur96] Durbin, S. D., Feher, G.: Protein crystallization, *Annual Review of Physical Chemistry*, 47 (1996) 171-204.
- [For99] Forsythe, E. L., Judge, R. A., Pusey, M. L.: Tetragonal Chicken Egg White Lysozyme Solubility in Sodium Chloride Solutions, *Journal of Chemical & Engineering Data*, 44 (1999) 3, 637-640.
- [Fro10] Froberg, P., Pietzsch, M., Ulrich, J.: Effect of crystalline substances in biodegradable films, *Chemical Engineering Research and Design*, 88 (2010) 9, 1148-1152.
- [Gar95] Garside J., Mass Crystallization, number balances and size distributions, in: J.P. van der Eerden, O.S.L. Bruinsma (Eds.), *Science and Technology of Crystal Growth*, Kluwer Academic Publishers, Dordrecht, 1995, p.209-220
- [Haa89] Haaland, P. D., *Experimental design in biotechnology*, Marcel Dekker Inc., N.Y., 1989.
- [Haa98] Haas, C., Drenth, J.: The Protein-Water Phase Diagram and the Growth of Protein Crystals from Aqueous Solution, *The Journal of Physical Chemistry*, 102 (1998) 21, 4226-4232.
- [Hek07] Hekmat, D., Hebel, D., Joswig, S., Schmidt, M. and Weuster-Botz, D.: Advanced protein crystallization using water-soluble ionic liquids as crystallization additives, *Biotechnology Letters*, 29 (2007) 11, 1703-1711.

- [Hen01] Henning S., Zur Migration flüssiger Einschlüsse in Schichten von Schmelzkristallisationsprozesse, Dissertation, Universität Bremen (Shaker, Aachen, 2001).
- [Mao12] Maosoongnern, S., Diaz Borbon, V.P., Ulrich, J., Flood, A.E., Introducing a fast method to determine the solubility and metastable zone width for proteins. –Case study Lyozyme-, Industrial and Engineering Chemistry Research, 2012, 10.1021/ie300799d.
- [Hof95] Hofmann, G., Crystallizers, in: J.P. van der Eerden, O.S.L. Bruinsma (Eds.), Science and Technology of Crystal Growth, Kluwer Academic Publishers, Dordrecht, 1995, p.221-232.
- [Hun67] Hunter, W. G., Hoff, M. E.: Planning Experiments To Increase Research Efficiency, Industrial & Engineering Chemistry, 59 (1967) 3, 43-48.
- [Jud98] Judge, R. A., Forsythe, E. L., Pusey, M. L.: The effect of protein impurities on lysozyme crystal growth, Biotechnology and Bioengineering, 59 (1998) 6, 776-785.
- [Jud95] Judge, R. A., Johns, M. R., White, E. T.: Protein purification by bulk crystallization: the recovery of ovalbumin, Biotechnology and Bioengineering, 48 (1995) 4, 316-23.
- [Kön03] König, A., Phase Diagrams, in: J. Ulrich, H. Glade (Eds.), Melt Crystallization Fundamentals, Equipment and Applications, Shaker Verlag, Aachen, 2003, p. 7-39.
- [Lei11] Leiser, M., Einsatz der “Solvent Freeze out”-Technologie für die Proteinkristallisation, Diploma Thesis, Martin-Luther-Universität Halle-Wittenberg, Halle (Saale), 2011.
- [Lig04] Lightfoot, E. N., Moscariello, J. S.: Bioseparations, Biotechnology and Bioengineering, 87 (2004) 3, 259-273.
- [Liu10] Liu, Y. X., Wang, X. J., Ching, C. B.: Toward Further Understanding of Lysozyme Crystallization: Phase Diagram, Protein-Protein Interaction, Nucleation Kinetics, and Growth Kinetics, Crystal Growth & Design, 10 (2009) 2, 548-558.

- [Loh04] Loher, M., Saladin, D., Keferstein, C., Vetter, W., Keppler-Ott, Th., Non-classical design of experiments in cold forging: process optimization with data-based process models, in proceedings of 4<sup>th</sup> CIRP Intelligent Computation in Manufacturing Engineering, Sorrento (Naples) Italy, 2004, p. 523-527.
- [Mec06] Mecitoglu, Ç., Yemenicioglu, A., Arslanoglu, A., Elmacl, Z. S., Korel, F., Çetin, A. E.: Incorporation of partially purified hen egg white lysozyme into zein films for antimicrobial food packaging, Food Research International, 39 (2006) 1, 12-21.
- [Mee02] Meenan, P. A., Anderson, S. R., D. L. Klung, The influence of impurities and solvents on crystallization, in: A. S. Myerson (Ed.), Handbook of Industrial Crystallization, Butterworth-Heinemann, Boston, 2002, p. 67-97.
- [Mon97] Montgomery D.M., Design and analysis of experiments, John Wiley and Sons, New York, 1997.
- [Mot98] Motoki, M., Seguro, K.: Transglutaminase and its use for food processing, Trends in Food Science & Technology, 9 (1998) 5, 204-210.
- [Mus97] Muschol, M., Rosenberger, F.: Liquid-liquid phase separation in supersaturated lysozyme solutions and associated precipitate formation/crystallization, The Journal of Chemical Physics, 107 (1997) 6, 1953-1962.
- [Mül12] Müller, C. "How to describe protein crystals correctly? -case study of lysozyme crystals-", Dissertation, an der Martin-Luther-Universität Halle-Wittenberg, (Winterwork, Borsdorf, 2012).
- [Neu95] Neumann M., Vergleich statischer und dynamischer Schichtkristallisation und das Reinigungspotential der Diffusionswäsche, Dissertation, der Universität Bremen (PAPIERFLIEGER, Clausthal-Zellerfeld, 1996)
- [Nyv78] Nyvlt. J., Industrial crystallization. State of the Art., Verlag Chemie GmbH, Weinheim, 1978.
- [Özo92] Özoguz, M.Y., Zur Schichtkristallisation als Schmelzkristallisationsverfahren, Dissertation, Universität Bremen, VDI-Verlag GmbH, Düsseldorf, 1992.

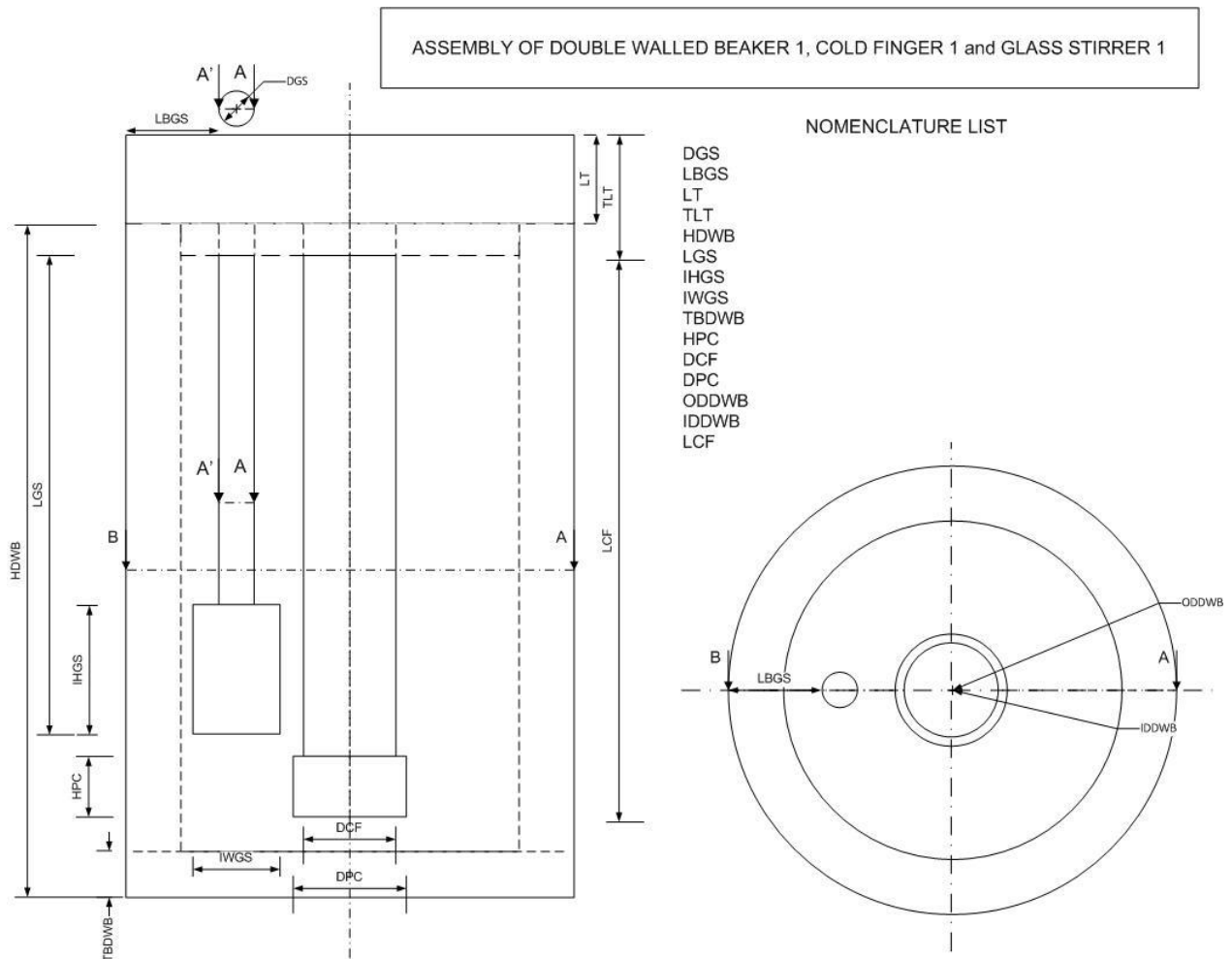
- [Oha73] Ohara, M., R. C. Reid, Modeling Crystal Growth Rates from Solution, Prentice Hall, Englewood Cliffs, NJ, 1973.
- [Phe90] Mc Pherson, A.: Current approaches to macromolecular crystallization, European Journal of Biochemistry, 189 (1990) 1, 1-23.
- [Phe09] Mc Pherson, A., Introduction to macromolecular crystallography, Wiley & Sons, New Jersey, 2009.
- [Por92] Porter, J. E., Ladisch, M. R.: Ion-exchange and affinity chromatography costs in  $\hat{\pm}$ -galactosidase purification, Biotechnology and Bioengineering, 39 (1992) 7, 717-724.
- [Pro88] Proctor, V. A., Cunningham, F. E., Fung, D. Y. C.: The chemistry of lysozyme and its use as a food preservative and a pharmaceutical, C R C Critical Reviews in Food Science and Nutrition, 26 (1988) 4, 359-395.
- [Ros96] Rosenberger, F.: Protein crystallization, Journal of Crystal Growth, 166 (1996) 1-4, 40-54.
- [Ros96a] Rosenbaum, D. F., Zukoski, C. F.: Protein interactions and crystallization, Journal of Crystal Growth, 169 (1996) 4, 752-758.
- [Roy04] Roy, J. J., Abraham, T. E.: Strategies in making cross-linked enzyme crystals, Chemical Reviews, 104 (2004) 9, 3705-3721.
- [Rüd11] Rüdiger, S: Proteinkristallisation mittels "Solvent Freeze Out"-Technologie, Diploma Thesis, Martin-Luther-Universität Halle-Wittenberg, 2011.
- [Ryu10a] Ryu, B.-H. Protein Crystallization by Solvent Freeze-Out Technology, Dissertation, der MLU Halle-Wittenberg (Shaker Verlag, Aachen, 2010).
- [Ryu10b] Ryu, B. H., Jones, M. J., Ulrich, J.: Crystallization of Hen Egg White Lysozyme by Solvent Freeze-Out: Effect of Cooling Rate on Protein Inclusion in the Ice Layer, Chemical Engineering & Technology, 33 (2010), 1695-1698.
- [Sha96] Schall, C. A., Arnold, E., Wiencek, J. M.: Enthalpy of crystallization of hen egg-white lysozyme, Journal of Crystal Growth, 165 (1996) 3, 293-298.

- [Sch04] Schmidt, S., Havekost, D., Kaiser, K., Kauling, J., Henzler, H.-J.: Kristallisation für die Aufarbeitung von Proteinen, *Chemie Ingenieur Technik*, 76 (2004) 6, 819-822.
- [Sch93] Scholz R., Die Schichtkristallisation als thermisches Trennverfahren, Dissertation, Universität Bremen (VDI-Verlag, Düsseldorf, 1993).
- [Shu52] Shugar, D.: The measurement of lysozyme activity and the ultra-violet inactivation of lysozyme, *Biochimica et Biophysica Acta*, 8 (1952) 302-309.
- [Scw02] Schwartz, A., Myerson, A., Solutions and Solution Properties, in: A. S. Myerson (Ed.), *Handbook of Industrial Crystallization*, Butterworth-Heinemann, Boston, 2002, p. 1-30.
- [Sta02] StatSoft, Inc. (2002). *STATISTICA for Windows [Computer program manual]*. Tulsa, OK: StatSoft, Inc., 2300 East 14th Street, Tulsa, OK, 74104-4442, (918) 749-1119, fax: (918) 749-2217, e-mail: info@statsoft.com, Web: <http://www.statsoft.com>.
- [Ste03] Stepanski M., Schäfer E., Separate organics by melt crystallization: A guide to when and how to use this technique, in: J. Ulrich, H. Glade (Eds.), *Melt Crystallization Fundamentals, Equipment and Applications*, Shaker Verlag, Aachen, 2003, p. 191.
- [Tam11] Tam, S. K., Chan, H. C., Ng, K. M., Wibowo, C.: Design of Protein Crystallization Processes Guided by Phase Diagrams, *Industrial & Engineering Chemistry Research*, 50 (2011) 13, 8163-8175.
- [Tre08] Trevino, S. R., Scholtz, J. M., Pace, C. N.: Measuring and increasing protein solubility, *Journal of Pharmaceutical Sciences*, 97 (2008) 10, 4155-4166.
- [Ulr02] Ulrich, J., Bülau, H.C., Melt crystallization, in: A. S. Myerson (Ed.), *Handbook of Industrial Crystallization*, Butterworth-Heinemann, Boston, 2002, p. 161-177.
- [Ulr03] Ulrich, J., Introduction, Laboratory tests for melt crystallization, in: J. Ulrich, H. Glade (Eds.), *Melt Crystallization Fundamentals, Equipment and Applications*, Shaker Verlag, Aachen, 2003, p.1-5, 148.

- [Ulr08] Ulrich, J., Nordhoff, S., Schmelzkristallisation, in: Goedecke R., Verfahrensentwicklung, in Fluidverfahrenstechnik, Wiley-VCH Verlag GmbH & Co. KGaA, Weinheim, 2008, p. 1131-1189.
- [Wan94] Wangnick, K., Das Waschen als Nachbehandlungsprozeß der Schichtkristallisation, Dissertation, Universität Bremen, (VDI-Verlag GmbH, Düsseldorf, 1994)
- [Web97] Weber, P. C., [2] Overview of protein crystallization methods, Methods in Enzymology, in Macromolecular Crystallography Part A, edited by Charles W. Carter, Jr., Academic Press, 1997, p. 13-22 (0076-6879).
- [Wie99] Wiencek, J. M.: New Strategies for Protein Crystal Growth, Annual Review of Biomedical Engineering, 1 (1999) 1, 505-534.
- [Yan95] Yang, C.-H., Lin, S.-M., Wen, T.-C.: Application of statistical experimental strategies to the process optimization of waterborne polyurethane, Polymer Engineering & Science, 35 (1995) 8, 722-730.
- [Yok04] Yokoyama, K., Nio, N., Kikuchi, Y.: Properties and applications of microbial transglutaminase, Applied Microbiology and Biotechnology, 64 (2004) 4, 447-454.
- [Zhu95] Zhu, Y., Rinzema, A., Tramper, J. Bol, J., Microbial transglutaminase: A review of its production and application in food processing, in: Applied Microbiology and Biotechnology. Volume 44. Springer Berlin / Heidelberg; 1995. p. 277-282.

## 9. Appendix

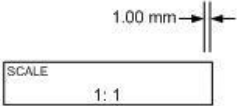
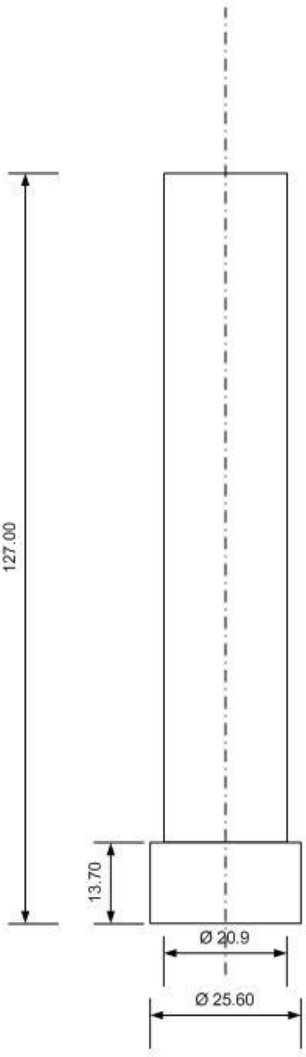
### I. SFO Equipment 1: Nomenclature



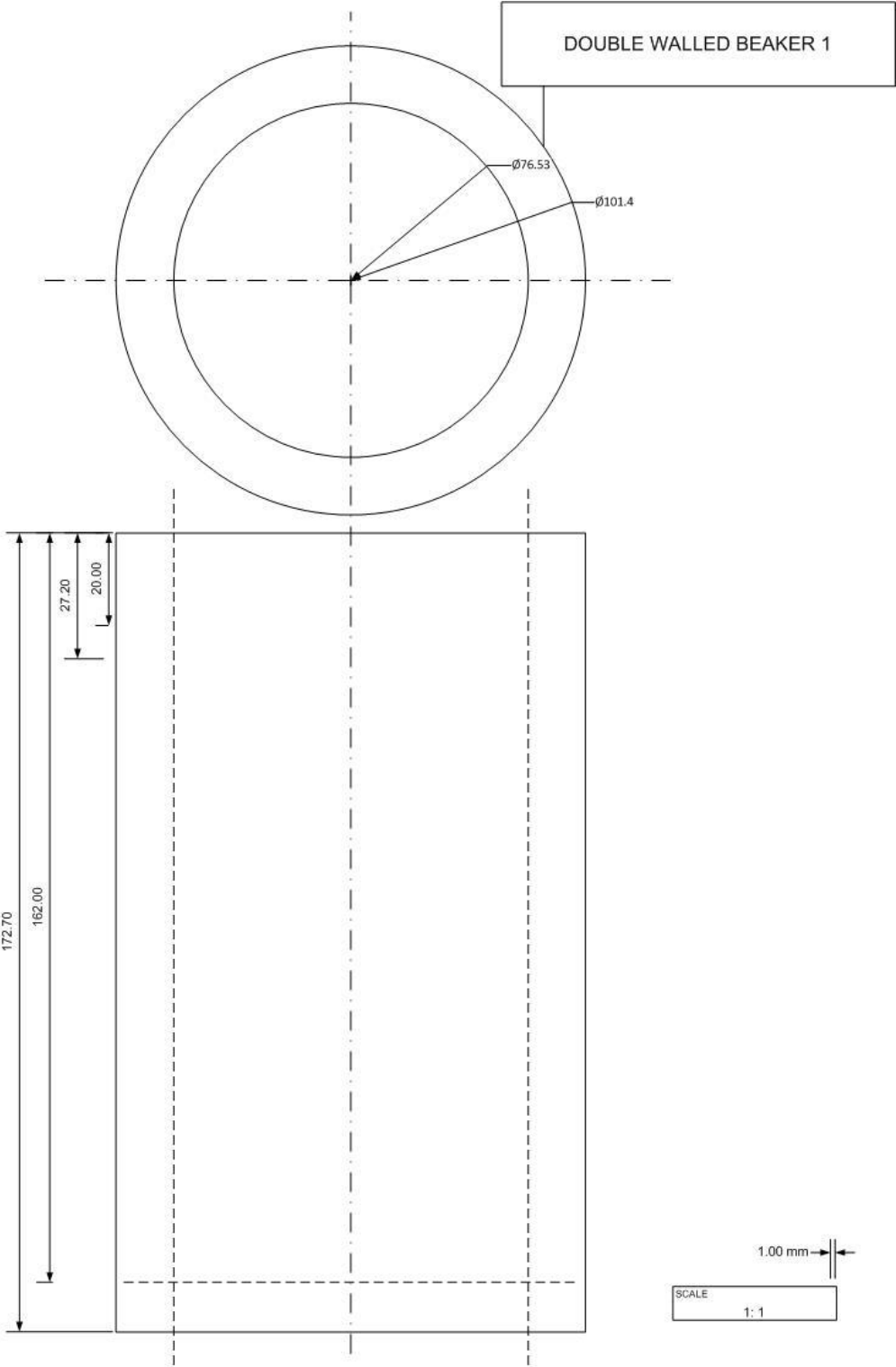


SFO Equipment 1: Cold Finger

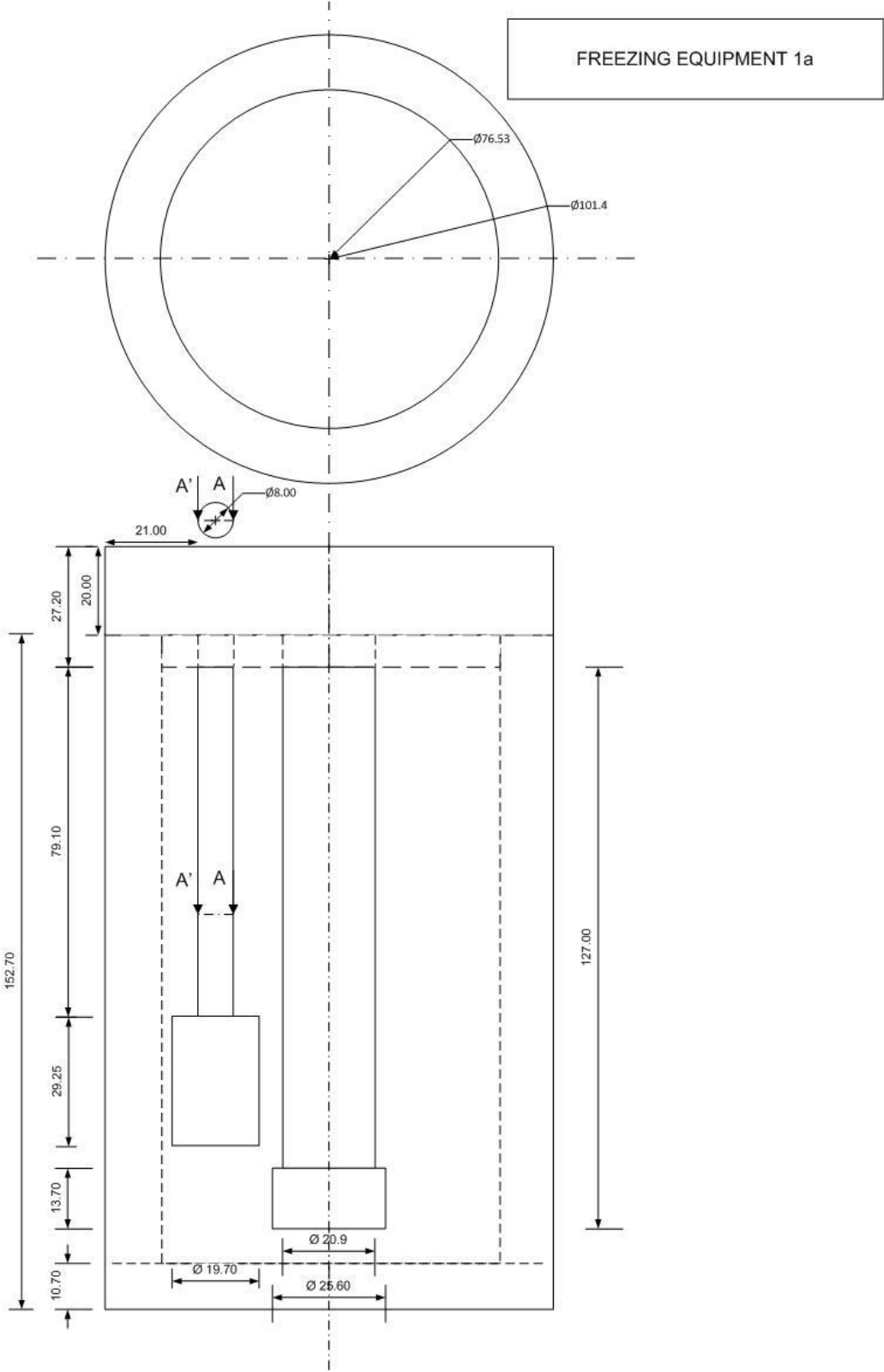
COLD FINGER 1



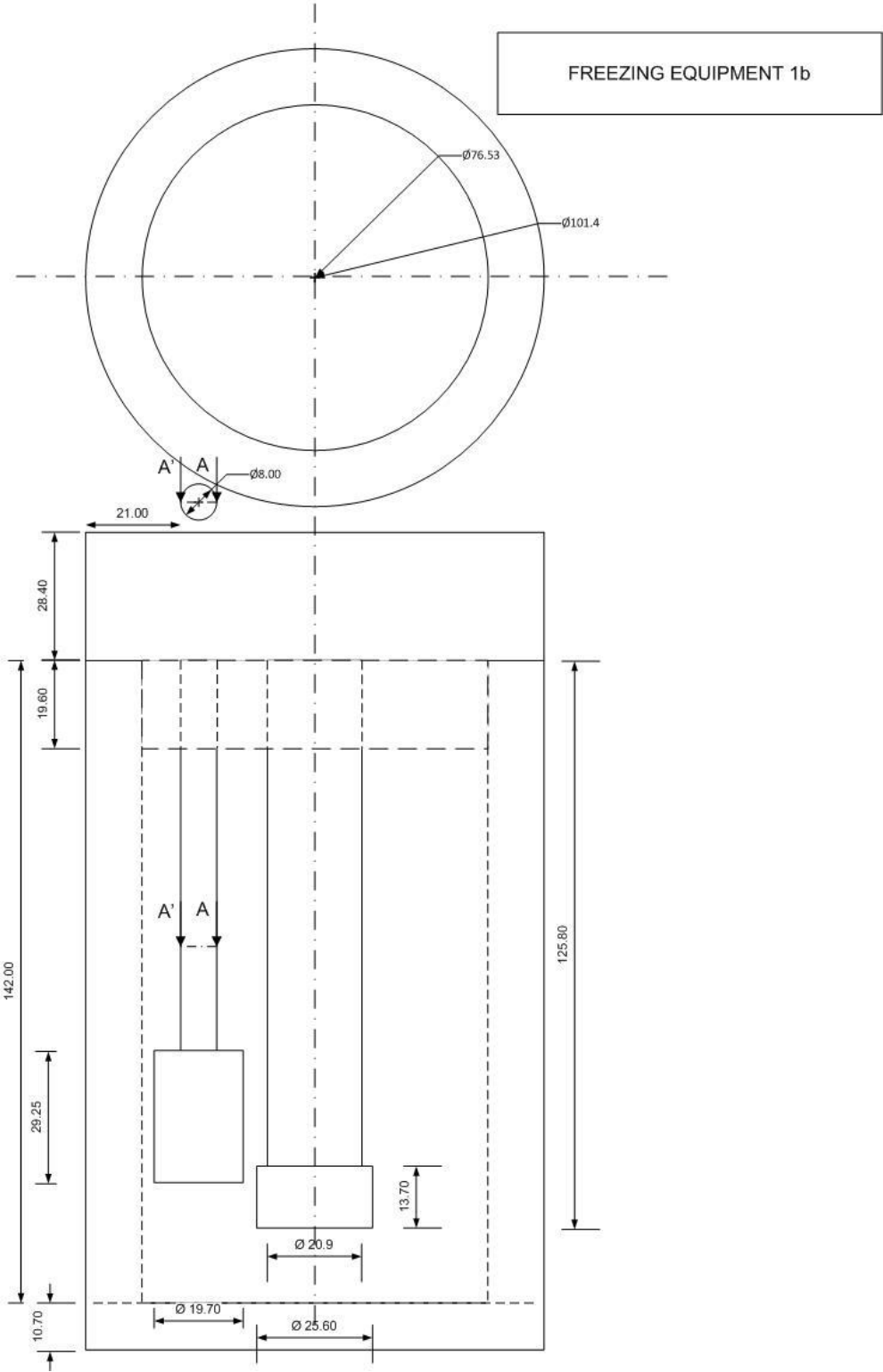
SFO Equipment 1: Double walled beaker



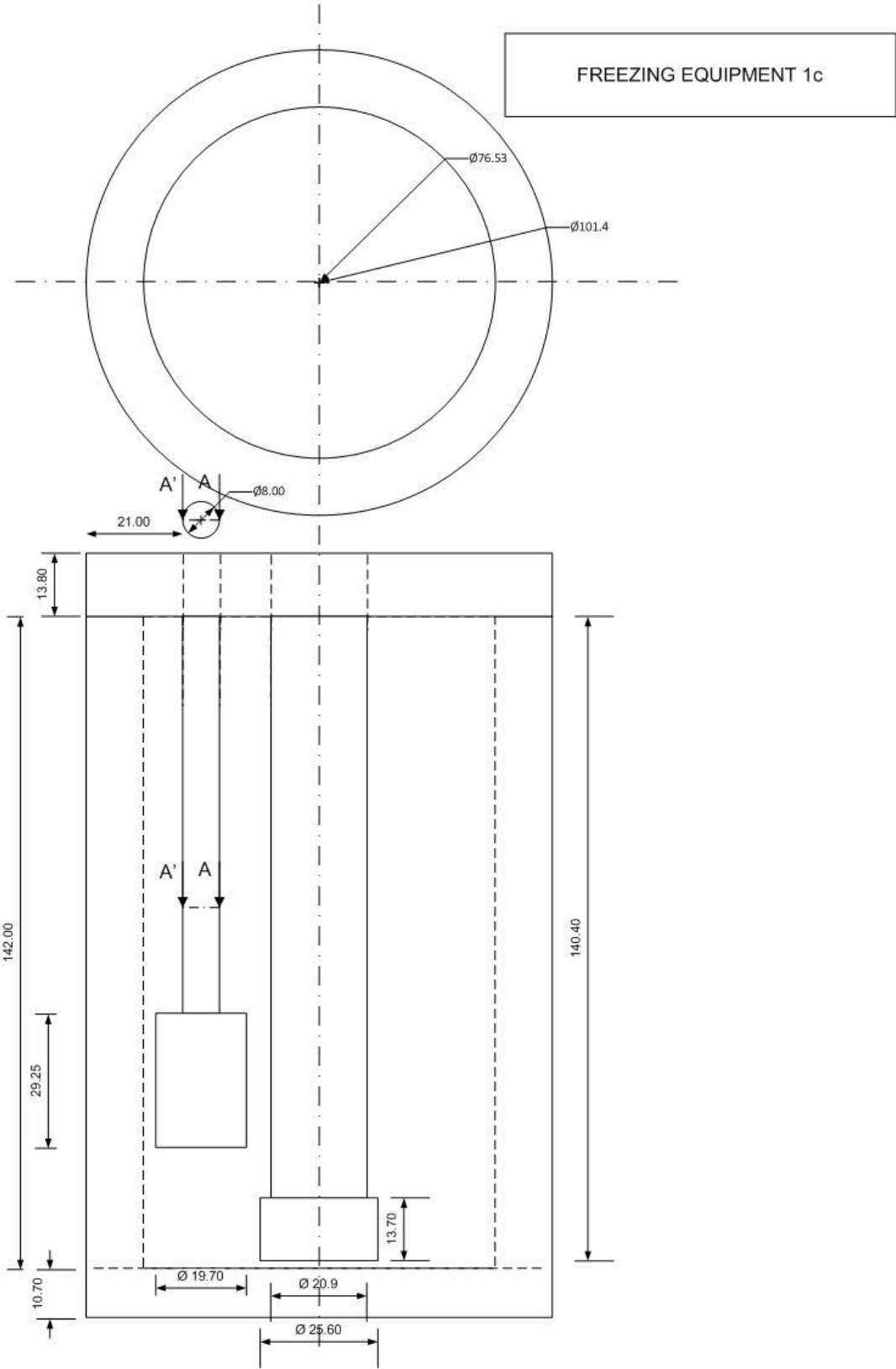
SFO Equipment 1: (a) Cold Finger with middle length



SFO Equipment 1: (b) Cold Finger with short length



SFO Equipment 1: c) Cold Finger with long length

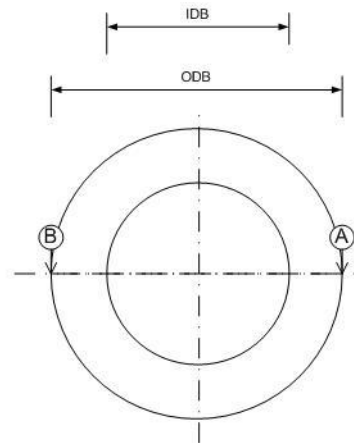
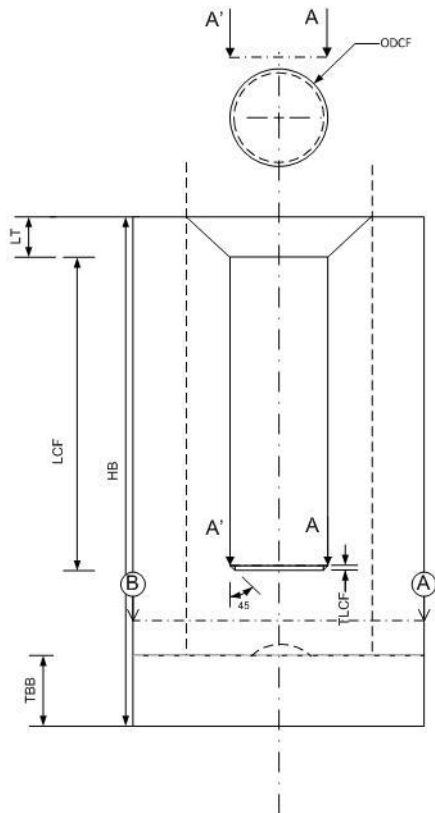


II. SFO Equipment 2: Nomenclature

ASSEMBLY OF DOUBLE WALLED BEAKER 2, COLD FINGER 2

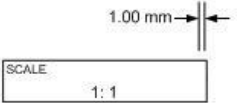
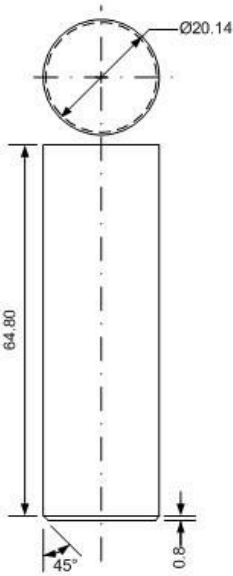
NOMENCLATURE LIST

- LT = LID THICKNESS
- ODCF = OUTER DIAMTER OF COLD FINGER
- LCF = LENGTH OF COLD FINGER
- HB = HEIGHT OF DOUBLE WALLED BEAKER
- TLCF = TIP LENGTH OF COLD FINGER
- TBB = THICKNESS AT THE BOTTOM OF DOUBLE WALLED GLASS
- IDB = INNER DIAMTER OF DOUBLE WALLED BEAKER
- ODB = OUTER DIAMETER OF DOUBLE WALLED BEAKER



SFO Equipment 2: Cold Finger

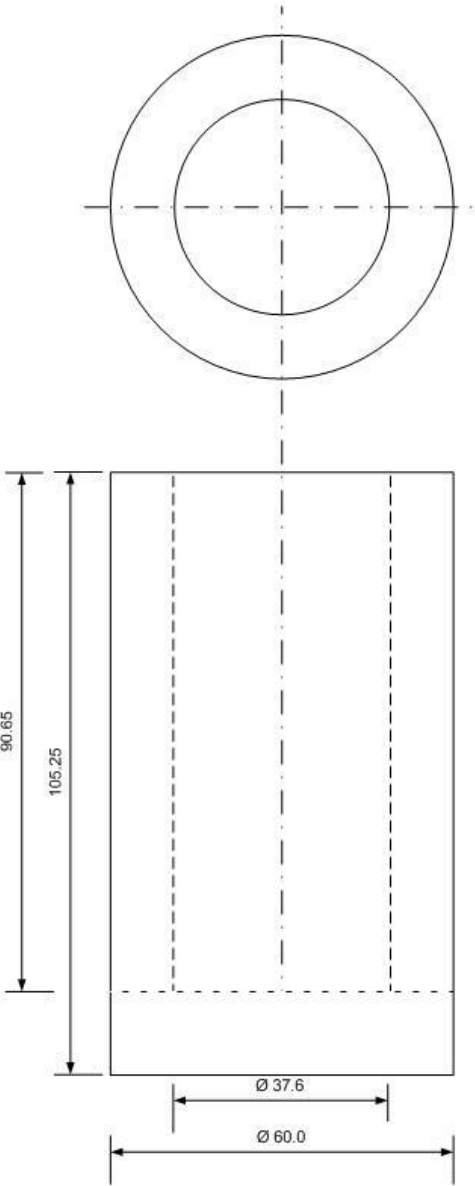
COLD FINGER 2





SFO Equipment 1: Double walled beaker

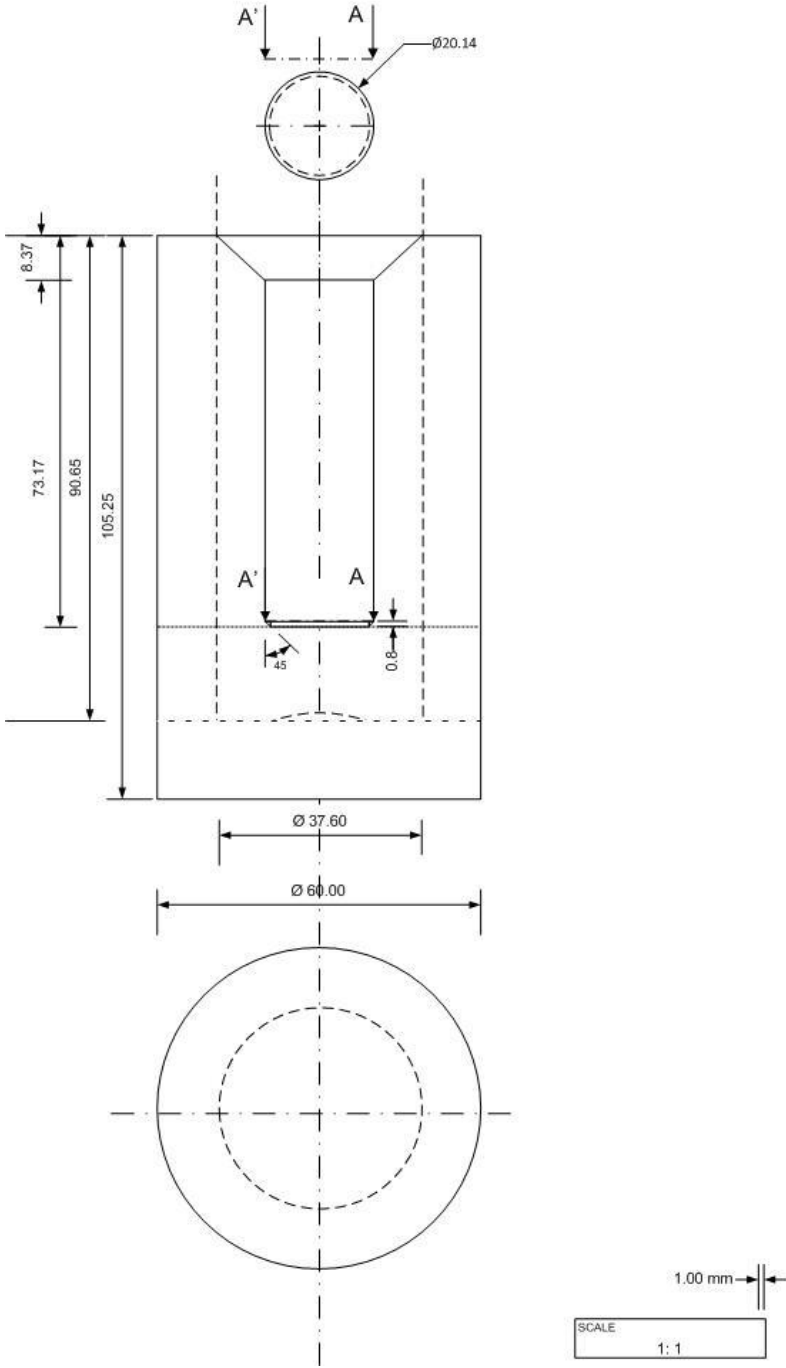
DOUBLE WALLED BEAKER 2



1.00 mm → ←

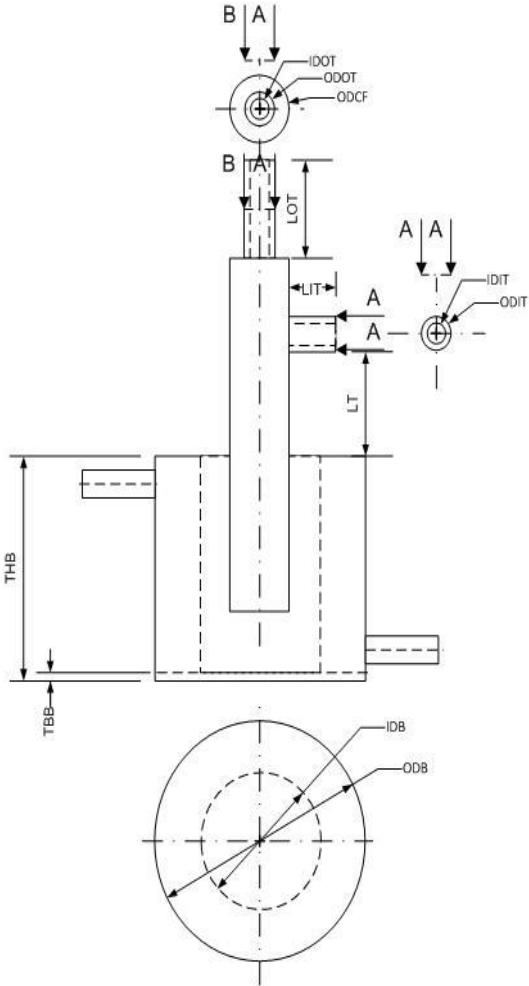
SCALE  
1: 1

ASSEMBLY OF DOUBLE WALLED  
BEAKER 2 and COLD FINGER 2



III. SFO Equipment 3: Nomenclature

ASSEMBLY OF DOUBLE WALLED BEAKER 3, COLD FINGER 3

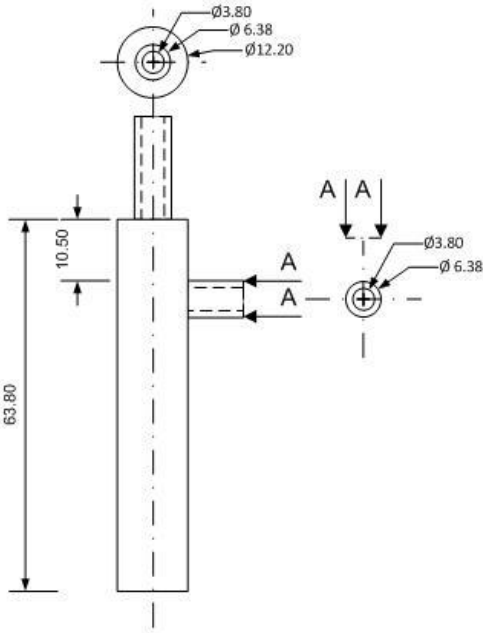


NOMENCLATURE LIST

- IDOT
- ODOT
- ODCF
- LOT
- LIT
- IDIT
- ODIT
- LT
- THB
- TBB
- ODB
- IDB

SFO Equipment 3: Cold Finger

COLD FINGER 3

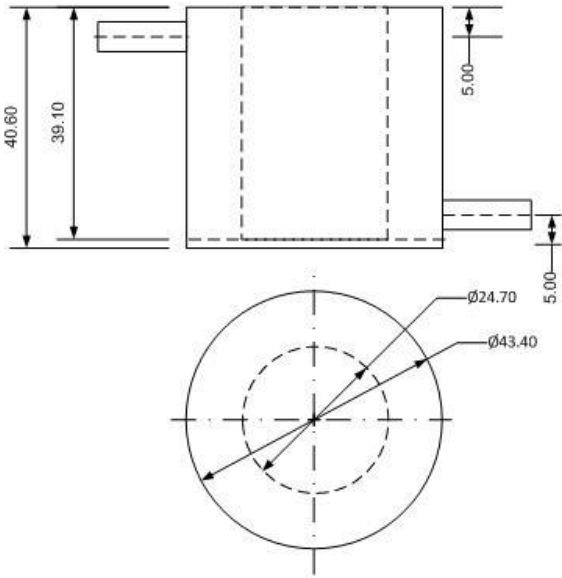


1.00 mm → ←

SCALE  
1:1

SFO Equipment 3: Double walled beaker

DOUBLE WALLED BEAKER 3

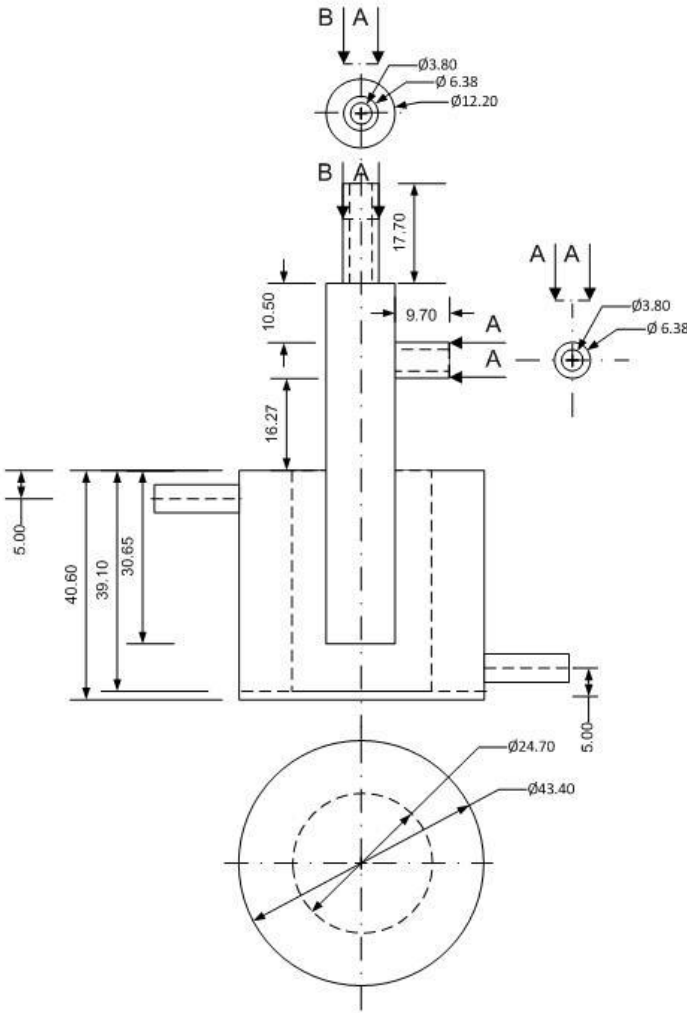


1.00 mm

SCALE  
1: 1

SFO Equipment 3: (a) Cold Finger short length

FREEZING EQUIPMENT 3a

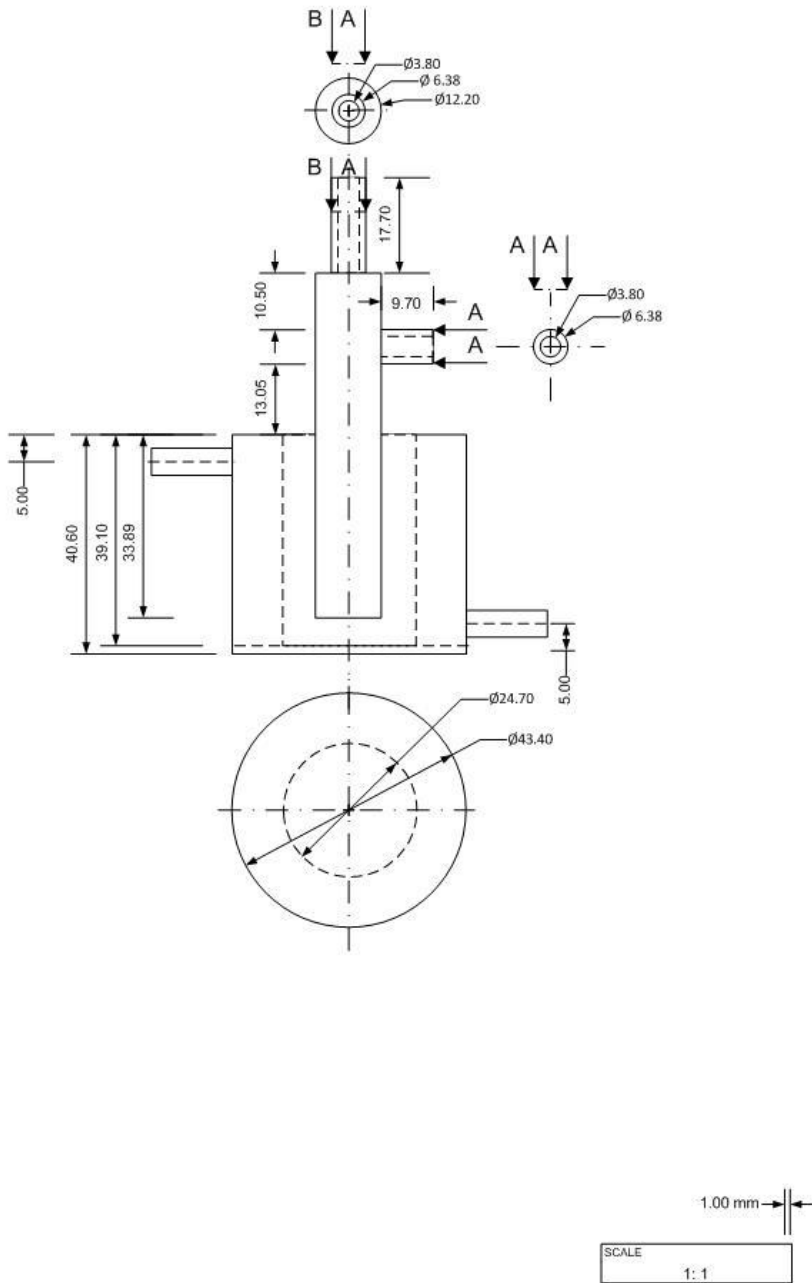






SFO Equipment 3: c) Cold Finger long length

FREEZING EQUIPMENT 3c



## Statement of Authorship

---

I declare that I have written this document on my own. It is a compilation of the results of work carried out by my own or by students under my supervision. The used resources and tools or previously cited information have been distinguished by quotation marks.

Düsseldorf den, 19.06.2013



Viviana Patricia Díaz Borbón

# Lebenslauf

## Persönliche Angaben

Name: Viviana Patricia Díaz Borbón  
Geburtsdatum: 05.10.1981 in Bogotá Kolumbien  
Staatsangehörigkeit: kolumbianisch – deutsche Erwerbstätigkeit gestattet  
Familienstand: verheiratet



## Hochschulstudium

01/2010 - 11/2012 **Promotionsstudentin** am Lehrstuhl für Thermische Verfahrenstechnik an der Martin-Luther-Universität Halle-Wittenberg.  
10/ 2006 - 04/2009 **Master Kurs** in Applied Polymer Science an der Martin-Luther-Universität Halle-Wittenberg, Abschluss: M.Sc., Note: 2,4.  
01/ 1999 - 07/2006 **Chemieingenieurwesen** an der Universidad Nacional de Colombia, Abschluss: Chemieingenieurin, entsprechende Note in Deutschland: 2,3.

## Wissenschaftliche Arbeiten

01/2010 - 11/2012 wissenschaftliche Arbeit auf dem Gebiet „**Optimierung industrieller Kristallisationsprozesse von Proteinen**“  
Zentrum für Ingenieurwissenschaften an der **Martin-Luther-Universität Halle-Wittenberg**, <http://tvt.iw.uni-halle.de/>  
07/2008 - 12/2008 Master Thesis in „**Fabrication and characterization of scaffolds for Tissue Engineering**“, Note: 2,1.  
**Fraunhofer-Institut für Werkstoffmechanik IWM**, <http://www.iwm.fraunhofer.de/>  
02/2008 - 04/2008 Projektarbeit „**Production of protein films using internal plasticizers**“, Note: 1,7.  
Arbeitsgruppe Aufarbeitung biotechnischer Produkte an der **Martin-Luther-Universität Halle-Wittenberg**, <http://downstream.pharmazie.uni-halle.de/>  
08/2007 – 10/2007 Praktikum in „ **Preparation of silk protein solutions and coating of scaffolds**“  
**Fraunhofer-Institut für Werkstoffmechanik IWM**, <http://www.iwm.fraunhofer.de/>  
02/2006 – 06/2006 Diplomarbeit „ **Analysis of different alternatives of bactericides in admixtures**“, entsprechende Note in Deutschland: 1,3.  
**Sika Colombia S.A. (Bogotá, Kolumbien)**, <http://www.sika.com/>  
01/2006 – 06/2006 Versuchsanlage Projektarbeit „**Rezepturenentwicklung auf Chitosan-Basis zur längeren Haltbarkeit von Rosen** “ entsprechende Note in Deutschland: 1,3.  
**Universidad Nacional de Colombia**, <http://www.unal.edu.co/english/>

## Berufliche Erfahrungen

Since	01/2012	Sales Manager, <b>GEA Messo PT, (Duisburg, Deutschland)</b>
	06/2005 – 12/2005	Praktikum „Unterstützung im Außenhandelsbereich: Marktanalyse der Bestandteile von Plastik- und Gummirohstoffen“, <b>Elastika Ltda. (Bogotá, Kolumbien)</b>
	04/2001 – 10/2001	Nebenjob als „Manager Assistent“, <b>Reyser (Bogotá, Kolumbien)</b>

## Veröffentlichungen

- Maosoongnern, S., Díaz Borbon, V.P., Ulrich, J., Flood, A.E.: **Introducing a fast method to determine the solubility and metastable zone width for proteins –Case study Lysozyme-**, Industrial & Engineering Chemistry Research 51 (2012) 46, 15251-15257.
- Díaz Borbon, V. P., Ulrich, J.: **SFO-solvent freeze out-technology for industrial proteins**, J. Cryst. Growth., 373 (2013) 38-44. <http://dx.doi.org/10.1016/j.jcrysgro.2012.09.031>.
- Díaz Borbón, V.P., Ulrich, J.: **Optimization and applicability of SFO-solvent freeze out-technology in protein crystallization**, *ACHEMA 2012* (Frankfurt am Main, 18-22 June 2012). Vortrag (Englisch).
- Díaz Borbón, V.P., Ulrich, J.: **Solvent freeze out crystallization of lysozyme from a lysozyme-ovalbumin mixture**, *Cryst. Res. Technol.*, 47 (2012) 5, 541-547.
- Díaz Borbón, V.P., Ulrich, J.: **Optimization of the novel technology: freeze out protein crystallization**, in proceedings of ISIC 18 (18th International Symposium on Industrial Crystallization), Zürich, edited by Biscans B., Mazzotti M., AIDIC, 2011, p. 496-497. Poster Präsentation.
- Díaz Borbón, V.P., **Verfahrensoptimierung von "Solvent Freeze Out" Proteinkristallisation**, Jahrestreffen des Fachausschusses Kristallisation (ProcesNet) 2011. Vortrag (Deutsch).
- Díaz Borbón, V.P., Ulrich, J.: **Advances toward optimization of a novel freeze out protein crystallization technology**, in proceedings of BIWIC'10 (17th International Workshop on Industrial Crystallization), Halle, edited by Stelzer, T., Ulrich J., Cuvillier Verlag Göttingen, 2010, p. 232-240. Poster Präsentation.

## Seminare

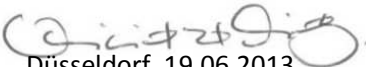
11. - 12.10/2011	Seminar in University of Szeged, Faculty of Pharmacy, Szeged, Ungarn (Vortrag) ( <a href="http://www.u-szeged.hu/english/">http://www.u-szeged.hu/english/</a> )
19.- 20.05/2011	Fortbildungsveranstaltung vom Haus der Technik: Grundlagen und Auslegung von Kristallisationen in der chemischen und pharmazeutischen Industrie, Berlin, Deutschland
02.12/2010	Seminar bei Orion Pharma, Espoo, Finland (Vortrag) ( <a href="http://www.orion.fi/en/">http://www.orion.fi/en/</a> )

## Auslandsaufenthalte

10/2002 - 01/2003	Fort Lauderdale, FL., USA, Englischsprachkurs
-------------------	---

## Kenntnisse

Sprache	Spanisch (Muttersprache), Englisch (verhandlungssicher), Deutsch (Höhere Mittelstufe)
EDV-Kenntnisse	MS Office, Origin, Statistica, CorelDRAW, ChemDraw, Hysis, Aspen, Endnote

  
Düsseldorf, 19.06.2013